BOOK of ABSTRACTS

20TH INTERNATIONAL COUETTE TAYLOR WORKSHOP

July 11-13th 2018 - Marseille France

INVITED SPEAKERS

Dr. Philippe Ghendrih, Directeur de recherche CEA-Institut de Recherche sur la Fusion Magnétique

Title: Burning plasma turbulence driven by a Rayleigh-Bénard like instability

Prof. Björn Hof, Institute of Science and Technology Austria

Title: Directed percolation transition to turbulence

Prof. Keith Julien, Applied Mathematics, University of Colorado, Boulder

Title: Rotating Rayleigh-Benard Convection: Theory, Experiments and Simulations

Prof. Francisco Marques Applied Physics**,** Universitat Politècnica de Catalunya

Title: Dynamics of thermal plumes in a uniform and a stratified ambient.

Dr. Benoit Pier, Directeur de recherche CNRS LMFA Ecole Centrale Lyon

Title: Complex dynamics in eccentric Taylor-Couette-Poiseuille flow

High-Order Compact scheme for High-Performance Computing of stratified rotating flows

Stéphane Abide[1], Stéphane Viazzo[2], Isabelle Raspo[2], Anthony Randriamampianina[2], Gabriel Meletti[3], Uwe Harlander[3], Andreas Krebs[3]

[1] Université de Perpignan Via Domitia, LAMPS EA 4217, Perpignan, France

[2] Aix-Marseille Univ., CNRS, Centrale Marseille, M2P2, France

[3] Department of Aerodynamics and Fluid Mechanics, Brandenburg University of Technology, Cottbus-Senftenberg, Germany

---

To take advantage of modern generation computing hardware, a scalable numerical method, based on high-order compact scheme, was developed to solve rotating stratified flows in cylindrical annular domains.

The azimuthal direction has been discretized using Fourier series expansion to benefit from the natural periodicity of the cylindrical geometry, and the favorable complexity algorithms for computing Fast Fourier Transforms. The space discretization in the two wall-bounded directions relies on the fourth-order compact scheme approximations. The code parallelization strategy combines two approaches. The first one is the $2d$-pencil decomposition to address the parallel solution of the implicit viscous terms and the pressure-like equations based on the diagonalization method. The second strategy of parallelization consists in the calculation of the compact derivatives/interpolations, using the approximate tridiagonal solver named reduced Partial Diagonal Dominant (rPDD) algorithm [1].The developed technique is validated with respect to analytical solutions, using the method of manufactured solutions, and available data for two specific configurations of rotating stratified flows : the Taylor-Couette setup under an axial thermal stratification and the baroclinic cavity. The purpose is to demonstrate its ability to correctly capture the flow characteristics in strato-rotational instability and in baroclinic instability with associated small-scale features. Moreover, this code is found to drastically reduce the huge execution times that often prevent detailed numerical investigations of these complex phenomena.

Figure 1 shows a strong scaling test carried out to assess the performance for up to 1024 cores using grid up to $128 \times 568 \times 568$ in radial, axial and azimuthal directions. Figure 2 shows instantaneous isocontours in the (θ, z) plane of the horizontal velocity divergence $\nabla_h.\mathbf{u}$ along the inner cold wall and along the outer hot cylinder in the baroclinic configuration. This variable is introduced to exhibit the occurrence of small-scale features simultaneously with the large-scale baroclinic waves. In the first plot, the small-scale structures, developing towards the bottom wall, have been identified as inertia gravity waves (IGWs) by different authors in similar water-filled cavities. The present observed features recall such IGWs reported by these authors. Recently, for the same present configuration, [2] mentioned the presence of ripples resulting from hydrodynamical instability along the outer hot cylinder. We also capture the same phenomenon, as illustrated by the isocontours of the horizontal divergence.

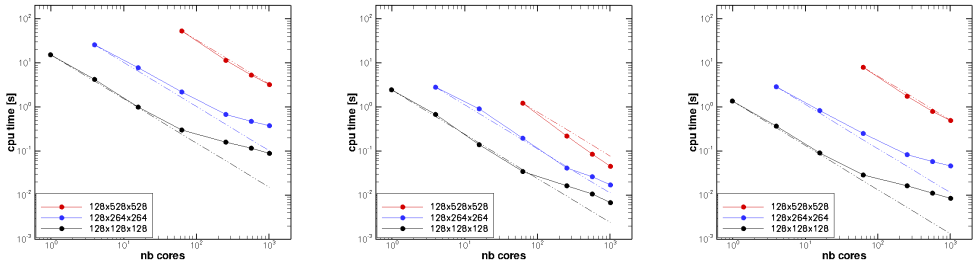

(a) (b) (c)

Figure 1: Baroclinic configuration - Strong scaling test a) temporal iteration b) solution of Poisson equation c) convective terms.

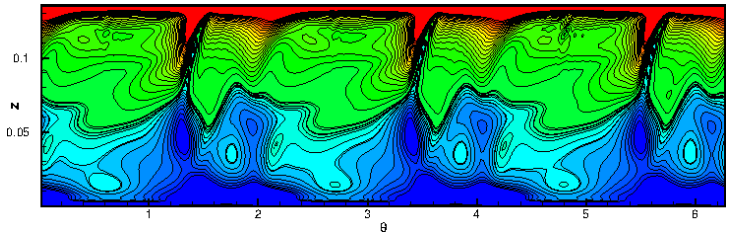

(a)

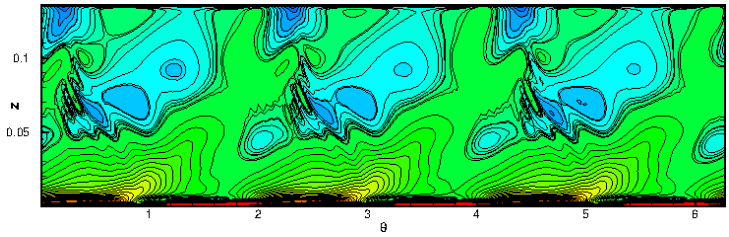

(b)

Figure 2: Baroclinic configuration - Instantaneous isocontours in (θ, z) plane of the horizontal divergence of the velocity: at radius close to inner wall (a), at radius close to outer wall (b).

References

[1] S. Abide, M. S. Binous, B. Zeghmati, *An efficient parallel high-order compact scheme for the 3D incompressible Navier-Stokes equations*, Int. J. Comp. Fluid Dynamics, **31**, (4-5), 214-229, 2017.

[2] T. Von Larcher, S. Viazzo, U. Harlander, M. Vincze, A. Randriamampianina, *Instabilities and small-scale waves within the Stewartson layers of a thermally rotating annulus*, J. Fluid Mech. **841**, 380-407, 2018.

Acknowledgements

This work was granted access to the HPC resources of CALMIP supercomputing center under the allocation 2017P17027 and to the HPC resources of Aix-Marseille Université financed by the project Equip@Meso (ANR-10-EQPX-29-01) of the program "Investissements d'Avenir" supervised by the "Agence Nationale de la Recherche". The authors acknowledge financial support from "Ministère des Affaires Étrangères", France, in the framework of a PROCOPE project (PHC 28369XH and 35299PM).

Alternating 'flip' solutions in ferrofluidic Taylor-Couette flow

Sebastian Altmeyer[1],

[1] Castelldefels School of Telecom and Aerospace Engineering (EETAC), Universitat Polytecnica de Catalunya (UPC), Spain

---

The flow confined between two concentric cylinders rotating with different velocity - Taylor-Couette flow - has been a paradigm to investigate fundamental non-linear dynamics, various hydrodynamic stabilities and pattern formation in fluid flows [1]. Although, classical fluids in this system setup (Taylor-Couette system, TCS) [2] have been studied for about hundred years the dynamics of complex fluids (e.g., ferrofluids [3]) have attracted attention mainly in recent years/modern era [4, 5, 7, 8]. A representative types of such complex fluids are ferrofluids, which are manufactured fluids consisting of dispersion of magnetized nanoparticles in a liquid carrier. A ferrofluid can be stabilized against agglomeration through the addition of a surfac- tant monolayer onto the particles. In the absence of any magnetic field, the nanoparticles are randomly orientated so that the fluid has zero net magnetization. In this case, the nanoparticles alter little the viscosity and the density of the fluid. Thus, in the absence of any external field a ferrofluid behaves as an ordinary (classical) fluid. However, when a magnetic field of sufficient strength is applied, the hydrodynamical properties of the fluid, such as the viscosity, can be changed *dramatically* [4, 9] and the dynamics can be vary altered. For instance, the magnetoviscous effect in ferrofluids is highly dependent on the orientation of the magnetic field with respect to the fluid flow. Studies indicated that, under a symmetry-breaking transverse magnetic field, all flow states in the TCS become intrinsically *three-dimensional* [6, 7], even increase the already huge number of flow states, known to exist in the TCS (being steady, time-independent or unsteady, time-dependent and its multiplicities).

This study treats with the influence of a *symmetry-breaking* transversal magnetic field on the nonlinear dynamics of ferrofluidic Taylor-Couette flow, consider axial periodic, counter-rotating cylinders with wide gap at low Reynolds number. We detected alternating 'flip' solutions (Fig. 1) which are flow states featuring typical characteristics of *slow-fast-dynamics* in dynamical systems. The flip corresponds to a temporal, periodic change in the axial wavenumber k and we find them to appear either as pure 2-fold axisymmetric (due to the symmetry-breaking nature of the applied transversal magnetic field) or involving non-axisymmetric, helical modes (flow contributions) in its interim solution. The latter ones show features of typical ribbon solutions. In any case the flip solutions have a preferential first axial wavenumber which corresponds to the more stable state (slow dynamics) and a second axial wavenumber, corresponding to the short appearing more unstable state (fast dynamics). However, in both cases the flip time grows exponential with increasing the magnetic field strength before the flip solutions, living on 2-tori invariant manifolds, cease to exist, with life-time going to infinity. Further we show that ferrofluidic flow turbulence differ from the classical, ordinary (usually at high Reynolds number) turbulence. The present/applied magnetic field *hinders* the *free motion* of ferrofluid partials and therefore 'smoothen' typical turbulent quantities and features so that speaking of mildly chaotic dynamics seems to be a more appropriate expression for the observed motion. The result is more a middle chaotic motion than typical high Reynolds number turbulence.

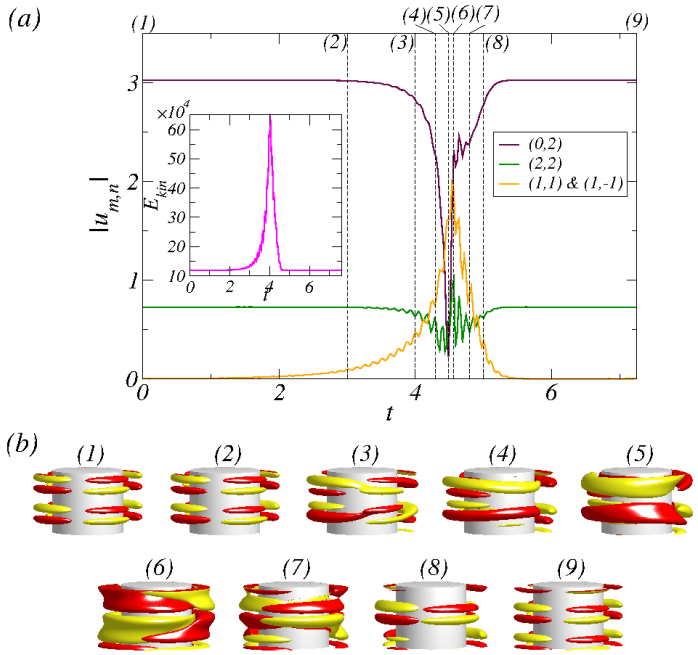

Figure 1: Visualization of the flip solution (slow-fast dynamics) 1-wTVF$^{\pi}_{2\pi}$. Shown are (a) dynamics with time of modes $|u_{m,n}|$ (inset shows E_{kin}) as indicated over a quarter period $\tau_p/4$ due to symmetries for $Re_i = 130$, $s_x = 0.7$ and times t as indicated. (b) presents corresponding visualisations for isosurfaces of $rv \pm 25$ [red (dark gray) and yellow (light gray) colors correspond to positive and negative values, respectively, of the flow structures during th 'flip' transition at times as indicated in (a).

References

[1] G. I. Taylor, *Stability of a viscous liquid contained between two rotating cylinders.* Philos. Trans. R. Soc. London A **223**, 289 (1923).

[2] C. D. Andereck, S. S. Liu, and H. L. Swinney, *Flow regimes in a circular Couette system with independently rotating cylinders.* J. Fluid Mech. **164**, 155 (1986).

[3] R. E. Rosensweig, *Ferrohydrodynamics.* Camb. University Press, Cambridge (1985).

[4] M. Niklas, *Influence of magnetic fields on Taylor vortex formation in magnetic fluids.* Z. Phys. B **68**, 493 (1987).

[5] H. W. Müller and M. Liu, *Structure of ferrofluid dynamics.* Phys. Rev. E **64**, 061405 (2001).

[6] S. Altmeyer, C. Hoffmann, A. Leschhorn, and M. Lücke, *Influence of homogeneous magnetic fields on the flow of a ferrofluid in the Taylor-Couette system.* Phys. Rev. E **82**, 016321 (2010).

[7] M. Reindl and S. Odenbach, *Effect of axial and transverse magnetic fields on the flow behavior of ferrofluids featuring different levels of interparticle interaction.* Phys. Fluids **23**, 093102 (2011).

[8] S. Altmeyer, Y.-H. Do, and Y.-C. Lai, *Transition to turbulence in Taylor-Couette ferrofluidic flow.* Sci. Rep. **5**, 10781 (2015).

[9] M. I. Shliomis, *Effective viscosity of magnetic suspensions.* Sov. Phys. JETP **34**, 1291 (1972).

Transient behavior between multi-cell flow states in ferrofluidic Taylor-Couette flow

Sebastian Altmeyer[1], Younghae Do[2], Soorok Ryu[2]

[1] Castelldefels School of Telecom and Aerospace Engineering (EETAC), Universitat Polytecnica de Catalunya (UPC), Spain

[2] Department of Mathematics, KNU-Center for Nonlinear Dynamics, Kyungpook National University, Daegu 41566, South Korea

---

We investigate transient behaviors induced by magnetic fields on the dynamics of the flow of a ferrofluid [1] in the gap between two concentric, independently rotating cylinders. Without applying any magnetic fields, we uncover emergence of flow states constituted by a combination of a localized spiral state in the top and bottom of the annulus and different multi-cell flow states with toroidally closed vortices in the interior of the bulk. However, when a magnetic field is presented, we observe the transient behaviors between multi-cell states passing through two critical thresholds in a strength of an axial (transverse) magnetic field [2]. Numerical simulations are carried out by solving the ferrohydrodynamical equation of motion using the Niklas approximation [3]. Before the first critical threshold of a magnetic field strength, multi-stable states with different number of cells can be observed. After the first critical threshold, we find the transient behavior between the three- and two-cell flow states. For stronger magnetic fields or after the second critical threshold, we discover that multi-cell states to disappear and a localized spiral state remains stimulated in the system.

Without applying any magnetic fields, we found the emergence of two flow states constituted by a combination of a localized spiral state (SPI_l) in the top and bottom of the annulus and different multi-cell flow states (SPI_{l+2v}, SPI_{l+3v}) with toroidally closed vortices in the interior of the bulk (SPI_{l+2v}= SPI_l + SPI_{2v} and SPI_{l+3v}= SPI_l + SPI_{3v}). The appearing of these multi-stable states is based on the initial conditions.

Applying any magnetic field and changing it's strength can trigger transitions among various flow states, for example, the two-cell and three-cell flow states. The emergence of the flow states, dynamical evolution, and transitions among the various flow states can be summarized in detail, as follows. By increasing the axial [transverse] magnetic field strength, we first identify a transition from SPI_{l+3v} [(SPI_{l+2v}] to SPI_{l+2v} [SPI_{l+3v}], respectively. However, for strong enough magnetic fields, we discover the second transition only leaving a SPI_l state behind.

Although the flow states under fairly large magnetic fields (s_x or s_z) are SPI_l, there is a significant difference between two final SPI_l states. For applying the strong transverse magnetic field (s_x), SPI_l is orientated close to top and bottom lid located in the Ekman vortex regime. But SPI_l under the strong axial magnetic field (s_z) is orientated more towards the center of the bulk. According to the different type of magnetic fields, SPI_l state can move to or away from the Ekman region.

As to expect, the transitions between the multi-cell flow states are always accompanied by a change in the wavelength and wavenumber, respectively. However, in the present study the symmetry breaking effect (a stimulated two-cell mode [4, 5]) of the transverse magnetic field is obviously present, but plays a significant minor role than in other studies. It becomes more and more pronounced for the larger magnetic field strength s_x and s_z.

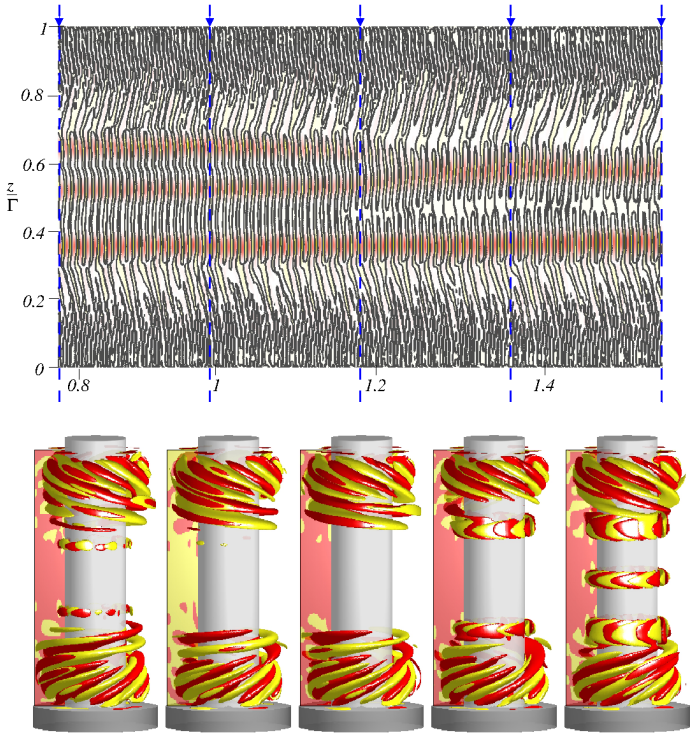

Figure 1: Transitions from SPIl_{l+3V} to SPI_{l+2V}. *Top:* Space-time plot of the azimuthal vorticity η during the transition at $r = r_1 + 0.1d$. Red (dark gray) and yellow (light gray) correspond to positive and negative values, with $\eta \in [-440, 440]$. *Bottom:* Snapshots of corresponding vortex structures during the transition.

References

[1] R. E. Rosensweig, *Ferrohydrodynamics*. Camb. University Press, Cambridge (1985).

[2] S. Altmeyer, Y. Do, and S. Ryu *Transient behavior between multi-cell flow states in ferrofluidic Taylor-Couette flow.* Chaos **27**, 113112 (2018).

[3] M. Niklas, *Influence of magnetic fields on Taylor vortex formation in magnetic fluids.* Z. Phys. B **68**, 493 (1987).

[4] S. Altmeyer, C. Hoffmann, A. Leschhorn, and M. Lücke, *Influence of homogeneous magnetic fields on the flow of a ferrofluid in the Taylor-Couette system.* Phys. Rev. E **82**, 016321 (2010).

[5] M. Reindl and S. Odenbach, *Effect of axial and transverse magnetic fields on the flow behavior of ferrofluids featuring different levels of interparticle interaction.* Phys. Fluids **23**, 093102 (2011).

On a new family of Tollmien-Schlichting Waves
20th International Couette-Taylor Workshop (ICTW20)

Roger Ayats[1], Alvaro Meseguer[1], Fernando Mellibovsky[2]

[1] Departament de Física, Universitat Politècnica de Catalunya, Jordi Girona 1-3–B5, 08034 Barcelona, Spain

[2] Castelldefels School of Telecom and Aerospace Engineering, Universitat Politècnica de Catalunya, Esteve Terradas 7–C3, 08034 Barcelona, Spain

---

Transition to turbulence in shear flows is still an open question that remains unsolved and far from completely being understood. Although it has been intensively studied, ever the simplest systems are still revealing unexpected solutions.

With the objective of understanding this transition in its simplest form, 2D Plane Poiseuille Flow (PPF, pressure-driven incompressible 2D flow between two infinite parallel plates) has been considered. It is governed by the Navier-Stokes equations assuming no-slip boundary conditions at the walls and periodic boundary conditions in the streamwise direction. For this particular case, constant mass flux is considered.

In particular, this system, which has been studied during decades, has several different solutions: subcritical bifurcation of its basic flow resulting in an *upper branch* (UB) and a *lower branch* (LB) of streamwise periodic solutions (Tollmien-Schlichting waves) [1, 2], superharmonic bifurcation of the UB solutions [3, 4, 5] and subharmonic bifurcation of streamwise localised wavepacket solutions [3, 4, 6].

Recent studies have evidenced the relevance of the role of the unstable LB travelling waves in the transition to turbulence (within the context of pipe Poiseuille flow [7, 8, 9, 10]). The present study focuses precisely on the new dynamics (symmetry breaking) that takes place in the LB of the Tollmien-Schlichting waves (TSW) in 2D PPF.

Arnoldi linear stability analysis carried out along wave length continuations of several travelling wave branches revealed a new family of TSW solutions. This new family is the result of a pitchfork bifurcation that breaks the usual half-period shift & reflect symmetry of the TSW. These new waves are henceforth referred to as *asymmetric* Tollmien-Schlichting waves (ATSW) and they are depicted in Figure 1.

Figure 1 (a) is the result of the aforementioned continuations at constant $Re = 10^4$ for both TSW (in grey) and ATSW (in black), where solid lines correspond to stable and dashed and dotted lines to unstable regions. Note that TSW-UB short-dashed line is an unstable region due to the superharmonic Hopf bifurcation (bullets), whereas LB long-dashed line is an unstable region due to the lower branch of the saddle node (squares) and simultaneously to the asymmetric pitchfork (triangles). Figure 1 (b) shows continuations for different values of constant wave number k (TSW in grey and ATSW colour coded).

It is worth mentioning that the ATSW branches contain different saddle node bifurcations which enable the existence of *stable solutions* inside them (see Figure 1). Furthermore, the saddle nodes found in the left TSW LB produce the same effect (see Figure 1 (a)). These results contradict the established idea that stable solutions can only be obtained from UBs and add more complexity into the problem.

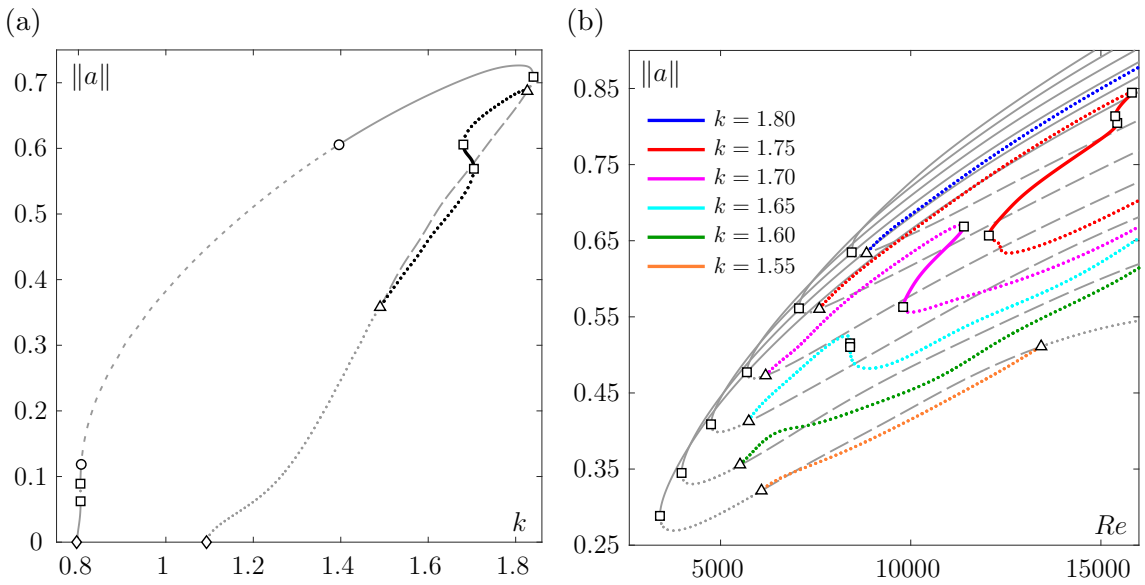

Figure 1: Continuation of both TSW and ATSW at constant $Re = 10^4$ (a) and at different values of constant wave number k (b). Solid, short-dashed, long-dashed and dotted lines denote stable, unstable superharmonic Hopf, double unstable saddle-pitchfork and LB unstable regions respectively. Squares, circles and triangles are saddle-node, Hopf and pitchfork bifurcation points. Diamonds at zero norm indicate subcritical bifurcations of the base flow.

In addition, recent Arnoldi linear stability analyses have revealed the existence of subharmonic Hopf bifurcations in the new ASTW branches if the lenght of the domain is increased.

An extension of the work presented by Mellibovsky and Meseguer [6] is being done in order to describe the role of these new ATSW solutions and understand if both symmetric and asymmetric families could lead to a streamwise snakes-and-ladders mechanism.

References

[1] Chen, T.S. and Joseph, D.D., J. Fluid Mech., **58**, 337-351, 1973.

[2] Zahn, J.P., Toomre, J., Spiegel, E.A. and Gough, D.O., J. Fluid Mech., **64**, 319-345, 1974.

[3] Jimenez, J., J. Fluid Mech., **218**, 265-297, 1990.

[4] Drissi, A., Net, M. and Mercader, I., Phys. Rev. E, **60**, 1781-1791, 1999.

[5] Casas, P.S. and Jorba, À., Comm. Nonl. Sci. Numer. Simul. , **17**, 2864-2882, 2012.

[6] Mellibovsky, F. and Meseguer, A., J. Fluid Mech., **779**, R1, 2015.

[7] Faisst, H. and Eckhardt, B., Phys. Rev. Letters, **91**, (22), 224502, 2003.

[8] Wedin, H. Kerswell, R.R., J. Fluid Mech., **508**, 333–371, 2004.

[9] Pringle, C.C.T. and Kerswell, R.R., Phys. Rev. Letters, **99**, 074502, 2007.

[10] Mellibovsky, F. and Meseguer, A., Phil. Trans. R. Soc. A, 2008.

Mayonnaise Taylor-Couette Turbulence

Dennis Bakhuis[1], Rodrigo Ezeta[1], Pim A. Bullee[1], Raymond H. J. Kip[1], Sander G. Huisman[1], Alvaro Marin[1], Detlef Lohse[1,3], Chao Sun[1,2]

[1] Physics of Fluids, Max Planck Institute for Complex Fluid Dynamics, MESA+ Institute and J. M. Burgers Center for Fluid Dynamics, University of Twente, P.O. Box 217, 7500 AE Enschede, The Netherlands

[2] Center for Combustion Energy and Department of Thermal Engineering, Tsinghua University, 100084 Beijing, China

[3] Max Planck Institute for Dynamics and Self-Organization, Am Fassberg 17, 37077 Go ttingen, Germany

---

It is well known that water and oil do not mix. Putting in some effort to mix the two will result in an emulsion of tiny oil droplets in water which is generally not stable and demixes quickly. By using the Twente Turbulent Taylor-Couette (T3C) apparatus [1], we continuously shear the mixture, Re= $\mathcal{O}(10^5)$, which becomes a dynamic equilibrium. A schematic of the setup is shown in figure 1a. The torque of the system is measured for oil volume fractions α between 0% and 100% and two different types of oil. The first oil has a viscosity ten times that of water. Figure 1b shows the system with $\alpha = 10\%$. The mixture is completely opaque due to tiny droplets of oil. We calculated the viscosity of the emulsion by assuming a Newtonian response of the system. Close to the inversion point (oil droplets in water change to water droplets in oil, or vice versa) the viscosity is much larger than the individual viscosities of the water and oil. This is due to a jamming behaviour of the tiny droplets that increase the apparent viscosity [2]. Using a second oil which has a viscosity similar to that of water, we can isolate this viscosity increase based on the droplet jamming and see if this has an effect on the inversion point.

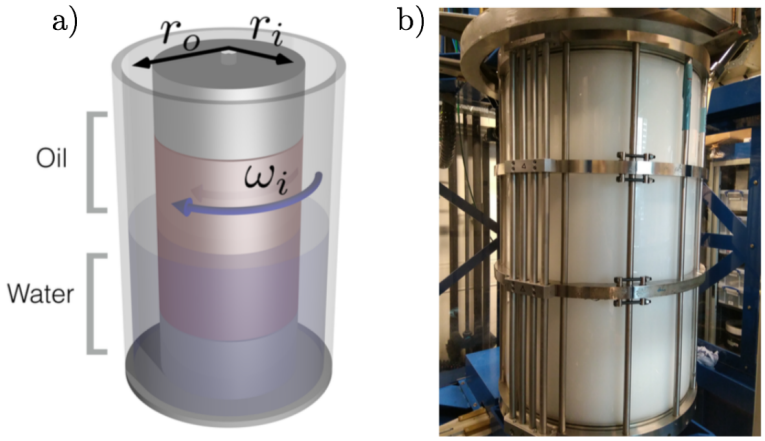

Figure 1: a) Schematic of the T^{3}C apparatus used for the experiments. The torque of the system is measured for various mixtures of water and oil. The separation of water and oil is only visible before the experiment. b) Picture of the system during an experiment using 10% of oil. The fluid is completely opaque due to microscopic oil droplets in the water.

References

[1] D.P.M. van Gils, G.W. Bruggert, D.P. Lathrop, C. Sun, and D. Lohse *The Twente turbulent Taylor-Couette (T3C) facility: Strongly turbulent (multiphase) flow between two independently rotating cylinders*, Rev. Sci. Instrum. **82**, 025105, 2011.

[2] S. R. Derkach *Rheology of emulsions*, Adv. Colloid Interface Sci. **151**, 1–23, 2009.

Acknowledgements

We would like to thank Ruben Verschoof and Pieter Berghout for various stimulating discussions. Also, we like to thank Gert-Wim Bruggert and Martin Bos for technical support. This work was funded by STW, FOM, ERC, and MCEC, which are part of the Netherlands Organisation for Scientific Research (NWO). Bakhuis and Sun acknowledges financial support from VIDI grant No. 13477. Sun acknowledges the Natural Science Foundation of China under Grant No. 11672156. Bullee acknowledges NWO-TTW (project 14504).

Spirals, ribbons and RZIF: frequency prediction from mean flows for counter-rotating Couette-Taylor flows

Yacine Bengana[1], Laurette Tuckerman[1],

[1] PMMH-CNRS, Sorbonne Université, ESPCI Paris France

A number of time-periodic flows have been found to have a property called RZIF: when a linear stability analysis is carried out about the temporal mean (rather than the usual steady state), an eigenvalue is obtained whose **Real** part is **Zero** and whose **Imaginary** part is the nonlinear **Frequency** [1]. In counter-rotating Couette-Taylor flow, a Hopf bifurcation gives rise to branches of the well-known spirals [2] and the somewhat lesser-known ribbons [3], which are an equal superposition of spirals moving axially upwards and downwards. Illustrations are shown in the left portion of figure 1. The spirals are traveling waves in both the axial z and azimuthal θ directions, while the ribbons are standing waves in z and traveling waves in θ, with functional forms for, e.g., the radial velocity

$$\begin{aligned} u^{\mathrm{SPI}\pm}(r,\theta,z,t) &= \sum_{k,m} \hat{u}^{\mathrm{SPI}}_{km}(r)\, e^{i(\pm k\alpha z + mM_0\theta - \omega_{\mathrm{SPI}}t)} + \text{c.c.} \\ u^{\mathrm{RIB}}(r,\theta,z,t) &= \sum_{k,m} \hat{u}^{\mathrm{RIB}}_{km}(r)\, \sin(k\alpha z)\, e^{i(mM_0\theta - \omega_{\mathrm{RIB}}t)} + \text{c.c.} \end{aligned}$$

We use a spectral finite-difference code [4] to solve the Navier-Stokes equations in a cylindrical geometry with resolution $(N_r, N_\theta, N_z) = (33, 16, 16)$. The parameters we use are those of [5]: radius ratio $\eta \equiv r_{\mathrm{in}}/r_{\mathrm{out}} = 0.5$, axial and azimuthal wavenumbers $\alpha = 2\pi/1.2$ and $M_0 = 2$, and inner Reynolds number $Re_{\mathrm{in}} = 240$. For these parameters, branches of spirals and ribbons bifurcate at $Re_{\mathrm{out}} \approx -586$ towards increasing Re_{out}. Their temporal means are equal to the azimuthal means and are shown in the right portion of figure 1. Linearizing about these mean flows leads to the results shown in figure 2. Both the spiral and the ribbon branches are seen to have the RZIF property: the imaginary parts of the eigenvalues are very close to their respective nonlinear frequencies and the real parts are close to zero.

References

[1] D. Barkley, Europhys. Lett., **75** 750, 2006; S.E. Turton, L.S. Tuckerman, D. Barkley, Phys. Rev. E, **91**, 043009, 2015.

[2] E.R. Krueger, A. Gross, R.C. Di Prima. J. Fluid Mech., **24**, 521–538, 1966; W.F. Langford, R. Tagg, E.J. Kostelich, H.L. Swinney, M. Golubitsky. Phys. Fluids, **31**,776–785, 1988; J. Antonijoan, F. Marquès, J. Sanchez, Phys. Fluids, **10**, 829–838, 1998.

[3] R. Tagg, W.S. Edwards, H.L. Swinney, P.S. Marcus, Phys. Rev. A, **39**, 3734, 1989; P. Chossat, G, Iooss, *The Couette-Taylor Problem*, Springer, 1994.

[4] A.P. Willis, *The Openpipeflow Navier–Stokes solver*, SoftwareX **6**, 124–127, 2017.

[5] A. Pinter, M. Lücke, C. Hoffmann, Phys. Rev. Lett., **96**, 044506, 2006; Phys. Rev. E, **78**, 017303, 2008; C. Hoffmann, S. Altmeyer, A. Pinter, and M Lücke, New J. Phys., **11**, 053002, 2009.

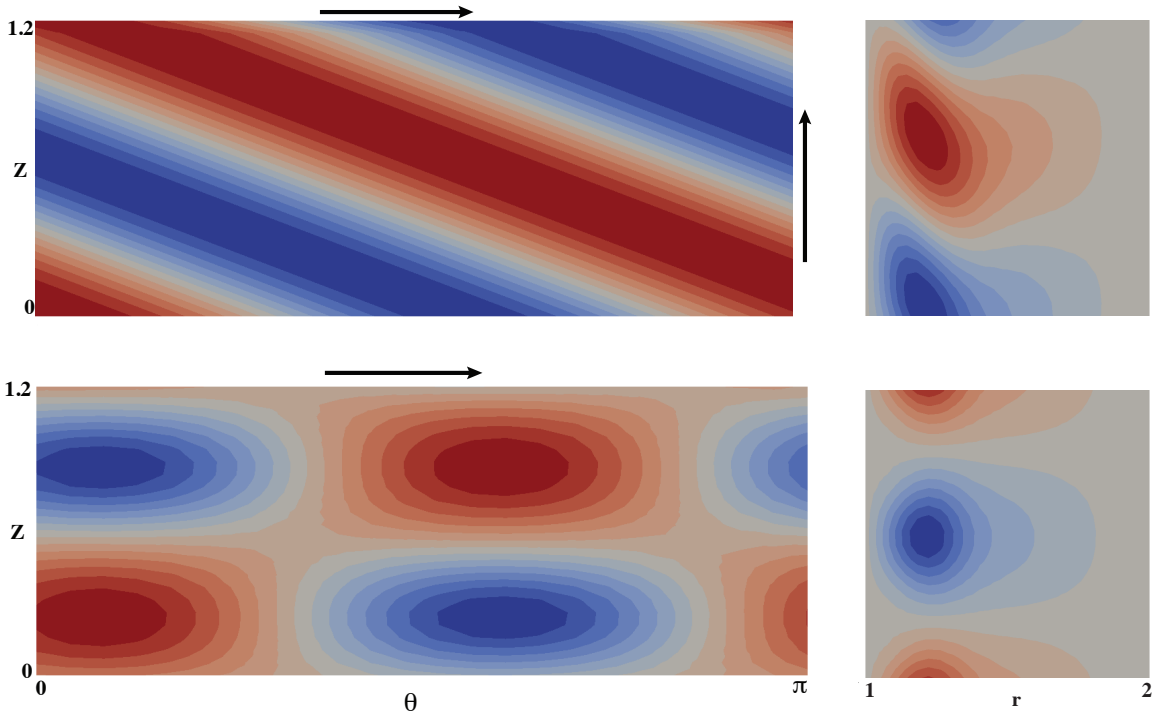

Figure 1: Upward-moving spirals (top) and ribbons (bottom). Left: Instantaneous flow visualized via radial velocity in (θ, z) view at mid-gap. Right: Mean flow visualized via azimuthal velocity in (r, z) view.

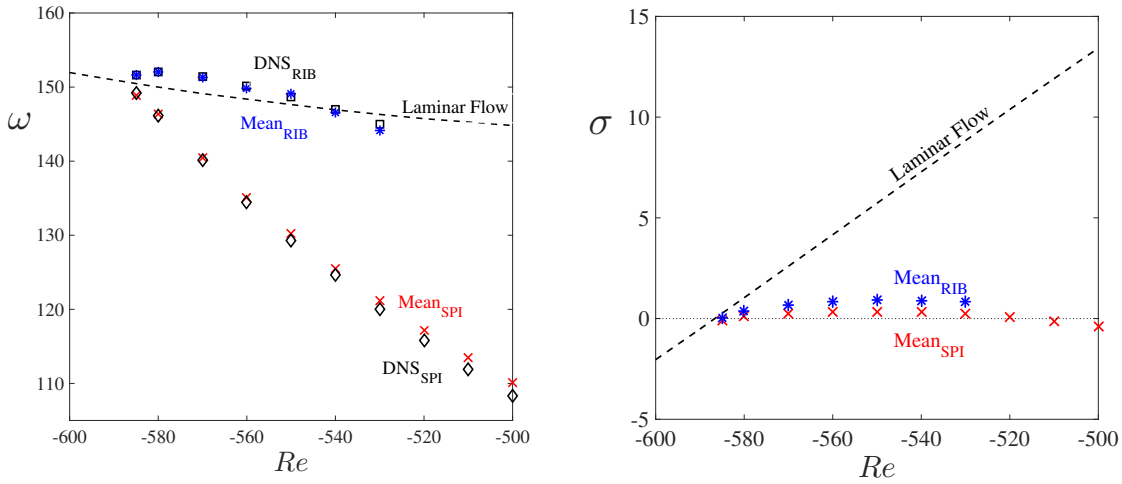

Figure 2: Frequencies (left) and growth rates (right). Nonlinear frequencies from DNS are shown as squares (for ribbons) and diamonds (for spirals). Imaginary parts of eigenvalues resulting from linearizing about the mean flow of ribbons (blue stars) and spirals (red crosses) match the nonlinear frequencies. Real parts of these eigenvalues are near zero. Frequencies and growth rates from linearization about laminar Couette flow are shown as dashed lines.

Dynamics and transport of a solute in Taylor-Couette flow bounded by permeable walls

Rouae BEN DHIA[1], Denis MARTINAND[1], Nils TILTON[2]

[1] Aix-Marseille Univ., CNRS, Centrale Marseille, M2P2, France

[2] Mechanical Engineering, Colorado School of Mines, CO 80401, USA

Performances of filtration techniques are known to deteriorate with the accumulation of retained materials near the semi-permeable membranes. In the case of a solution considered here, the osmotic pressure induced by the concentration boundary layer forming near the membrane tends to cancel out the operating pressure driving the permeate flux accross the device. Dynamic filtration devices make use of hydrodynamic instabilities to mix the solution and abate the concentration boundary layer. However, no quantitative results exist to assess the couplings between mixing, osmotic pressure and instabilities, the effectiveness of dynamic filtration and how to optimize it.
This study adresses those couplings in a controled fashion by considering a Taylor-Couette cell, with a fixed outer cylinder and a rotating inner one. Moreover, the gap is filled with a solution and both cylinders are semi-permeable membranes totally rejecting the solute. Imposing an operating pressure accross the gap drives a radial in- or outflow and the transmembrane flow of pure solvent builds up a concentration boundary layer near the inner or outer cylinder. The osmotic pressure related to the concentration increase at the membrane then opposes the operating pressure and reduces the radial flow. For fixed operating conditions, a stationary state can be obtained analytically(figure 1a).

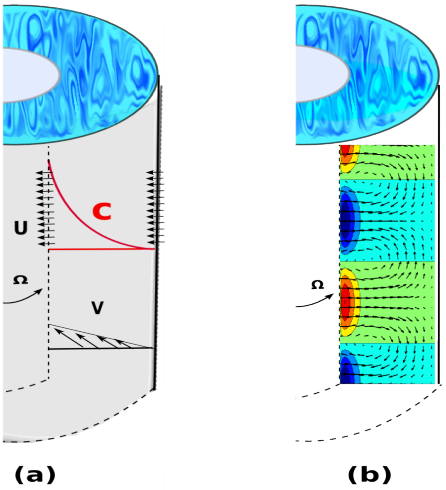

Figure 1: Figure of studied situation: a) Configuration and sketch of the base state (U,V : radial and azimuthal velocity components, C : concentration profile), b) Perturbation to this base state in a meridional plane.

As the rotation rate of the inner cylinder is increased, centrifugal instabilities emerge in the form of toroidal vortices. These instabilities are studied both analytically (figure 1b), using the previous stationary state as a base state, and numerically, using dedicated Direct Numerical Simulations implementing accurate boundary conditions for the transmembrane flow and pressure. Osmotic pressure is found to promote these centrifugal instabilities as a result of an original self-sustained mechanism coupling the advection of the concentration boundary layer by the vortices, molecular diffusion and osmotic pressure driving a transmembrane flow fostering the vortices. This mechanism can induce a substantial reduction of the critical rotation rate above which vortices are observed.

Direct Numerical Simulations of a Finite–Wavelength Modulation within Taylor–Couette Flow

Pieter Berghout[1], Rick Dingemans[1], Xiaojue Zhu[1], Roberto Verzicco[1,2], Richard J.A.M. Stevens[1], Wim van Saarloos[4], Detlef Lohse[1,3]

[1] Physics of Fluids Group and Max Planck Center Twente, MESA+ Institute and J. M. Burgers Centre for Fluid Dynamics, University of Twente, P.O. Box 217, 7500AE Enschede, Netherlands

[2] Dipartimento di Ingegneria Industriale, University of Rome 'Tor Vergata', Via del Politecnico 1, Roma 00133, Italy

[3] Max Planck Institute for Dynamics and Self-Organisation, 37077 Göttingen, Germany

[4] Instituut-Lorentz, Universiteit Leiden, Postbus 9506, 2300 RA Leiden, The Netherlands

---

In this talk we will present Direct Numerical Simulations (DNS) of counter rotating Taylor–Couette (TC) flow at low Reynolds numbers. We simulate a radius ratio of $\eta = r_i/r_0 = 0.91$ and a large aspect ratio of $\Gamma = L/d = 64$. In particular we investigate the part of the TC parameter space [1] in which we find the turbulent spiral structure, see Figure 1. In analogy to the very high radius ratio ($\eta = 0.98$) experiments [2], we too observe a turbulence intensity modulation of the finite–wavelength pattern for varying inner cylinder Reynolds number, which fits the phenomenology of the Ginzburg-Landau equations [3]. We find similar modulations of the pressure field and the turbulence intensity with varying outer cylinder rotation. In pursuit of a better understanding of this pattern, we also study the behavior of the instability curve for varying inner cylinder Reynolds number.

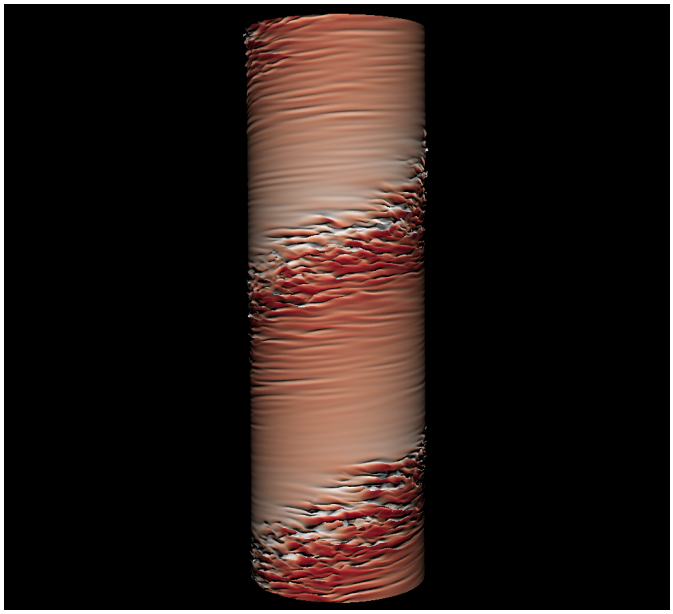

Figure 1: A snapshot of the azimuthal velocity (v_θ) at the $r = r_i + d/2$ exhibits a turbulent spiral structure. Aspect ratio $\Gamma = L/d = 64$ and radius ratio $\eta = r_i/r_0 = 0.91$.

References

[1] C. D. Andereck, S. S. Liu, H. L. Swinney. Flow regimes in a circular Couette system with independently rotating cylinders. J. Fluid Mech. (1986), vol.164, pp. 155–183

[2] A. Prigent, G. Grégoire, H. Chaté, O. Dauchot, W. Saarloos. Large-Scale Finite-Wavelength Instability within Turbulent Shear Flow. Physical Review Letters, 89, 14501 - (2002).

[3] M. Cross, H. Greenside. Pattern Formation and Dynamics in Nonequilibrium Systems. Cambridge: Cambridge University Press. (2009)

Acknowledgements

This project is funded by the Priority Programme SPP 1881 Turbulent Superstructures of the Deutsche Forschungsgemeinschaft. We also acknowledge PRACE for awarding us access to Marconi, based in Italy at CINECA under PRACE project number 2016143351. This work was partly carried out on the national e-infrastructure of SURFsara, a subsidiary of SURF cooperation, the collaborative ICT organization for Dutch education and research.

The effect of spanwise rotation on turbulence and passive scalar transport in channel flow

Geert Brethouwer[1]

[1] Linné FLOW Centre, KTH Mechanics, SE-100 44 Stockholm, Sweden

---

Turbulent channel flow subject to spanwise system rotation has been studied by DNS [**?**]. The Reynolds number $Re = U_b h/\nu$ is varied from a low 3000 to a moderate 31 600 and the rotation number $Ro = 2\Omega h/U_b$ is varied from 0 to 2.7 corresponding to very rapid rotation. Here, U_b is the mean bulk velocity, h the channel half gap and Ω the system rotation rate. The mean streamwise velocity profile U displays also at higher Re the characteristics linear part with a slope $dU/dy \approx 2\Omega$ corresponding to an absolute mean vorticity equal to zero. With increasing Ro a distinct unstable side with large spanwise and wall-normal Reynolds stresses and a stable side with much weaker turbulence develops in the channel and the flow starts to relaminarize. Persisting turbulent-laminar patterns emerge at higher Re (Figure **??**). If Ro is further increased the flow on the stable side becomes laminar-like while at yet higher Ro the whole flow relaminarizes, although the calm periods might be disrupted by repeating bursts of turbulence caused by a linear instability of Tollmien-Schlichting-like waves [**?**], see Figure **??**. The influence of Re is considerable, in particular on the stable side of the channel where velocity fluctuations are stronger and the flow relaminarizes less quickly at higher Re. Visualizations and spectra show that at $Ro = 0.15$ and 0.45 large counter-rotating streamwise roll cells develop on the unstable side at low and high Re. These become smaller and eventually vanish when Ro increases, especially at higher Re.

In some of the DNS a passive scalar was included to study the effect of rotation on passive scalar transport [**?**]. In these DNS Re is fixed at 20 000 and Ro is varied from 0 to 1.2. The scalar is constant but different at the two walls, leading to steady scalar transport across the channel. The distinct turbulent-laminar patterns observed at certain Ro on the stable channel side induce similar patterns in the scalar field. On the unstable channel side the streamwise turbulent scalar flux is strongly reduced due to rotation and this leads to an alignment between the turbulent scalar flux vector and mean scalar gradient. On the stable channel side rotation strongly reduces the wall-normal turbulent scalar transport. The main conclusions of the study are that rotation reduces the similarity between the scalar and velocity field and that the Reynolds analogy for scalar-momentum transport does not hold for rotating turbulent channel flow. This follows from a reduced correlation between velocity and scalar fluctuations, and a strongly reduced turbulent Prandtl number of less than 0.2 on the unstable channel side away from the wall at higher Ro (Figure **??**). Scalar scales also become larger than turbulence scales on the unstable side according to spectra and two-point correlations.

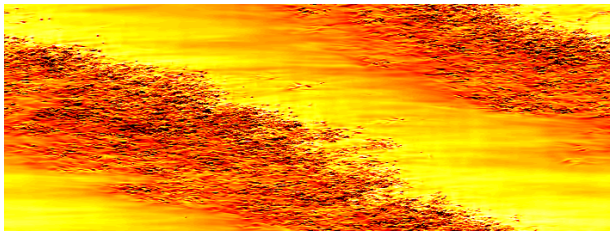

Figure 1: Streamwise flow field on the stable channel side in a plane parallel and close to the wall at $Re = 20\,000$ and $Ro = 0.45$.

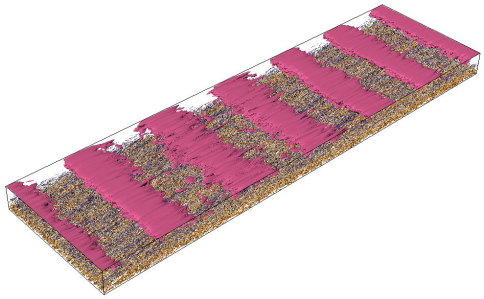

Figure 2: Contours of instantaneous positive wall-normal velocity (magenta) showing TS-like waves on the stable channel side and vortices (blue to yellow) on the unstable side at $Re = 31600$ and $Ro = 1.2$.

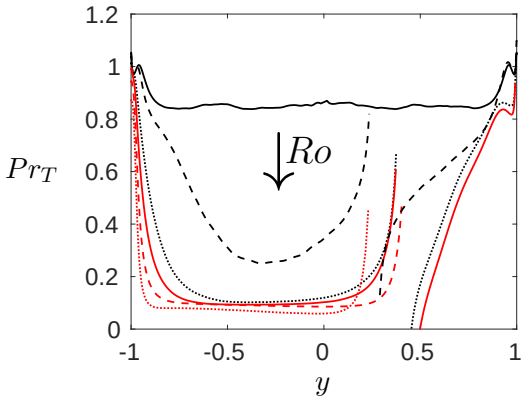

Figure 3: Turbulent Prandtl number Pr_T as function of Ro.

References

[1] G. Brethouwer, *Linear instabilities and recurring bursts of turbulence in rotating channel flow simulations*, Phys. Rev. Fluids. **1**, 054404, 2016.

[2] G. Brethouwer, *Statistics and structure of spanwise rotating turbulent channel flow at moderate Reynolds numbers*, J. Fluid Mech. **828**, 424-458, 2017.

[3] G. Brethouwer, *Passive scalar transport in rotating turbulent channel flow*, J. Fluid Mech. **844**, 297-322, 2018.

Particle separation in a narrow-gap Taylor-Couette setup

Philipp Brockmann[1], Hamid Tabaei Kazerooni[1,2], Luca Brandt[2] Jeanette Hussong[1]

[1] Laboratory for Laser-Measurement Technique in Multiphase Flows (LLMM), Institute of Thermo- and Fluiddynamics, Ruhr University Bochum (RUB), Germany

[2] SeRC and Linne FLOW Centre, KTH Mechanics, Stockholm, Sweden

---

It is known that suspended particles in rotating horizontal drum and free surface Taylor-Couette (TC) flows accumulate in band-shaped patterns at specific operation conditions. The existence of this so-called particle banding-phenomenon in a completely filled rotating horizontal drum was first discoverd by Lipson [1] for a dilute suspension of settling crystals. This phenomenon was also observed by Tirumkudulu et al. [2] in a partially filled TC flow laden with neutral buoyant particles. Different numerical and experimental studies have been conducted since then to investigate this phenomenon. However, the driving hydrodynamic mechanism responsible for the formation of the bands is not fully understood yet. In the present work, we report the observation of particle banding for a dilute suspension of settling particles in a fully filled horizontally aligned narrow-gap (1 mm) TC flow. In particular, we observed an almost complete separation of suspended non-neutrally buoyant particles with different sizes to multiple bands in a laminar Couette flow. Figure 1a shows a snapshot of this phenomenon where particles separate based on their size and form a symmetric pattern. Furthermore, in a monodisperse suspension, we observed that a single particle band decomposed to multiple stripes when the rotation axis of flow is inclined with respect to horizon (Fig.1b).

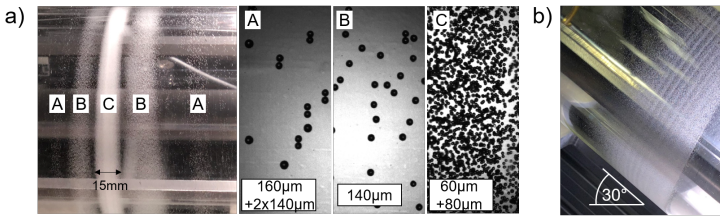

Figure 1: Particle bands in the TC cell. a) particle separation effect, b) striped bands at an inclination angle of 30 degrees.

To investigate particle dynamics and underlying hydrodynamic effects, an Astigmatism-based Particle-Tracking-Velocimetry (APTV) procedure was developed based on Cierpka et al. (2010). This method is suitable to determine the out-of plane position of large microparticles ($d_p > 60\mu m$) with an accuracy of less than 30 percent of the particle radius. The main difference compared to previous works is that particles are illuminated in a brightfield mode, such that each particle act as a ball lens yielding a focal point of light rays passing through it. Due to its curvature, the outer cylinder of the TC setup acts as a cylindrical lens which induces astigmatism and changes the shape of this focal point from circle to ellipsoid based on the location of particles along the gap. The shape of this focal point is very sensitive to

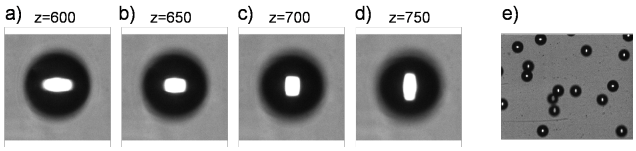

Figure 2: (a- d) Evolution of the aspect ratio of the focal point of a particle with $d_p = 196\mu m$ located at the inner cylinder, e) image of particles in the TC rig ($d_p = 148\mu m$).

the out-of-plane position of the particles and is the key parameter to reconstruct the particle location (Fig. 2 a-d).

Finally, a unique TC-facility was built to achieve optimal conditions for calibrating the APTV-technique and to measure the particle and flow velocities, as well as the radial particle concentration in any desired azimuthal and axial position (Fig. 3). The setup is designed in such a way that the orientation of the rotation axis can be varied with respect to horizon which enable us to explore the effect of gravity on the banding phenomenon.

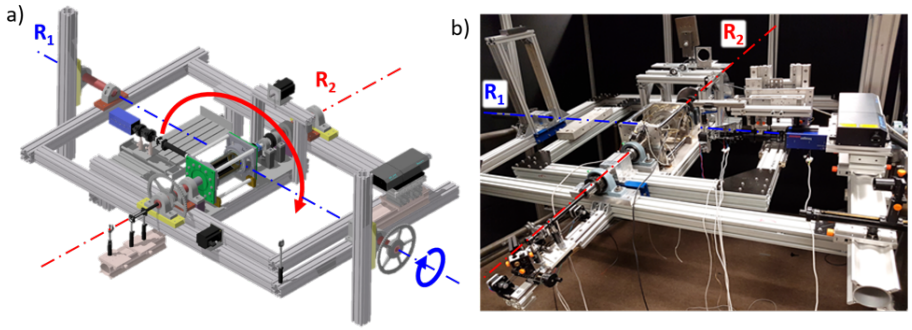

Figure 3: a) Schematic sketch of TC facility illustrating the degrees of freedom, b) picture of current state of the setup with highlighted degrees of freedom.

References

[1] S. G. Lipson, *Periodic banding in crystallization from rotating supersaturated solutions.*, Journal of Physics: Condensed Matter **13(21)**, 507-509, 2001.

[2] M. Tirumkudulu, A. Tripathi, A. Acrivos, *Particle segregation in monodisperse sheared suspensions.*, Physics of Fluids **11(3)**, 507-509, 1999.

[3] C. Cierpka, R. Segura, R. Hain, C. J. Kaehler, C. J. (2010), *A simple single camera 3C3D velocity measurement technique without errors due to depth of correlation and spatial averaging for microfluidics*, Measurement Science and Technology, **21(4)**, 045401, 2001.

Drag reduction in Taylor–Couette turbulence with a superhydrophobic inner cylinder

Pim A. Bullee,[1,2] Ruben A. Verschoof,[1] Dennis Bakhuis,[1] Sander G. Huisman,[1] Chao Sun,[1,3] Rob G. H. Lammertink[2] and Detlef Lohse[1,4]

[1] Physics of Fluids, Max Planck Institute for Complex Fluid Dynamics, MESA+ Institute and J. M. Burgers Center for Fluid Dynamics, University of Twente, P.O. Box 217, 7500 AE Enschede, The Netherlands

[2] Soft matter, Fluidics and Interfaces, MESA+ Institute for Nanotechnology, University of Twente, P.O. Box 217, 7500 AE Enschede, The Netherlands

[3] Center for Combustion Energy and Department of Thermal Engineering, Tsinghua University, 100084 Beijing, China

[4] Max Planck Institute for Dynamics and Self-Organization, Am Fassberg 17, 37077 Göttingen, Germany

---

In this research, we investigate a highly turbulent flow over a non-wetting surface of micro-scale roughness. To accurately measure drag and to visualize the flow we use the Taylor–Couette geometry. For this study, the inner cylinder is rotating, whereas the outer cylinder is kept stationary. The gap-width based Reynolds number is $\mathcal{O}(10^6)$. The inner cylinder is coated with a rough, hydrophobic material. We vary the void fraction of air α present in the working fluid to introduce bubbles to the flow. For smaller volume fractions of air, up to $\alpha \leq 2\%$, we see that the increased surface roughness from the coating also increases the drag. For larger fractions of air, $\alpha > 2\%$, the drag decreases compared to a smooth hydrophilic, uncoated cylinder using the same volume fraction of air. This suggests that two mechanisms play a role: the roughness that increases the drag and the more effective drag-reducing mechanism of the superhydrophobic surface. The balance between these effects determines if bubble drag reduction is more effective when using a superhydrophobic surface compared to using a smooth hydrophilic surface.

Acknowledgements

We thank Dennis van Gils, Gert-Wim Bruggert, Martin Bos, Jan van Nieuwkasteele and Ineke Punt for their technical support. The work was financially supported by NWO-TTW (project 14504). Verschoof acknowledges NWO-TTW (project 13265). Huisman acknowledges financial support from MCEC. Sun and Bakhuis acknowledge financial support from VIDI grant No. 13477, and the Natural Science Foundation of China under grant no. 11672156.

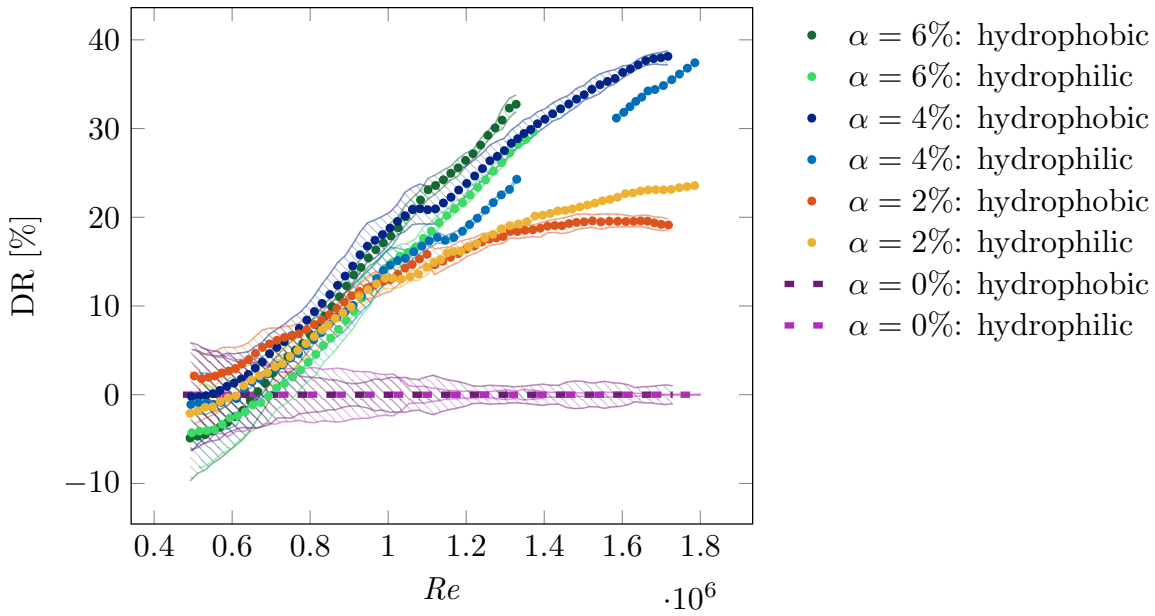

Figure 1: Skin friction drag reduction (DR) results from torque measurements. DR is defined as the ratio in skin friction coefficient between bubbles ($\alpha > 0$) and no bubbles ($\alpha = 0$): $\mathrm{DR} = 1 - (C_f(\alpha)/C_f(0))$. Compared is an uncoated, *hydrophilic*, smooth inner cylinder, to a coated, *hydrophobic* inner cylinder with micro-scale roughness. Different void fractions of air α are studied under Reynolds numbers increasing between 0.5×10^6 and 1.7×10^6. The data are an average of at least four measurements, with extremes denoted by the error bar area.

High-speed standard magneto-rotational instability

Kengo Deguchi[1],

[1] School of Mathematical Sciences, Monash University, Victoria 3800, Australia

---

The magneto-rotational instability (MRI), found by Velikhov (1959) and Chandrasecher (1961), could destabilise hydrodynamically stable flows by an imposed magnetic field. The work by Balbus & Hawley (1991) popularised this instability among astrophysicists as this could possibly explain the origin of the mysterious instability seen in certain astrophysical objects obeying Kepler's law, which is hydrodynamically stable. The instability has been tested in Taylor-Couette flow by numerous researchers as summarised in the recent review by Rudiger et al. (2017). While the general trend of the neutral curves is well-understood, it may be worth to consider the large Reynolds number limit of them because the Reynolds number of astrophysical flows is indeed quite large. Here we use the method of matched asymptotic analysis to find the mathematical asymptotic limit of the neutral curves.

In most of the previous theoretical studies 'locally periodic approach' has been employed assuming asymptotically short wavelengths of perturbations. However, they do not produce accurate approximation of the neutral curve because that assumption is not valid for the most dangerous perturbation. In fact, there are two important ingredients missing in those analyses: (i) the effect of boundary conditions, (ii) the effect of curvature.

Our analysis begins by considering the narrow gap limit of Taylor-Couette flow which is merely a rotating channel flow. The locally periodic result can be obtained when the periodic boundary conditions are used at the walls. Using the no-slip and perfectly conducting or insulating boundary conditions, we shall highlight the similarities and differences to the locally periodic case. The results are compared with the numerical solutions of full resistive magneto-hydrodynamic equations.

Then the theory is extended to the fully wide-gap Taylor-Couette flows (the radius ratio η, the inner and outer Reynolds numbers R_i, R_o). In particular, here it is found that the neutral solution branch asymptotically approaches to a line in the R_o–R_i parameter space

$$R_i = \frac{C + P_m^2 B_0^2 \eta^2}{\eta(C + P_m^2 B_0^2)} R_o$$

which exists between the Rayleigh line and solid-body rotation line. Here C is a function of η and obtained by the numerical computation of the asymptotically reduced equations. This means that the multiple of the magnetic Prandtl number and the imposed non-dimensional axial magnetic field strength, $P_m B_0$, should be larger than some critical value in order to observe the MRI at the quasi-Kepler rotation.

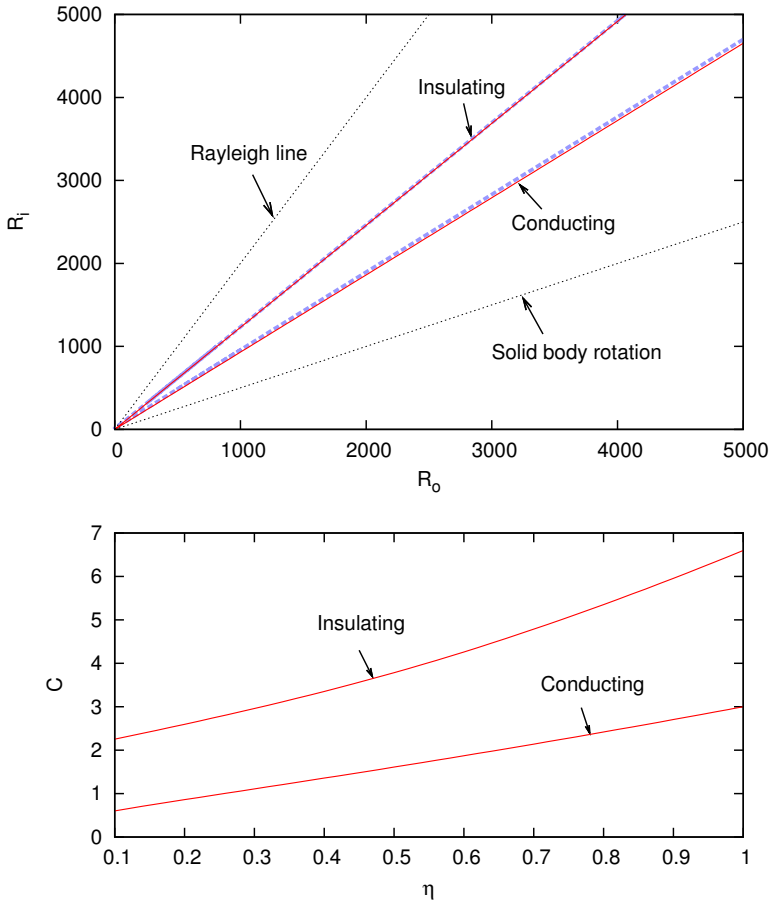

Figure 1: Upper: The neutral curve of Taylor-Couette flow between perfectly conducting or insulating cylinders with the radius ratio $\eta = 0.5$. A constant axial magnetic field $B_0 = 2$ is imposed. The magnetic Prandtl number is unity. The thick blue dashed curves are the full numerical solutions, while the thin red lines are the asymptotic results. Lower: the value of C found by the asymptotic analysis.

References

[1] E. P. Velikhov, *Stability of an ideally conducting liquid flowing between cylinders rotating in a magnetic field*, J. Expl. Theoret. Phys. (USSR) **36**, 1398-1404, 1959.

[2] S. Chandrasekhar, *Hydrodynamic and Hydromagnetic stability*, Clarendon. 1961.

[3] S. Balbus, J. Hawley, *A powerful local shear instability in weakly magnetized disks. I. Linear analysis*, ApJ **376**, 214-222, 1991.

[4] G. Rudiger, G. Marcus, R. Hollerbach, M. Schultz, F. Stefani *Stability and instability of hydromagnetic Taylor-Couette flows*, Physics Reports **741**, 1-89, 2018.

Acknowledgements

This work is supported by Australian Research Council Australian Discovery Early Career Award DE170100171 funded by the Australian Government.

Instability of a quasi-periodic pulsed Taylor-Couette flow

DENNI Chaimaa[1], ANISS Said[1], ELJAOUAHIRY Abdelouahab[1]

[1] University of Hassan II, Faculty of Sciences Aïn-Chock, Laboratory of Mechanic, B.P.5366 Maarif, Casablanca, Morocco. chaimaadenni@gmail.com

Abstract:

In the present work, a linear stability analysis of a pulsed Taylor-Couette flow is investigated in a quasi-periodic situation, where the inner and the outer cylinders oscillating respectively with the angular velocities $\Omega_o \cos(\omega_1 t)$ and $\Omega_o \cos(\omega_2 t)$, here ω_1 and ω_2 are two incommensurate frequencies. We study the influence of the frequency ratio, $\omega = \frac{\omega_2}{\omega_1}$, on the critical parameters (Taylor number and wave number). The numerical results show that the modulation with two incommensurate frequencies has a stabilizing or destabilizing effect with respect to the periodic case, where the two frequencies are considered equal.

1 Introduction

The stability of a periodic basic flow in Taylor-Couette geometry, with zero mean angular velocity, has been considered in [1] and [2], respectively in the case where the inner cylinder is fixed and the outer cylinder is oscillating periodically and in the case where the two cylinders are modulated in phase or in out of phase. Subsequently, Aouidef et *al.* [3] studied theoretically and experimentally the stability of periodic flow in the case where the inner and outer cylinders oscillate with the same modulated angular velocity. In contrast to these works, we perform in this paper a linear stability analysis of the pulsed Taylor-Couette flow in a quasi-periodic situation. The numerical resolution is done using spectral method for spatial resolution [4] and Runge-Kutta method for temporal resolution.

2 Linear stability analysis

We consider an incompressible fluid filling the annulus between two infinitely long cylinders subject to the boundary conditions $\Omega_1(r = R_1) = \Omega_o \cos(\omega_1 t)$ and $\Omega_2(r = R_2) = \Omega_o \cos(\omega_2 t)$. By assuming $R_2 - R_1 << R_1$, the basic flow is given by

$$\rho \frac{\partial v_B}{\partial t} = \mu \frac{\partial^2 v_B}{\partial x^2} \tag{1}$$

$$v_B(x,t) = F_1(x)\cos(\omega_1 t) + F_2(x)\sin(\omega_1 t) + G_1(x)\cos(\omega_2 t) + G_2(x)\sin(\omega_2 t) \tag{2}$$

The expressions $F_1(x)$, $F_2(x)$, $G_1(x)$ and $G_2(x)$ are

$$F_1(x) = \frac{\cos(\gamma_1 x)\cosh(\gamma_1(2-x)) - \cosh(\gamma_1 x)\cos(\gamma_1(2-x))}{\cosh(2\gamma_1) - \cos(2\gamma_1)} \quad ; \quad F_2 = \frac{1}{\omega_1}\frac{d^2 F_1}{dx^2}$$

$$G_1(x) = \frac{\cos(\gamma_2(1-x))\cosh(\gamma_2(1+x)) - \cosh(\gamma_2(1-x))\cos(\gamma_2(1+x))}{\cosh(2\gamma_2) - \cos(2\gamma_2)} \quad ; \quad G_2 = \frac{1}{\omega_2}\frac{d^2G_1}{dx^2}$$

where $\gamma_1 = \sqrt{\frac{\omega_1}{2}}$ and $\gamma_2 = \sqrt{\frac{\omega_2}{2}}$

The axisymmetric disturbances are considered with a perturbed velocity field as

$$(u(x,t), v(x,t), w(x,t))) = (\widehat{u}(x,t), \widehat{v}(x,t), \widehat{w}(x,t))\, exp(ikz) \tag{3}$$

After linearization of the Navier-Stokes equations and elimination of the pressure and vertical velocity component w, we obtain the equations for the components u and v

$$\begin{cases} (\frac{\partial^2}{\partial x^2} - k^2 - \frac{\partial}{\partial t})M\widehat{u} = 2k^2Ta^2 v_B \widehat{v} \\ (\frac{\partial^2}{\partial x^2} - k^2 - \frac{\partial}{\partial t})\widehat{v} = \widehat{u}\frac{\partial v_B}{\partial x} \end{cases} \tag{4}$$

where k is the wave number and $Ta = \frac{R_1\Omega_0 d}{\nu}\sqrt{\frac{d}{R_1}}$ is the Taylor number. The associated boundary conditions are

$$\widehat{u} = \widehat{v} = \frac{\partial \widehat{u}}{\partial x} = 0 \qquad at \;\; x = 0, 1 \tag{5}$$

3 Results and discussion

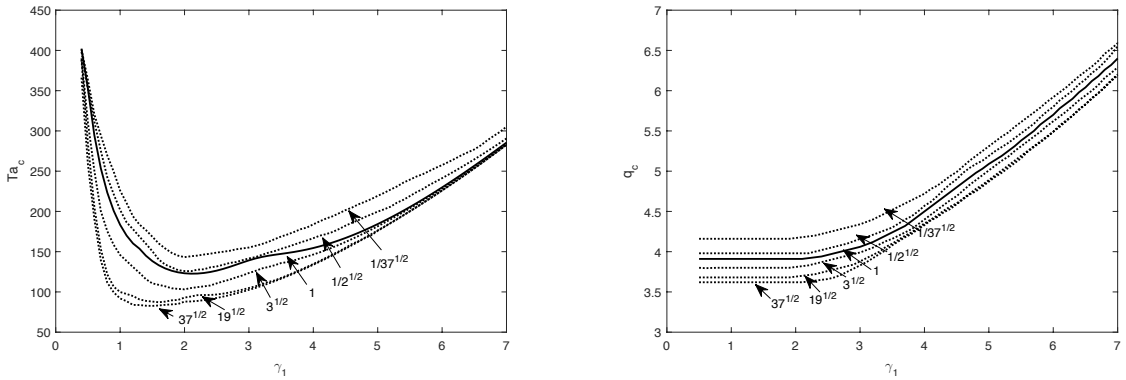

Figure 1: Critical Taylor number and wave number versus the frequency for different values of the frequency ratio, ω

The critical Taylor number and wave number as a function of γ_1 for different values of frequency ratio ω are reported in Figure 1. In the low frequency limit, ($\gamma < 1$), the Taylor number decreases with increasing ω and for intermediate frequency, the flow remains potentially unstable for an intermediate frequency γ_p. The critical Taylor number increases when ω decreases and also the critical wave number decreases. According to the numerical results, the frequency ratio has a stabilizing or a destabilizing effect compared to the situation of Aouidef et *al* [3], corresponding to $\omega = 1$. Regarding the critical wave number, it remains constant for low frequencies and it starts to increase from $\gamma_1 = 3$. We also find that for a fixed value of the frequency, the critical wave number increases when ω decreases.

References

[1] P. J. Riley and R. L. Laurence. *Linear stability of modulated circular couette flow*, J. Fluid Mech, 75,625, 1976.

[2] S. Carmi and J. I. Tustaniwskyj. *Stability of modulated finite-gap cylindrical Couette flow: linear theory*, J. Fluid Mech.43, 108, 19, 1981.

[3] A. Stegner, A .Aouidef, C. Normand and J. E. Wesfreid. *Centrifugal instability of pulsed flow* , American Institute of Physics, 1994.

[4] J. A. C. Weideman. S. C. Reddy. *A MATLAB differentiation matrix suite*. ACM transaction on mathematical software, 26,2000.

Convection in the spherical gap under micro-gravity conditions: From Earth's mantle to atmospheric flows.

Christoph Egbers[1], Florian Zaussinger[1], Peter Haun[1],
Peter Canfield[2], Vadim Travnikov[1], Andreas Froitzheim[1]

[1] BTU Cottbus-Senftenberg, Dept. Fluid Mechanics and Aerodynamics, Germany

[2] Airbus Defence and Space, Friedrichshafen, Germany

The Geoflow and AtmoFlow experiments are designed to investigate geophysically motivated flows in the spherical gap geometry. GeoFlow aims to study Earth's core and mantle-like flows, AtmoFlow will investigate global atmospheric flows. In both experiments the radial gravitational field is established by an artificial force field based on the dielectrophoretic effect. Axial gravity is eliminated by conducting the experiments under micro-gravity conditions on the ISS. We present latest results from the GeoFlow IIc experiment and first results from the planned AtmoFlow experiment.

GeoFlow IIc - Influence of dielectric heating on convection

Dielectric heating occurs in situations where an alternating electric field is applied on an insulating dielectric material (cf. in domestical micro-wave stoves) where the fluids molecules have a strong dipole structure. This effect can produce thermal convection through the thermo-electric coupling by the dielectrophoretic force. The working fluid of GeoFlow shows dielectric heating properties. Hence, it is used to investigate dielectric heating on convective processes. Three regimes are in the scope of GeoFlow IIc. First, the influence of dielectric heating on isothermal stratification. Second, the interaction of dielectric heating with a convectively unstable fluid. Third, the impact of heating on rotational instabilities. All three regimes are investigated by means of interferograms and accompanying numerical simulations, [2], [3]. Dielectric heating creates a stable parabola-shaped mean temperature profile with a maximum in the interior of the spherical gap for initially isothermal fluids, [1]. This stratification is known from certain stellar objects, too. In the convection state, the temperature distribution is more homogeneous with a lower maximum temperature, cf. Fig. 1 (left). For the comparison, a numerical interferogram is applied to temperature fields obtained in the simulation. The onset of convection as well as basic spatial properties of the resulting internally heated convective zone are in very good agreement with the experiment. The computed velocity field reveals strong downdrafts which lead to recognizable fringe patterns in the interferograms, see Fig. 1 (right).

Investigation of atmospheric-like flows in the spherical gap geometry: AtmoFlow

The main objective of the AtmoFlow experiment is the investigation of convective flows in the spherical gap geometry that are of interest for geophysical, astrophysical and especially here for atmospheric research. The main feature of AtmoFlow is its spherical geometry and aims to observe flows in thin gaps that are subjected to a central force field. Such a condition, obviously impossible to reach on ground, is achieved by simulating buoyancy driven convection through a central dielectrophoretic field in microgravity conditions e.g. on the ISS. Without losing its overall view on the complex physics, circulation in planetary atmospheres

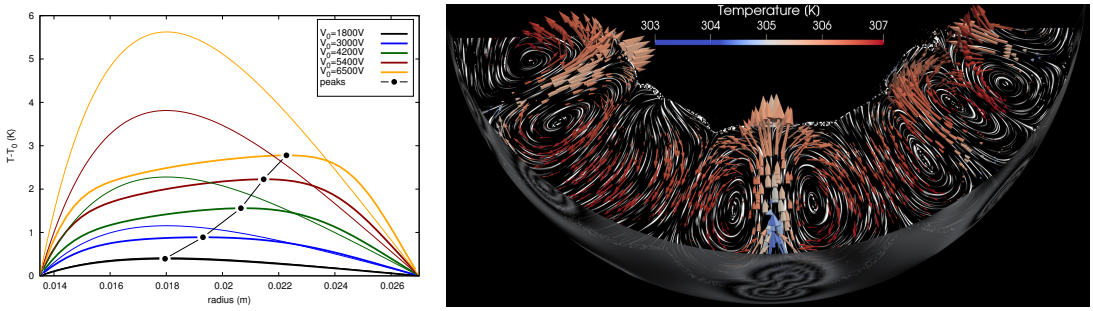

Figure 1: GeoFlow IIc: Mean temperature profile as function of the radius. Thick lines represent the conductive case, thin lines show the averaged temperature for the 3D case (left). Numerical reconstruction of a convective downdraft. Ring structures are numerical interferograms which are used to compare numerical with experimental results (right).

can be reduced to a simple model of the in- and outgoing energy (e.g. radiation) and rotational effects. Both input parameters are determined by the boundaries of the system, see Fig. 2 (right). This strongly simplified assumption makes it possible to break some generic cases down to test models which can be investigated by laboratory experiments and numerical simulations, Fig 2 (left). Therefore, it is possible to study atmospheric circulations by means of this spherical shell experiment, where varying differential rotation rates and temperature boundary conditions represent different types of planets. This is a very basic approach, but various open questions regarding weather, climate change and global warming can be answered with that simplified setup. We find a rich variety of typical flow patterns for radius ratio 0.7, including baroclinic waves, occluded fronts, strong tropical convergence, sub-tropical jets and complex polar vortices.

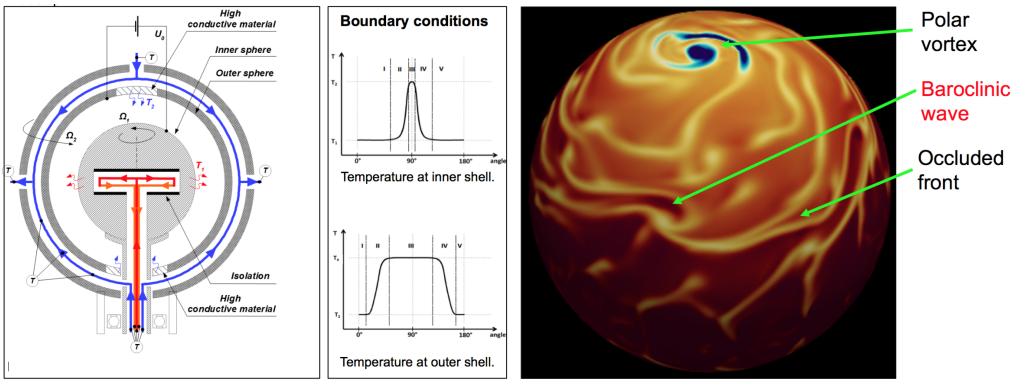

Figure 2: AtmoFlow: Sketch of the experimental setup of AtmoFlow (left). Numerical simulations in the experimental parameter space (right).

References

[1] F. Zaussinger, P. Haun, M. Neben, T. Seelig, V. Travnikov, Ch. Egbers, H. Yoshikava, I. Mutabazi, Phys Rev Fluids, 2018, submitted

[2] F. Zaussinger, A. Krebs, V. Travnikov, Ch. Egbers, *Adv. Space Res.*, **60**, 1327–1344, 2017.

[3] V. Travnikov, F. Zaussinger, Ph. Beltrame, Ch. Egbers, *Phys Rev E*, **96**, 023108, 2017.

Effect of amplitude ratio of a quasi-periodic gravitational modulation on the thermal instability in a Hele-Shaw cell

Abdelouahab El jaouahiry[1], Said Aniss[1],

[1] Faculty of Sciences, Laboratory of Mechanics, University Hassan II Ain-Chock, Casablanca,Morocco

---

1 Abstract

We study the influence of the amplitude ratio of accelerations which is introduced in the quasi-periodic Mathieu equation studied by Boulal et *al.* [2]. In this equation there are two incommensurate frequencies ω_1 and ω_2, i.e, the ratio, $\omega = \frac{\omega_2}{\omega_1}$, is an irrational number. We show that the increase of the ratio of accelerations, A_c, has a destabilizing effect.

2 Introduction

The periodic gravitational modulation of Rayleigh-Bénard convection in Hele-Shaw cell has been studied in [1]. Boulal et *al.* [2] have extend this configuraion to quasi-periodic gravitational modulation with two incommensurate frequencies. Boulal et *al.* [2] have showed that a modulation with two incommensurate frequencies has astabilizing or a destabilizing effect strongly depending on the frequencies ratio, ω. However, no study provides quantitative results regarding the influence of accelerations ratio on the onset of instability without assuming equal accelerations. Unlike the previous work, the present study aims to use a new maner to treat the problem of quasi-periodic oscillator using Floquet analysis after approximating an irrational number by a rational number.

3 Quasi-periodic Mathieu equation

Consider a Newtonian liquid confined in a horizontal Hele-Shaw cell of infinite extent in the x direction. Denote by d the height of the cell, e the distance between the vertical planes and $\epsilon = e/d$ the aspect ratio of the cell; the values $y = \pm e/2$ and z=0, d, correspond to the boundaries of the cell. The lower and upper walls are maintained respectively at temperatures T_1 and T_2 ($T_1 > T_2$). We consider that the Hele-Shaw cell is submitted to the volumic force $\rho[\mathbf{g} - (b_1\omega_1^2 \cos\omega_1 t + b_2\omega_2^2 \cos\omega_2 t)\ \mathbf{k}]$. Where ω_1 and ω_2 are two-dimensional incommensurate frequencies. The parameters b_1 and b_2 are the amplitudes of motion. Following the recent study in [3], we use the fact that an irrational number, ω , can be approximated by a rational number of the form $\omega = p/q$, where p and q are prime integers. The linearized equation in the Hele-Shaw approximation [1, 2] is written as

$$\frac{d^2 f}{d\tau^2} + 2\mu\ \frac{df}{d\tau} + \frac{4q^2\ h\ Pr^*}{\Omega_1^2}\ \left[R_0 - Ra\ (1 + Fr_1\Omega_1^2(\cos 2q\tau + A_c \cos 2p\tau))\right] f = 0 \qquad (1)$$

where $2\mu = \frac{2q(\pi^2+k^2+12Pr^*)}{\Omega_1}, h = \frac{k^2}{k^2+\pi^2}, R_0 = \frac{12k^2}{h^2}, \omega = \frac{\Omega_2}{\Omega_1} = \frac{\omega_2}{\omega_1}, A_c = \frac{b_2\omega_2^2}{b_1\omega_1^2}$; Ra is the Rayleigh number, Fr_1 is the Froude number, Pr^* is the Prandtl number and k is the wave number.

4 Rsultats et discussion

Figure 1 illustrates the results of the case where the fluid layer is heated from below and for values frequencies ratio, $\omega = \sqrt{37}$, effective Prandtl number, $Pr^* = 1$, Froude number, $Fr_1 = 1.6 \times 10^{-4}$ and for different values of the ratio of accelerations A_c. We see that near $\Omega_1 = 0$, the critical Rayleigh and wave numbers tend, respectively, to the values of the unmodulated case, namely $Ra_c = 48\pi^2$ and $k_c = \pi$. Here, it turns out that the effect of the accelerations ratio, A_c, is destabilizing for all values of Ω_1.

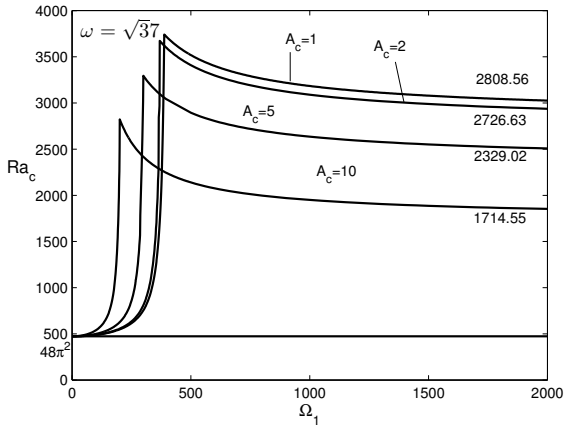

Figure 1: Evolution of the critical Rayleigh number, Rac, as a function of the dimensionless frequency Ω_1 for $\omega = \sqrt{37}$.

References

[1] S. Aniss, M. Souhar and M. Belhaq, "Asymptotic study of the., convective parametric instability in hele-shaw cell," Phys.Fluids. **90**, 262-268, 2000.

[2] T. Boulal, S. Aniss, M. Belhaq and A. Azouani, "Effect of quasi-periodic gravitational modulation on the convective instability in Hele-Shaw cell,", J. Nonlinear Mech., Issue 9, **43**, 852-857, 2008.

[3] M. Yagoubi and S. Aniss, "Effect of vertical quasi-periodic vibrations on the stability of the free surface of a fluid layer", Eur. Phys. J. Plus. **90**, 2017.

Acknowledgements

The organizers of the ICTW20 wish to thank all senders for their interest on the upcoming workshop.

Drag reduction due to vapor bubbles in high-Reynolds number Taylor-Couette flow

Rodrigo Ezeta[1], Sander G. Huisman[1], Dennis Bakhuis[1], Sander Bonestroo[1], Chao Sun[2,1]
Detlef Lohse[1,3]

[1] Physics of Fluids, Max Planck Institute for Complex Fluid Dynamics, MESA+ Institute and J. M. Burgers Center for Fluid Dynamics, University of Twente, P.O. Box 217, 7500 AE Enschede, The Netherlands

[2] Center for Combustion Energy and Department of Thermal Engineering, Tsinghua University, 100084 Beijing, China

[3] Max Planck Institute for Dynamics and Self-Organization, Am Fassberg 17, 37077 Göttingen, Germany

---

The presence of air bubbles in high-Reynolds number Taylor-Couette (TC) flow has proven to be successful when reducing the drag in the flow [1]. Approximately, 40% drag reduction (DR) was achieved when the volume fraction α is approximately 4% with a Reynolds number of $Re = 2.0 \times 10^6$. In this study, we explore the drag reduction mechanism in TC flow using vapor bubbles instead. We conduct experiments in the Boiling Twente Taylor-Couette (BTTC) apparatus [2]. A low-boiling point liquid (*Novec Engineered Fluid 7000*) is used as the fluid phase; this liquid boils at 34°C when the pressure is atmospheric.

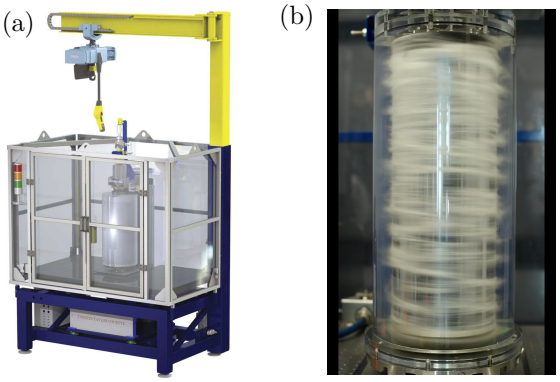

Figure 1: (a) Rendering of the BTTC facility. (b) A snapshot of the experiment where the distribution of the vapor bubbles can be appreciated.

The experiment is as follows: we fix the rotation of the inner cylinder (the outer cylinder is at rest) and measure the torque that is required to drive the cylinder at constant speed along with the pressure of the system. We gradually increase the temperature of the flow from 20°C to 50°C. When the pressure of the system equals the vapor pressure at the boiling temperature T_{boil}, we observe the formation of vapor bubbles which has a nearly uniform distribution along the axial direction. A snapshot of the experiment can be observed in Fig. 1(b). Due to the dynamic heating process, α is observed to increase during the experiment. Using a conservation of mass argument, in combination with the pressure signal, we can estimate α during the experiment as shown in Fig. 2(a). Using the measured $\alpha(t)$, we correct the liquid viscosity due to the presence of the vapor bubbles with the Einstein

correction, i.e. $\nu = \nu_\ell(1 + (5/2)\alpha)$, where ν_ℓ is the liquid viscosity. With both ν and $\mathcal{T}$ at hand, we calculate both the driving parameter of the flow expressed by the Taylor number Ta, and the Nusselt number Nu_ω, which quantifies the response of the flow. Here, $\mathrm{Ta} = (1/4)((1+\eta)/(2\sqrt{\eta}))^4(r_o - r_i)^2(ri + r_o)^2\omega_i^2/\nu^2$, where $r_{i,o}$ are the inner and outer radii respectively, $\eta = r_i/r_o = 5/7$ is the radius ratio, ω_i is the inner angular frequency and ν is the liquid viscosity; while $\mathrm{Nu}_\omega = ((r_o^2 - r_i^2)/(4\pi\ell r_i^2 r_o^2\omega_i))(\mathcal{T}/\rho\nu)$, where ℓ denotes the height of the cylinder, ρ is the liquid density and $\mathcal{T}$ is the torque. Finally, we evaluate the amount of drag reduction due to the vapor bubbles by computing $\mathrm{Nu}_\omega/\mathrm{Nu}_\omega(T_{\mathrm{boil}})$ and find DR of approximately 40% for $\mathrm{Ta} = 1.6 \times 10^{12} (Re = \mathcal{O}(10^6))$ for a volume fraction of $\alpha \approx 5\%$ (Fig. 2(b)). Using high-speed imaging, we have estimated the Weber number of the bubbles to be $\mathcal{O}(10)$ which is consistent with the study of drag reduction due to air bubbles in [1]. Our results support the idea that bubble deformability is crucial in order to achieve strong drag reduction.

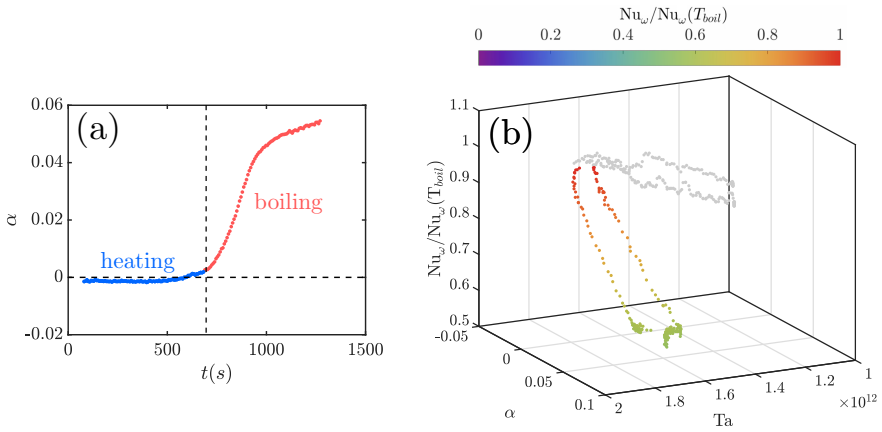

Figure 2: (a) The calculated volume fraction α during the experiment. (b) A 3D plot of the drag reduction achieved due to the presence of the vapor bubbles. Here two different experiments are shown. The colorbar represents the amount of drag reduction. The gray data points correspond to $\alpha \approx 0$.

References

[1] D. P. M. van Gils, D. Narezo, C. Sun, D. Lohse, *The importance of bubble deformability for strong drag reduction in bubbly turbulent Taylor-Couette flow*, J. Fluid Mech., **722**, 317-347, 2013.

[2] S. G. Huisman, R. C. A. van der Veen, G.-W. Bruggert, D. Lohse, C. Sun, *The boiling Twente Taylor-Couette (BTTC) facility: Temperature controlled turbulent flow between independently rotating, coaxial cylinders*, Rev. Sci. Instrum., **86**, 065108, 2015.

Acknowledgements

The authors acknowledge NWO and MCEC for their financial support. The authors would also like to thank G.-W. Bruggert, Martin Bos and Bas Benschop for their technical assistance. C. Sun acknowledges the financial support from the Natural Science Foundation of China under the Grant No. 11672156.

The linear instability of the stratified plane Couette flow

Giulio Facchini[1], Benjamin Favier[1], Meng Wang[2], Michael Le Bars[1], **Patrice Le Gal**[1]

[1] Aix-Marseille Univ, CNRS, Centrale Marseille, IRPHE, France

[2] Department of Mechanical Engineering, University of California, Berkeley, CA 94709, USA

We present the stability analysis of a plane Couette flow which is stably stratified in the vertical direction orthogonally to the horizontal shear (see Figure 1)[1]. Interest in such a flow comes from geophysical and astrophysical applications where background shear and vertical stable stratification commonly coexist. We first perform the linear stability analysis of the flow in a domain which is periodic in the stream-wise and vertical directions and confined in the cross-stream direction. The stability diagram is constructed as a function of the Reynolds number Re and the Froude number Fr, which compares the importance of shear and stratification. We find that the flow becomes unstable when shear and stratification are of the same order (i.e. $Fr \sim 1$) and above a moderate value of the Reynolds number $Re \geq 700$. The instability results from a resonance mechanism already known in the context of channel flows, for instance the unstratified plane Couette flow in the shallow water approximation [2].

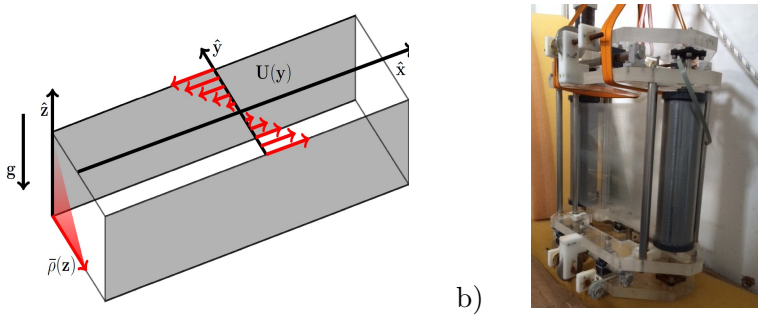

Figure 1: a) Sketch of the stratified plane Couette flow. b) The experimental setup with the transparent belt driven by vertical rollers; this shearing device is then introduced in a tank filled with salt stratified water.

The result is confirmed by fully non linear direct numerical simulations and to the best of our knowledge, constitutes the first evidence of linear instability in a vertically stratified plane Couette flow. We also report the study of a laboratory flow generated by a transparent belt entrained by two vertical cylinders and immersed in a tank filled with salty water linearly stratified in density. We observe the emergence of a robust spatio-temporal pattern close to the threshold values of Fr and Re indicated by linear analysis, and explore the accessible part of the stability diagram. Figure 2 presents spatio-temporal diagrams of the perturbation (left) and velocity fields (right) in the plane $y = 0$. With the support of numerical simulations we conclude that the observed pattern is a signature of the same instability predicted by the linear theory, although slightly modified due to streamwise confinement.

The mechanism at the origin of this instability relies on a resonance of internal gravity waves which are trapped close to the boundaries and Doppler shifted, thus allowing two counter

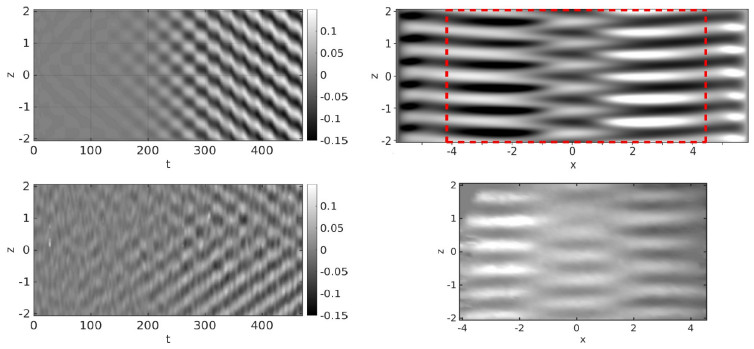

Figure 2: Left: Spatio-temporal diagram of the perturbation u at the center line $x = 0, y = 0$ for a reference case $Re = 969$, $Fr = 0.82$ for confined DNS (top) and experiment (bottom). Right: perturbation u in the plane y = 0 once the flow has become unstable for confined DNS (top) and the experiment (bottom). The red dashed rectangle indicates the area accessible to experimental measurements.

propagating waves to become stationary and mutually resonant. An analogous mechanism was also invoked to be at the origin of Strato-Rotational instability both in the plane Couette [3, 4] and the Taylor-Couette [5, 6, 7] geometries. More generally this wave interaction process identifies a class of instability which is characteristic of shear flows (e.g. [8]).

References

[1] G. Facchini, B. Favier, P. Le Gal, M. Wang, M. Le Bars, *The linear instability of the stratified plane Couette flow*, arXiv preprint arXiv:1711.11312, 2018.

[2] T. Satomura,*An investigation of shear instability in a shallow water*, Journal of the Meteorological Society of Japan. Ser. II **59 (1)**, 148-167, 1981.

[3] P. J. Kushner, M. E. McIntyre, T. G. Shepherd *Coupled Kelvin-wave and mirage-wave instabilities in semigeostrophic dynamics*, Journal of Physical Oceanography **28 (3)**, 513-518, 1998.

[4] J. Vanneste, I. Yavneh, *Unbalanced instabilities of rapidly rotating stratified shear flows*, Journal of Fluid Mechanics **584**, 373-396, 2007.

[5] I. Yavneh, J.C. McWilliams, J. C. Molemaker, M. Jeroen *Non-axisymmetric instability of centrifugally stable stratified Taylor-Couette flow*, Journal of Fluid Mechanics **448**, 1-21, 2001.

[6] J. Park, P. Billant *The stably stratified Taylor Couette flow is always unstable except for solid-body rotation*, Journal of Fluid Mechanics **725**, 262280, 2013.

[7] M. Le Bars, P. Le Gal, *Experimental analysis of the stratorotational instability in a cylindrical Couette flow*, Physical Review Letters **99**, 064502, 2007.

[8] P. G. Baines, H. Mitsudera, *On the mechanism of shear flow instabilities*, Journal of Fluid Mechanics **276**, 327342, 1994.

Influence of boundary conditions on instabilities in free surface rotating flows

Antoine Faugaret[1,2], **Laurent Martin Witkowski**[1,3], Yohann Duguet[1], Yann Fraigneau[1]

[1] LIMSI-CNRS, Université Paris-Saclay, F-91405 Orsay, France

[2] Sorbonne Université, Collège Doctoral, F-75005 Paris, France

[3] Sorbonne Université, Faculté des Sciences et Ingénierie, UFR d'Ingénierie, F-75005 Paris, France

---

The study of rotating flows in one of its most simple configurations (fixed cylindrical vessel, rotating disk at the bottom, free surface at the top) reveals much more complicated physics than expected. This flow, for low aspect ratios, is known to develop travelling instabilities as the angular velocity of the disk exceeds a finite threshold [1]. We revisit this flow case using distilled water experiments, direct numerical simulation and linear stability analysis. The comparison reveals a robust discrepancy in the instability thresholds. After a critical assessment of the possible issues in the experimental set-up, we eventually question the modelling of the free surface in the presence of water contaminants [2].

The influence of this numerical boundary condition was first tested by considering a new 'frozen' boundary condition where the radial velocity vanishes at the liquid interface [3]. In a second stage we generalise this new boundary condition into a linear combination of both 'free' and 'frozen' conditions, thereby introducing an additional free parameter α.

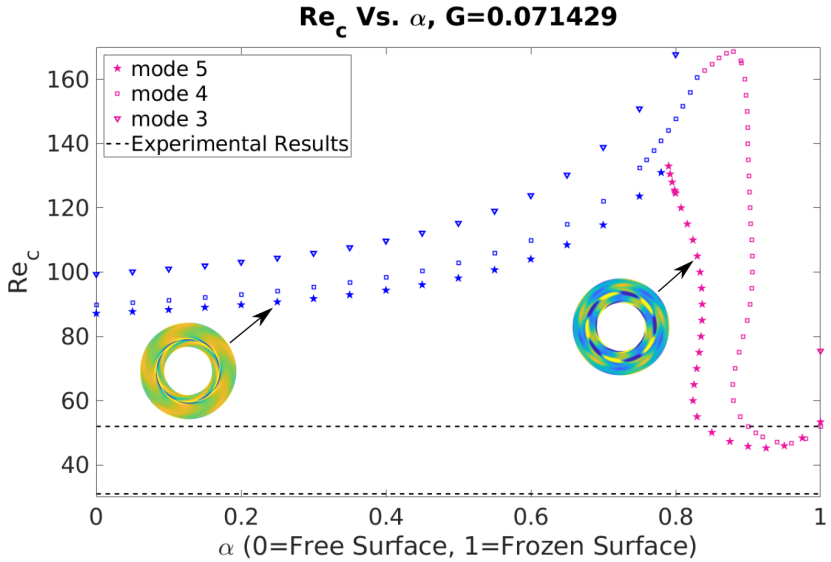

Figure 1: Evolution of the critical Reynolds number of three modes, for α between 0 (ideal free surface condition) and 1 ('frozen' condition), and a geometrical aspect ratio $G = 1/14$.

The search for the critical Reynolds number, parametrized by α, reveals a second branch of unstable modes with a lower critical threshold. The visual and quantitative agreeement between this new instability mode and the experimentally observed structures (cf Fig. 2) is very encouraging.

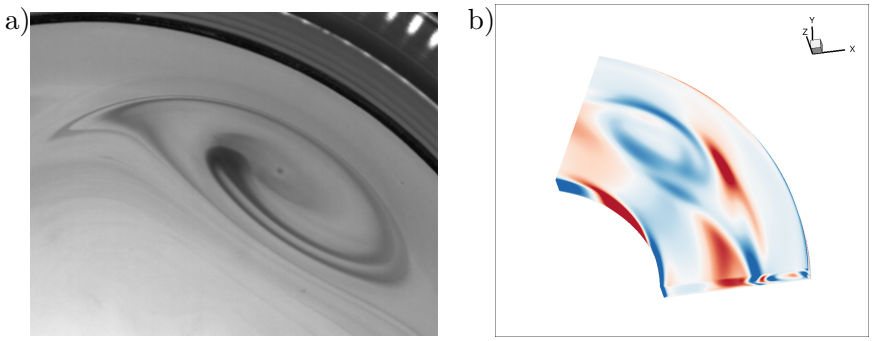

Figure 2: (a) Experimental visualization at $Re \sim 30$. (b) Axial vorticity computed at $Re = 53$, with frozen surface condition ($\alpha = 1$).

References

[1] S. Poncet and M.P. Chauve, *Shear-layer instability in a rotating system*, Journal of Flow Visualisation & Image Processing, **14**, 85-105, 2007.

[2] J.M. Lopez, F. Marques, A.H. Hirsa and R. Miraghaie, *Symmetry breaking in a free-surface cylinder flows*, J. Fluid Mech., **502**, 99-126, 2004.

[3] A. Spohn and O. Daube, *V Int. Conf. Computational Methods and Experimental Measurement*, 155-166, 1991.

Large scale vortices in the Taylor-Couette flow

Andreas Froitzheim[1], Sebastian Merbold[1], Christoph Egbers[1], Rodrigo Ezeta[2], Detlef Lohse[2], Chao Sun[2]

[1] Department of Aerodynamics and Fluid Mechanics, Brandenburg University of Technology Cottbus-Senftenberg, Siemens-Halske-Ring 14, 03046 Cottbus, Germany

[2] Physics of Fluids Group, MESA+ Institute and J.M. Burgers Centre for Fluid Dynamics, University of Twente, P.O. Box 217, 7500 AE Enschede, The Netherlands

---

In this study, which has been performed within the European High Performance Infrastructures (EuHIT) program, we investigate turbulent Taylor-Couette (TC) flow. It is the flow between concentric rotating cylinders serving as a famous reserve model for rotating flows in fluid mechanics. The TC geometry is defined by the radius ratio $\eta = r_1/r_2$ and the aspect ratio $\Gamma = L/d$ with the cylinder length L, the cylinder radii r_1 and r_2 for the inner and outer one respectively and the gap width $d = r_2 - r_1$. To describe the cylinder speeds, we use the ratio of angular velocities $\mu = \omega_2/\omega_1$ and the shear Reynolds number $Re_S = 2r_1r_2d|\omega_2 - \omega_1|/(\nu(r_1 + r_2))$ [3]. ν represents the kinematic viscosity.
In our study we focus on the impact of turbulent Taylor vortices on a fully turbulent TC flow, whose remnants have been found at very high Reynolds numbers [4] for pure inner cylinder rotation. Further, these remnants are strengthend again for slightly counter rotation and are responsible for a torque maximum, indicating the importance of turbulent Taylor vortices in that regime [1].
To investigate these vortices we performed PIV measurements in horizontal planes at 23 different cylinder heights at the torque maximum rotation rate ($\mu_{max}(\eta = 0.714) = -0.36$). The experiments were carried out inside the Boiling-Turbulent-Taylor-Couette experiment of the University of Twente within the EuHIT-program. The geometric parameters are $\eta = 0.714$, $\Gamma = 18.3$ and $d = 0.03m$. As working fluid distilled water is used with a kinematic viscosity of $1.004 \cdot 10^{-6} m^2/s$ at $20°C$ and fluorescent PMMA-Rhodamine B-particles are added as tracers. In summary we measured the radial $u_r(r, \varphi, z, t)$ and azimuthal velocity component $u_\varphi(r, \varphi, z, t)$ in horizontal planes scanning the axial coordinate in a range of $\pm 44mm$ around midheight with a step size of $4mm$ to analyse the flow in quasi-threedimensional space.

As the transport of angular momentum is constant across cylinder surfaces concentric to the rotation axis, we analyse the probability density function (PDF) of the azimuthal velocity component relative to these surfaces at specific radii r. In the axial direction, we limit the space to a length of one vortex pair and indicate the PDF as f_A. In figure 1, the PDFs (f_A) for $Re_S = 2.1 \cdot 10^5$ and $\mu = 0$ (case 1) as well as $\mu = -0.36$ (case 2) are shown. To get a deeper understanding for case 2, where dominant vortices are present inside the flow, also the PDFs for the axial position of the vortex center, inflow and outflow are added and denoted as $f_{vortex\ position}$.
For pure inner cylinder rotation (case 1), f_A is in good agreement with a Gaussian distribution independent of the radial location for $\tilde{r} \geq 0.05$. At the rotation ratio of the torque maximum (case 2), f_A strongly deviates from a Gaussian distribution. Close to the inner cylinder wall, the outflow region of the Taylor vortex ($f_{outflow}$) becomes important and shifts up the right flank of f_A. At the center of the gap, the distribution becomes quite symmetric to the origin of the x-axes in good agreement with the findings of [2]. With our measurements and

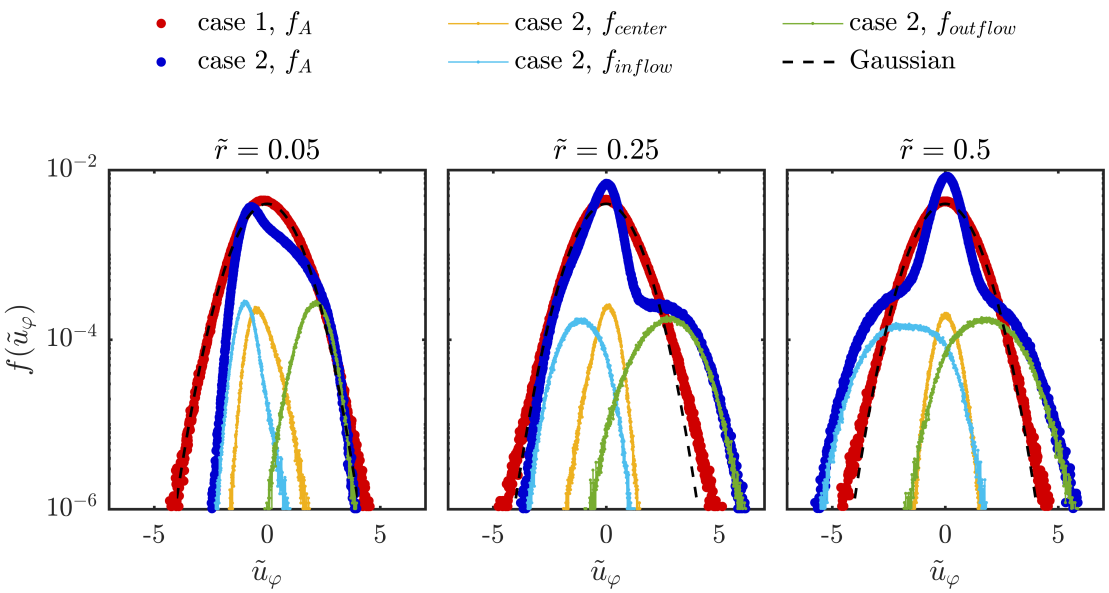

Figure 1: Probability density functions of the azimuthal velocity component for $Re_S = 2.1 \cdot 10^5$ and $\mu = 0$ (case 1) as well as $\mu = -0.36$ (case 2) relating to cylinder surfaces across one vortex pair. In addition, PDFs at the axial position of specific vortex locations of Taylor vortices are shown for case 2. The PDFs are normalized to have zero mean and a variance of one. The radial location, where the PDFs are evaluated, is normalized to be $\tilde{r} = 0$ at the inner and $\tilde{r} = 1$ at the outer cylinder.

the planned statistical analysis, we are confident to shed some more light on fully turbulent Taylor vortices at high Reynolds numbers.

References

[1] H. J. Brauckmann & B. Eckhardt, *Intermittent boundary layers and torque maxima in Taylor-Couette flow*, Phys. Rev. E **87**, 033004, 2013.

[2] H. J. Brauckmann, B. Eckhardt, J. Schumacher, *Heat transport in Rayleigh-Bnard convection and angular momentum transport in TaylorCouette flow: a comparative study*, Phil. Trans. R. Soc. A **375**, 20160079, 2017.

[3] B. Dubrulle, F. Dauchot, P. Y. Longaretti, D. Richard, J. P. Zahn, *Stability and turbulent transport in Taylor-Couette flow from analysis of experimental data*, Phys. Fluids **17**, 095103, 2005.

[4] S. G. Huisman, R. C. A. van der Veen, C. Sun, D. Lohse, *Multiple states in highly turbulent Taylor-Couette flow*, Nat. Commun. **5**, 3820, 2014.

Acknowledgements

Financial support by the Deutsche Forschungsgemeinschaft (DFG FOR1182 EG100\15-1, EG100\15-2) and the European High-Performance Infrastructures in Turbulence (EuHIT) is gratefully acknowledged.

New non-modal stability analysis and algebraic growth rate of a Taylor Couette model problem in an infinite domain

Tim Gebler[1], Judith Kahle[1], Martin Oberlack[1,2]

[1] Chair of Fluid Dynamics, TU Darmstadt, Otto-Berndt-Str. 2, 64287 Darmstadt, Germany

[2] Graduate School of Excellence CE, TU Darmstadt, Dolivostr. 15, 64293 Darmstadt, Germany

---

Since Taylor's experiment in 1923 [1], the Taylor Couette (TC) flow represents a paradigmatic system to study the stability of rotating shear flow. It is common to study the stability by employing the normal-mode approach. Although a two dimensional TC flow is found to have only stable eigenvalues by linear stability analysis [2], the non-normality of the eigenfunctions leads to a transient growth instability, which often appears to admit an algebraic growth rate [3]. It has been shown by the present group [4], [5], [6] that the normal-mode ansatz has its basis in symmetries and, moreover, that many classical shear flows admit new non-modal symmetry induced eigenfunctions. For the TC azimuthal base velocity $u_\varphi = Ar + Br^{-1}$ we obtain the new eigenfunction

$$\Psi(r, \varphi, t) = \widetilde{\psi}\left(\frac{r}{\sqrt{t}}\right) e^{im(-At+\varphi)} t^s \tag{1}$$

where s represents the complex exponent of the algebraic growth rate and Ψ is the stream function of the perturbation. As the variable $x = \frac{r}{\sqrt{t}}$ of the eigenfunction is depending on the variables in time and space, the usual geometry of the Taylor Couette flow with two finite radii has to be altered into a rotating wire flow in an infinite domain, which is a kind of TC model system for the wide-gap TC flow (figure 1).

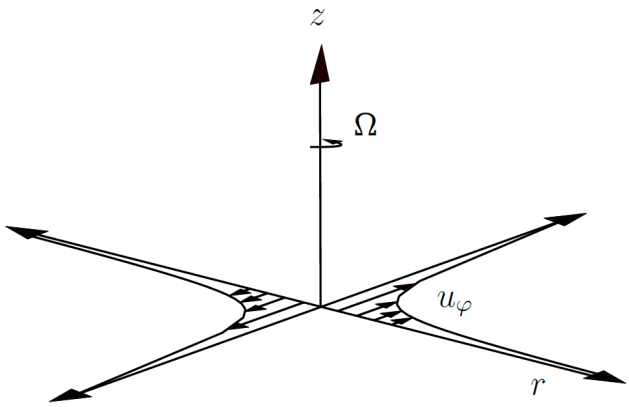

Figure 1: Infinitesimal thin wire in an infinite domain.

Together with appropriate boundary conditions at $x \to 0$ and $x \to \infty$ the underlying eigenvalue problem was completely solved, yielding a continuous eigenvalue spectrum with

$\Re(s) < \frac{1}{2}$ for arbitrary $m \neq 0$. Hence, the eigenfunctions (1) give rise to new instable modes for the plane TC model system, i.e. $\frac{1}{2} > \Re(s) > 0$. Considering the vorticity of the disturbed flow, a spiral movement can be observed (figure 2). Hereby, the parameter m determines the number of spiral arms, the imaginary part of the eigenvalue s defines the direction and degree of turns.

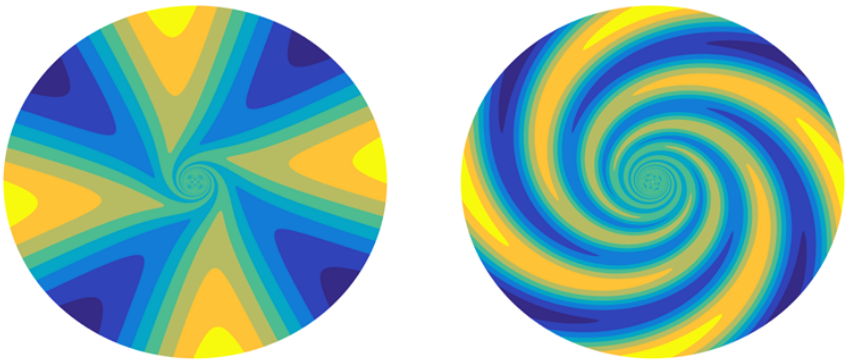

Figure 2: Appearance of spiral structures in the vorticity field with $m = 4$, $\Re(s) = 2$ and $\Im(s) = 0$ (left), $\Im(s) = 5$ (right)

In the next step the Fokas unifying method will be employed as such that solution (1) may also be used for finite radii of the classical TC flow.

References

[1] G. I. Taylor, *Stability of a Viscous Liquid Contained between Two Rotating Cylinders*, Transactions of the Royal Society London, **223**, 605-615, 1923.

[2] S. Grossmann, *The onset of shear flow turbulence*, Rev. Mod. Phys. **72**, 603-618, 2000.

[3] S. Maretzke, B. Hof and M. Avila, *Transient growth in linearly stable Taylor Couette flows*, Journal of Fluid Mechanics, **742**, 254-290, 2014.

[4] A. Nold and M. Oberlack, *Symmetry analysis in linear hydrodynamic stability theory: Classical and new modes in linear shear*, Physics of Fluids, **25**, 104101, 2013.

[5] A. Nold, M. Oberlack and A. F. Cheviakov, *On new stability modes of plane canonical shear flows using symmetry classification*, Journal of Mathematical Physics, **56**, 113101, 2015.

[6] J. Hau, M. Oberlack and G. Chagelishvili, *On the optimal systems of subalgebras for the equations of hydrodynamic stability analysis of smooth shear flows and their group-invariant solutions*, Journal of Mathematical Physics, **58**, 043101, 2017.

Finite element simulation of thermal electro-hydrodynamic driven flow in annular geometry

Philipp Gerstner[1], Martin Baumann[1], Vincent Heuveline[1]

[1] Engineering Mathematics and Computing Lab (EMCL), Heidelberg University, Germany

---

We consider the hydrodynamical behavior of dielectric fluids contained in a vertical annulus under applied voltage and temperature gradient between inner and outer wall. This setting gives rise to a body force, that is a superposition of buoyancy and dielectrophoretic force [1]. The situation can be modeled by means of the thermal electro hydrodynamical equations which are based on the standard Boussinesq approximation for natural convection, augmented by DEP force and Gauss law for describing the electric field inside the fluid as a function of temperature. These equations for fluid velocity u, pressure p, temperature θ and electric potential Φ are given by

$$\begin{aligned} \partial_t u + u \cdot \nabla u - \nu \Delta u + \frac{1}{\rho_1} \nabla p &= \alpha_f (\nabla \Phi)^2 \nabla \theta - \alpha_g \vec{g} \theta \\ \nabla \cdot u &= 0 \\ \partial_t \theta + u \cdot \nabla \theta - \kappa \Delta \theta &= 0 \\ -\nabla \cdot ((1 - e\theta) \nabla \Phi) &= 0 \end{aligned} \tag{1}$$

under appropriate initial and boundary conditions [2].

Our method for approximately solving system (1) is based on the Finite Element Method for discretization in both, space and time. For the spatial part, we make use of stable Taylor-Hood elements, whereas temporal discretization is implemented by a Petrov-Galerkin formulation with continuous trial and discontinuous test functions. In this way, the resulting discretized problem can be solved in a time-stepping manner, with an arising set of nonlinear algebraic equations for each time step which are solved by Newtons method. Here, the main computational effort lies in the solution of large-scale linear systems whose dimensions are in the order of several millions of variables when using a reasonable spatial resolution in 3D. To cope with these systems, we developed a parallel linear preconditioner which is based on a Schur complement approach for splitting the complete system into several subsystems according the underlying physics of the model. These subsystems correspond to discretized elliptic problems, which are well suited for being solved with highly scalable methods. We make use of the Algebraic Multigrid Method [3] and construct the way of solving the subsequent subsystems such that the overall solution process exhibits good parallel efficiency. The implementation is based on the open source Finite Element package HiFlow^3 [4].

In our talk, we present a computational study to demonstrate parallel scalability of our method. Moreover, we present simulation results for a cylinder annulus of aspect ratio $\Gamma = 20$ with electric Rayleigh number in the order of 10^5. The numerical solution shows the transition from initially azimuthally aligned vortices to axially aligned columnar structures, where the latter are present in the final state of the dynamic system. Due to these vortices, radial heat transfer is enhanced as an increase of the associated Nusselt number shows.

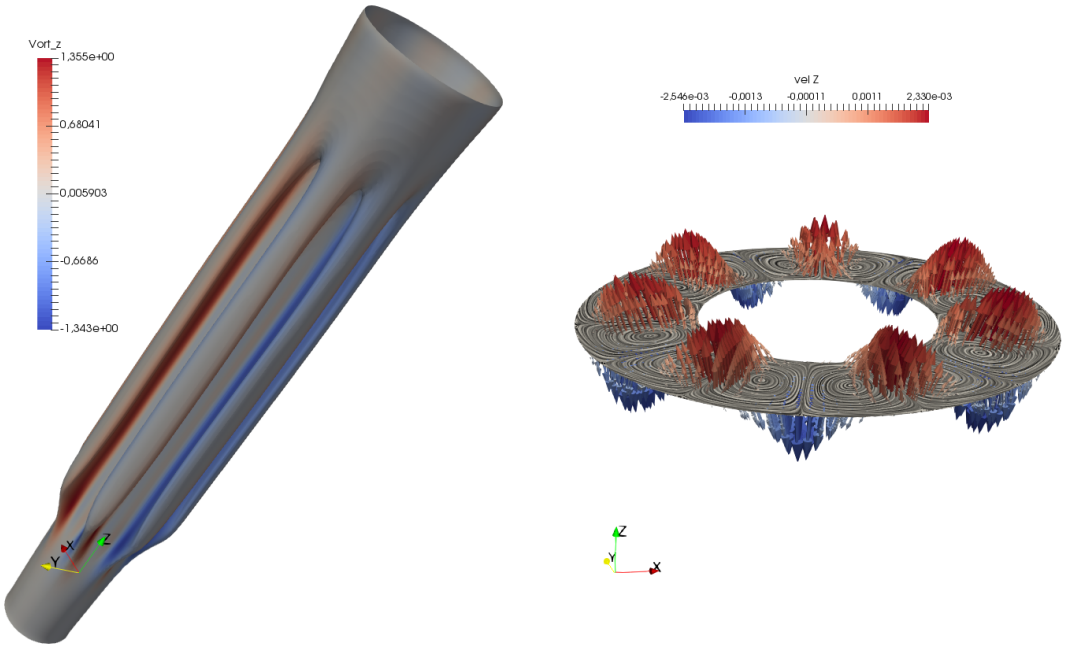

Figure 1: Fluid velocity and temperature in a vertical cylinder gap of aspect ratio $\Gamma = 20$ under applied temperature difference of $\Delta T = 7K$ and effective voltage $\Delta V = 7kV$ between inner and outer wall. Left: isosurface of median temperature with color map indicating the strength of axial vorticity. Right: illustration of the flow field on an horizontal cut at the middle height of the cylinder. Shown are both 3D field, indicated by arrows, and its projection onto the horizontal plane, illustrated by streamlines.

References

[1] A. Meyer, M. Jongmanns, M. Meier, C. Egbers, I. Mutabazi, *Thermal convection in a cylindrical annulus under a combined effect of the radial and vertical gravity*, Comptes Rendus Mécanique **345**,11 - 20, 2017.

[2] H.N. Yoshikawa, O. Crumeyrolle, I. Mutabazi, *Dielectrophoretic force-driven thermal convection in annular geometry*, Physics of Fluids **25**, 024106, 2013.

[3] H. Van Emden, U. Meier Yang, *BoomerAMG: A parallel algebraic multigrid solver and preconditioner*, Applied Numerical Mathematics **41**, 155 - 177, 2002.

[4] S. Gawlok, et. al., *HiFlow3 Technical Report on Release 2.0*, EMCL Preprint Series **6**, 2017.

Acknowledgements

This work was supported by the German Research Foundation (DFG) grant "Thermo-elektro-hydrodynamisch TEHD getriebene Wärmetransporterhöhung im vertikalen Zylinderspalt - Experimente und numerische Simulation im Kontext von Messunsicherheiten und optimaler Versuchsplanung (EG 100/20-1)". The authors acknowledge support by the state of Baden-Württemberg through bwHPC and the DFG through grant INST 35/1134-1 FUGG.

Gravity waves in baroclinic jet flows: a survey of laboratory experiments

Uwe Harlander[1], Costanza Rodda[1], Ion D. Borcia[2], Patrice Le Gal[3]

[1] BTU Cottbus-Senftenberg, Dept. Aerodynamics and Fluid Mechanics, Germany

[2] BTU Cottbus-Senftenberg, Dept. Computational Physics, Germany

[3] Aix-Marseille Univ., CNRS, Centrale Marseille, IRPHE, France

---

Inspecting animations of upper tropospheric jets provided e.g. by operational weather services it can be seen that the degree of turbulence of the jets is rather low but still, small-scale gravity waves seem to be steadily emitted from the jet cores. This observation is puzzling since the emission seems to be disconnected from classical instabilities and turbulence. Today the small-scale waves are attributed to an imbalance of the jet. For some part, a re-adjustment of the jet towards the geostrophic equilibrium leads to the radiation of gravity waves, however, another significant part seems to be connected to so called spontaneous imbalance. The latter denotes the fact that the geostrophic part of a flow can work as forcing for the unbalanced part [1]. Since a number of years the signature of spontaneous imbalance has been looked for in laboratory experiments. In the frame of the DFG research unit MSG-Waves we try to detect this phenomenon by means of a differentially heated rotating annulus experiment.

The differentially heated rotating annulus is a laboratory experiment originally designed for modeling large-scale features of the mid-latitude atmosphere. In the present study we investigate (i) a modified version of the classical baroclinic experiment in which a juxtaposition of convective and motionless stratified layers is created by introducing a vertical salt stratification. For large enough rotation rates, the baroclinic instability destabilizes the flow in the top and the bottom shallow convective layers, generating eddies and inertia-gravity waves separated by the stable stratified layer. We further investigate spontaneous imbalance (ii) in a shallow fluid layer filling a large differentially heated rotating annulus (Fig. 1). In this setup the ratio between stratification and rotation is larger than for the classical small heated rotating annulus and the gravity wave signature should hence be closer to the atmosphere. We observe gravity waves trapped at the jet core but also sporadic bursts of gravity wave emission from the baroclinic front in regions where the local

Rossby number is large. This points to spontaneous imbalance as wave generation mechanism. First results on numerical simulations [1, 2] and experimental findings [4, 3] have been published.

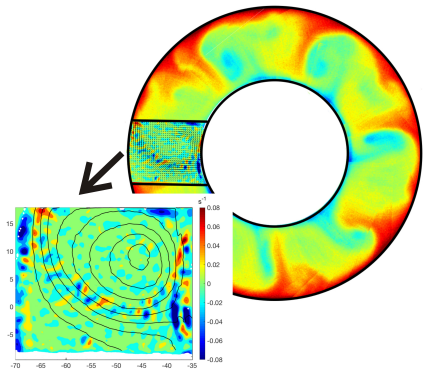

Figure 1: Infrared image of the large tank's surface temperature. The inset shows the horizontal part of the velocity divergence capturing the small-scale gravity wave signal along the jet core.

References

[1] S. Borchert, U. Achatz, M.D. Fruman, *Gravity wave emission in an atmosphere-like configuration of the differentially heated rotating annulus experiment,* J. Fluid Mech. **758**, 287311, 2014.

[2] S. Hien, J. Rolland, S. Borchert, L. Schoon, C. Zülicke, and U. Achatz, *Spontaneous inertia-gravity wave emission in the differentially heated rotating annulus experiment,* J. Fluid Mech. **838**, 541, 2018.

[3] C. Rodda, I. D. Borcia, P. Le Gal, M. Vincze, and U. Harlander, *Baroclinic, Kelvin and inertia-gravity waves in the barostrat instability experiment*, Geophys. and Astrophys. Fluid Dyn., https://doi.org/10.1080/03091929.2018.1461858, 2018.

[4] M. Vincze, I.D. Borcia, U. Harlander, and P. Le Gal, *Double-diffusive convection and baroclinic instability in a differentially heated and initially stratified rotating system: the barostrat instability*, Fluid Dyn. Res. **48**, 061414, 2016.

Acknowledgements

This work was supported by DFG (Germany), EuHIT (Europe), and CNRS (France).

20th International Couette-Taylor Workshop (ICTW20)
Stability of a Viscoelastic Pulsed Flow in Taylor Couette Geometry

HAYANI Mohamed[1], ANISS Said[1],

[1] University of Hassan II, Faculty of Sciences Ain-Chock,
Laboratory of Mechanics, B.P.5366 Maarif, Casablanca, Morocco

---

The present work is devoted to the study of the effect of a phase modulation, imposed on the inner and the outer cylinders, on the threshold of instability within a viscoelastic fluid in a Taylor-Couette geometry. In this context, we assume that the behavior of the fluid is governed by a non-linear Oldroyd-B law and the modulation is sinusoidal.
We perform a linear stability analysis of the base flow and a spatial resolution with spectral methods (Chebyshev-Gauss-Lobatto collocation method) combined with a temporal resolution using the Runge-Kutta method with Floquet Theory. The results obtained in this framework, allow us to highlight, the effect of the modulation and the viscoelastic nature on critical Taylor number.

1 Introduction

The Taylor-Couette flow of a viscoelastic fluid features a completely contrary scenario. Even at vanishing Reynolds numbers far below the critical condition for primary inertial instability, i.e. in the absence of inertia, the initially laminar flow of a viscoelastic fluid may become linearly unstable. This transition is non-inertial by nature and it originates from the elastic instability mechanisms: elastic normal stresses are amplified in the presence of small perturbations of the radial velocity field and couple to the curvature of streamlines. They build up a so-called hoop stress which actuates a secondary flow in the radial direction towards the center of the Taylor-Couette cell when the elastic forces are big enough (Weissenberg effect) [1, 2, 3, 4, 5]. Consider an incompressible viscoelastic fluid filling the annulus between two infnitely long cylinders of radii R_1 and $R_2 = R_1 + d$ where d is the gap length (Fig. 1). The angular velocity of each cylinder is $\Omega_o \cos(\omega t)$, Ω_0 and ω denote respectively the amplitude and the frequency of the modulated rotation.

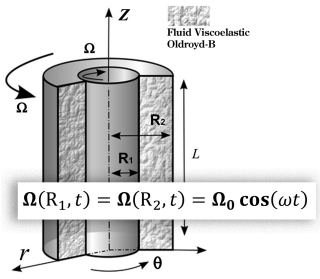

Figure 1: Taylor-Couette geometry.

2 Linear stability analysis

The set of equations (equations of momentum and behavioral law equations) is solved numerically using the Chebyshev pseudo-spectral collocation method based on the discretized Gauss-Lobatto points grid and a temporal resolution by the method of Runge-Kutta with Floquet Theory. With these considerations, we have a relation between the frequency γ, the Taylor's number T_a and the wave number k.

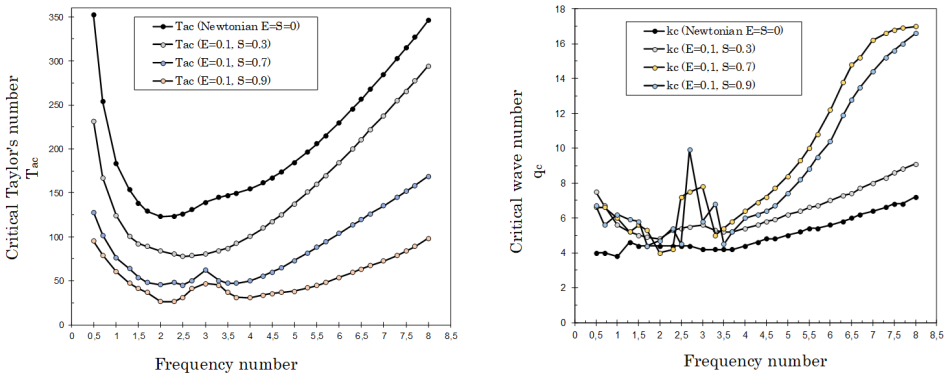

In this context, the critical Taylor number T_a, as a function of γ is presented in figure 2 for different values of the elasticity number and the composition number S. For the low values of elasticity, an hydrodynamic behavior similar to that of the Newtonian fluid is obtained for different values of the parameter S. Indeed, the flow is potentially unstable in the intermediate frequencies and a stabilization effect is obtained in the low and high frequencies. In addition to the destabilizing effect of the composition parameter in all frequency ranges.

References

[1] Ginn R. F. and Denn M. M., *Rotational stability in viscoelastic liquids: Theory*, AIChE Journal, 15(3):450454 (1969).

[2] Denn M. M. and Roisman J. J.,*Rotational stability and measurement of normal stress functions in dilute polymer solutions*, AIChE Journal, 15(3):454459 (1969).

[3] Larson, R. G., Shaqfeh, Eric S. G., Muller, S. J.,*A purely elastic instability in Taylor-Couette flow*, Journal of Fluid Mechanics, 218:573600 (1990).

[4] R.G. Larson, S. J. Muller, E. S. G. Shaqfeh,*The effect of fluid rheology on the elastic Taylor-Couette instability*, Journal of Non-Newtonian Fluid Mechanics, 51(2):195-225 (1994).

[5] Shaqfeh, Eric S. G., Muller, Susan J., Larson, Ronald G., *The effects of gap width and dilute solution properties on the viscoelastic Taylor-Couette instability*, Journal of Fluid Mechanics, 235:285-317 (1992).

[6] R. Byron Bird, Ole Hassager,*Dynamics of polymeric liquids: Fluid mechanics*, John Wiley and Sons Inc., New York, NY, 1 (1987).

On the stability of a Couette-Taylor flow between rotating porous cylinders to three-dimensional perturbations

Konstantin Ilin[1], Andrey Morgulis[2]

[1] Department of Mathematics, University of York, Heslington, York YO10 5DD, UK

[2] Department of Mathematics, Mechanics and Computer Science, The Southern Federal University, Rostov-on-Don and South Mathematical Institute, Vladikavkaz Center of RAS, Vladikavkaz, Russian Federation

---

We consider the stability of a steady incompressible flow between rotating porous cylinders with radial flow to small three-dimensional perturbations. This problem attracted considerable attention in the last 50 years and is still a very active research area (see, e.g. a recent paper [1]). Let r_1 and r_2 ($r_1 < r_2$) be the radii of the cylinders, Ω_1 and Ω_2 their angular velocities and ν the kinematic viscosity of the fluid. The basic flow is an exact solution of the Navier-Stokes equation, given by

$$u = \frac{Q}{r}, \quad v = V(r) = Ar^{R+1} + \frac{B}{r}, \quad p = -\frac{Q^2}{2r^2} + \int \frac{V^2(r)}{r}\, dr \tag{1}$$

where u and v are the radial and azimuthal components of the velocity, p is the pressure divided by (constant) density, Q is the (constant) volume flux of the fluid across the gap between the cylinders (per unit length in the axial direction), A and B are constants depending on r_1, r_2, Ω_1 and Ω_2, and $R = Q/\nu$ is the radial Reynolds number. It is also convenient to define azimuthal (inner and outer) Reynolds numbers as $Re_1 = r_1(r_2 - r_1)\Omega_1/\nu$ and $Re_2 = r_2(r_2 - r_1)\Omega_2/\nu$ respectively.

The azimuthal velocity profile $V(r)$ depends on R: it reduces to the Couette-Taylor profile for $R = 0$ (no radial flow) and, in the limits $R \to \pm\infty$, the flow becomes irrotational everywhere except for a thin boundary layer either at the outer cylinder (if $R \to +\infty$) or at the inner one (if $R \to -\infty$). It is well known that the classical Couette-Taylor flow is linearly stable to all perturbations if $\Omega_2 r_2^2 \geq \Omega_1 r_1^2$. It turns out that the presence of radial flow cardinally changes the situation. As has been shown in [2, 3], the basic flow (1) can be linearly unstable for $\Omega_2 r_2^2 \geq \Omega_1 r_1^2$ provided that the radial Reynolds number is sufficiently high ($|R| \gg 1$).

The aim of the present study is to investigate whether this instability can occur for moderate values of R. So, we consider the linear stability problem for flow (1). Perturbations are assumed to have the form of normal modes, i.e. they are proportional to $e^{\sigma t + in\theta + ikz}$ (where n and k are azimuthal and axial wave numbers), and the stability problem reduces to an eigenvalue problem for σ. The eigenvalue problem is solved using an adapted version of a Fourier-Chebyshev Petrov-Galerkin spectral method [4].

We have computed the neutral curves on the (Re_2, Re_1) plane for various values of the radial Reynolds number R and the geometric parameter $a = r_2/r_1$. Calculations show that even a relatively weak radial flow may lead to an instability which does not occur in the classical Couette-Taylor problem (without radial flow). An example of neutral curves for $a = 2$ is shown in Fig. 1: the circles represent computed points, and the curves are a result of linear spline interpolation based on these points. Each point is obtained by maximizing the unstable area on the (Re_2, Re_1) plane over azimuthal and axial wave numbers (n and k), i.e.

at each point in the unstable region, there is a least one unstable eigenvalue for some $n \geq 0$ and $k \geq 0$. Due to this maximization, some curves in Fig. 1 exhibit points where they are not smooth. These points correspond to the change in the azimuthal wave number of the most unstable mode. For example, the red solid curve in Fig. 1 corresponds to $Re = 40$ and consists of two smooth branches: on the left branch, the most unstable mode is the axisymmetric mode ($n = 0$) and, on the right one, it is the non-axisymmetric mode with $n = 1$; the two branches merge at $Re_2 \approx 485$. Figure 1 shows that for $R \geq 40$ the computed instability domains extend to the region where the classical Couette-Taylor flow is stable.

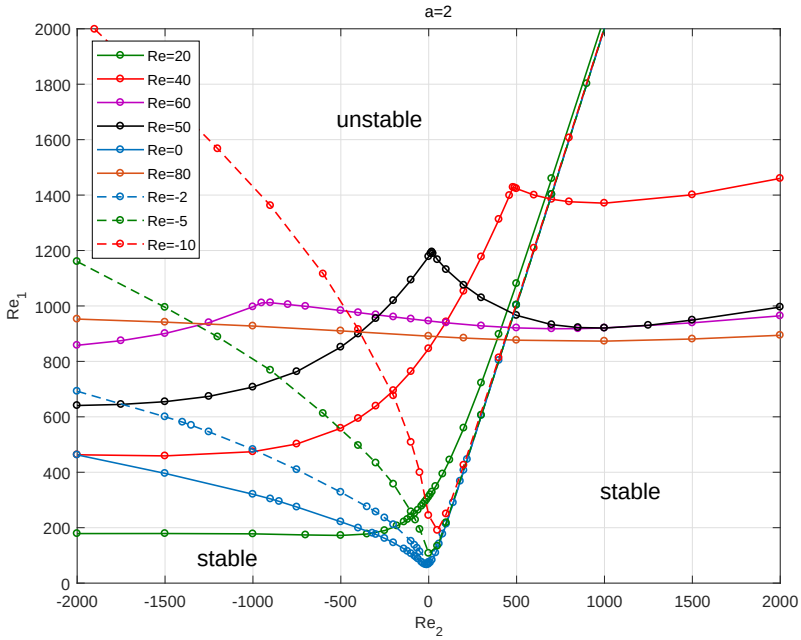

Figure 1: Instability regions for $a = r_2/r_1 = 2$ and various values of R.

References

[1] D. Martinand, E. Serre, R. M. Lueptow, *Linear and weakly nonlinear analyses of cylindrical Couette flow with axial and radial flows*, J. Fluid Mech. **824**, 438-476, 2017.

[2] K. Ilin, A. Morgulis, *Instability of an inviscid flow between porous cylinders with radial flow*, J. Fluid Mech. **730** (2013) 364–378.

[3] K. Ilin, A. Morgulis, *Inviscid instability of an incompressible flow between rotating porous cylinders to three-dimensional perturbations*, Eur. J. Mech. - B/Fluids **61**(1), 46-60, 2017.

[4] A. Meseguer, L.N. Trefethen, *Linearized pipe flow to Reynolds number* 10^7, J. Comput. Phys. **186**(1), 178-197 (2003).

Numerical Study of Thermoelectric Convection in a Finite Cylindrical Annulus

Changwoo Kang[1], Innocent Mutabazi[1],

[1] Normandie Université, UNILEHAVRE, CNRS-UMR 6294, LOMC, Le Havre, France

---

We study the transition to turbulence in a flow of a dielectric liquid with a radial temperature gradient and an alternating electric voltage $V(t)=V_0 sin\omega t$ with a frequency $\omega/2\pi$ much larger than the inverses of the liquid characteristic times. The liquid has the density ρ, the kinematic viscosity ν, the thermal diffusivity κ, the permittivity ϵ. It is confined inside a vertical cylindrical annulus of a radius ratio η=0.5 and an aspect ratio Γ=20. The inner and outer cylinders are kept at constant temperatures T_1 and T_2, leading to a temperature gradient (ΔT=T_1-T_2) acting on the fluid. The resulting gradient induces a vertical Archimedean buoyancy and a radial dielectrophoretic (DEP) force acting on the fluid. We assyme the validity of the electrohydrodynamic Boussinesq approximation [1, 2] i.e. $\rho = \rho_0(1-\alpha(T-T_0)$ and $\epsilon = \epsilon_*(1-e(T-T_0)$ where $\rho_0 = \rho(T_0)$ and $\epsilon_* = \epsilon(T_0)$. The coefficients α and e represent the thermal expansion and the thermal variation of permittivity respectively. The flow is characterized by two external control parameters : the Grashof number $Gr = \alpha\Delta T g d^3/\nu^2$ and the dimensionless electric tension $V_E = V_0/\sqrt{\rho\nu\kappa\epsilon_2}$. In the absence of the electric field, there is no dielectropheoretic force ($V_E = 0$) and a weak temperature gradient induces a large convective cell in the gap with an ascending flow near the hot surface and a descending flow near the cold surface. The stability of this convective cell has been investigated by many authores [3, 4]. On the other hand, when the effect of the Archimedean buoyancy can be neglected ($Gr = 0$ e.g. in the microgravity environment), the dielectrophoretic force can induce a thermal convection above a threshold of the electric tenson applied to the dielectric fluid [1, 2, 5]. A recent linear stability analysis of the the flow induced by both the Archimedean and dielectrophoretic buoyancies has shown the existence of the columnar modes in a certain range of the electric voltage values [6]. We carry out direct numerical simulations (DNS) to investigate the effect of the DEP force on the laminar large convective cell generated in a liquid with $Pr = 65$ for a fixed value of ΔT corresponding to $Gr = 530 < Gr_c = 776$. The dimensionless electric potential difference (V_E)varied from 0 to 10,000. Above a critical value of V_E, the base flow bifurcates to the state of columnar vortices. These stationary and counter-rotating vortices appear in the central part of the annulus while the flow remains laminar near the endplates (Fig. 1(a)). As the electric voltage increases,regular waves traveling downward are developed on columnar vortices (Fig. 1(b)). For large enough values of the electric voltage, there is a transition to chaotic flow with broken vortices(Fig. 1(c)). A further increase of V_E leads to a flow with small-scale structures (Fig. 1(d)). We provide time-averaged values associated with the kinetic energy and the heat transfer for different values of V_E to evaluate the performance on the electric voltage on the thermal convection, and we compare the present result to the experimental and theoretical available studies [5, 6].

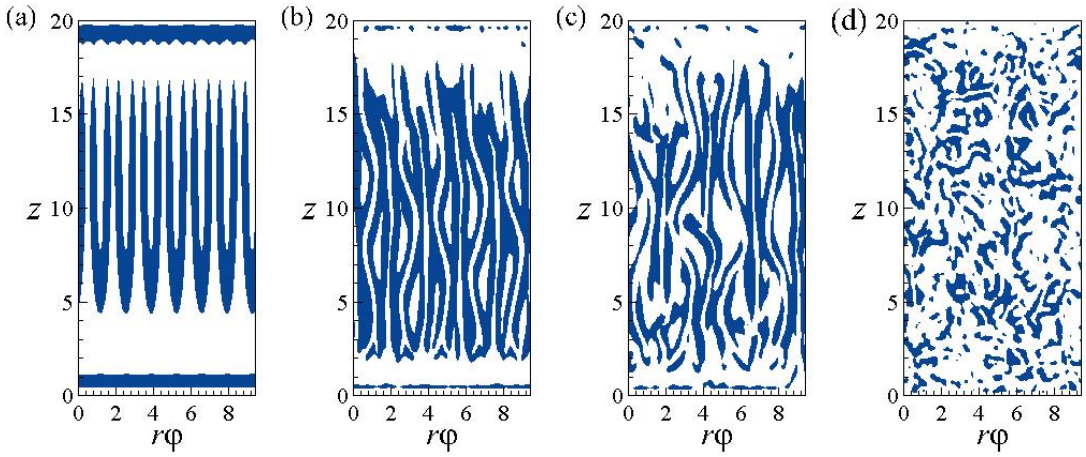

Figure 1: Instantaneous vortical structures at the central surface; (a) V_E=1,200, (b) V_E=2,500, (c) V_E=3,000, (d) V_E=8,000.

References

[1] P. H. Roberts, *Electrohydrodynamic convection*, Q. J. Mech. Appl. Math, **22**, 211-220, 1969.

[2] H.N. Yoshikawa, O. Crumeyrolle I. Mutabazi, *Dielectrophoretic force-driven thermal convection in annular geometry*, Phys. Fluids **25**, 024106, 2013.

[3] A. Bahloul, I. Mutabazi A. Ambari, *Codimension 2 points in the flow inside a cylindrical annulus with a radial temperature gradient*, Eur. Phys. J. AP **9**, 253-264, 2000.

[4] J. Pécheux P. Le Quéré *Numerical simulations of multiple flow transitions in axisymmetric annulus convection* J. Fluid Mech. **206**, 517, 1989.

[5] V. Travnikov, O. Crumeyrolle, I. Mutabazi, *Numerical investigation of the heat transfer in cylindrical annulus with a dielectric fluid under microgravity*, Phys. Fluids **27**, 054103, 2015.

[6] A. Meyer, M. Jongmans, M. Meier C. Egbers, *Thermal convection in a cylindrical annulus under a combined effect of the radial and vertical gravity*, C.R. Mécanique **345**, 11-20, 2017.

Acknowledgements

The present work has been realized within the LIA ISTROF (CNRS 1092), and it was partially supported by the CNES under the project INTEHLDI. C. Kang is supported by the project BIOENGINE, CPER-FEDER Normandie.

Effect of aspect ratio on steady liquid metal through the Gratz flow system in MHD
20th International Couette-Taylor Workshop (ICTW20)

S. Lecheheb[1,2], A. Bouabdallah[1], Z. Tigrine[1]

[1] Laboratory of Thermodynamics and energetic systems, Faculty of Physics, USTHB, BP 32 El alia, Babezzouar Algiers, Algeria

[2] Centre de Dveloppement des Energies Renouvelables, CDER, 16340, Algiers, Algeria

---

This work dealt with the geometrical effect on the Gratz flow system following the influence of the duct length to width ratio, aspect ratio , on heat-transfer rates, pressure distribution and thermal performances as local and mean Nusselt numbers of molten metal flow through horizontal rectangular channel in the Poiseuille flow conditions subjected to uniform transversal magnetic field.

We modelled the process to establish the properties related to heat transfer involving the both thermal regions of Gratz system in MHD. Thus, using a computational fluid dynamics procedure based on finite volume method (Fluent Code), we studied numerically the problem in order to characterize and control the viscous MHD flow according to an imposed axial temperature gradient. As a result of the effect of aspect ratio on the liquid metal for the considered geometry this one is connected with the sensitive parameters, namely, the Brinkman number Br, the Hartmann number Ha and the Peclet number Pe. The advantage of such modifications will directly affect the probable distribution of the temperature field, with or without a magnetic field effect. Under these conditions, we note that an early transition regime from the laminar flow to turbulence and therefore by decreasing Γ to enhance both heat transfer rates and flow mixing by pressure drop as Γ deceases.

keyword

Gratz flow system, Thermal performance, Poiseuille flow, Aspect ratio, Nusselt number.

Acknowledgements

The organizers of the ICTW20 wish to thank all senders for their interest on the upcoming workshop.

On the coalescence of anticyclones in stratified rotating flows

Patrice Le Gal[1], Raùl Cruz Gomez[2], Anne Cros[2]

[1] Aix-Marseille Univ, CNRS, Centrale Marseille, IRPHE, France

[2] Departamento de Fìsica, CUCEI , Universidad de Guadalajara, Guadalajara, Mexico

---

Oceanic meso-scale lenticular vortices play an important role in the redistribution of heat, salt and momentum in oceans and thus contribute to the climate equilibrium on Earth. These vortices are governed by geostrophic and hydrostatic balances between pressure gradients, Coriolis and buoyancy forces from where they get their shape and aspect ratio [1, 2]. This equilibrium leads to quasi-2D balanced motions in which energy is prevented to feed small scales by the conservation of potential vorticity. Understanding the way energy escapes from this mesoscopic turbulence to feed the smallest oceanic scales where dissipation occurs, is the subject of an intense research. Among several different routes to dissipation, the emission of internal gravity waves has been evoked to be a possible conveyor of energy redistribution [3]. On another hand, vortex pairing events are observed in oceans [4] where they participate to the complex dynamics of the mesoscopic turbulence. The aim of the present study is to describe and parametrize the merging of two lenticular anticyclones by means of stratified flow experiments performed on a rotating table. For this purpose, we generate pairs of anticyclonic vortices by the gentle injection of a small volume of water inside a continuously stably stratified rotating layer in the same way that Griffiths and Hopfinger [5] did thirty years ago for a two layer system. Figure 1 presents an example of a sequence of such a merging.

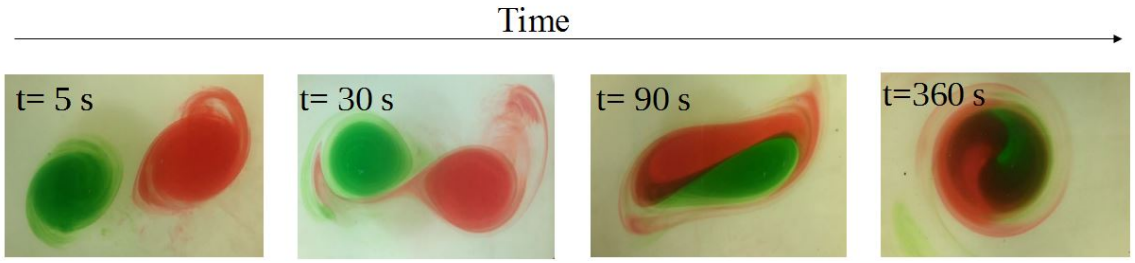

Figure 1: Temporal sequence of the merging of a pair of anticyclones for a Coriolis frequency $f = 1.57$ rad/s, a buoyancy frequency $N = 3.3$ rad/s and an initial separation $d_0 = 8$ cm.

Aside from describing the different regimes that lead or not to the coalescence of the pairs, in particular the determination of the critical initial separation distance [6] (to our knowledge this problem has never been revisited experimentally in the case of a continuously stratified layer), the final goal of this research will be to quantify the amount of the ageostrophic energy loss when two lenticular vortices are coalescing. Indeed, during the transient time of their merging, the dipolar unbalanced structure that forms radiate away internal gravity waves that will dissipate the excess of energy of the pair compared to the final balanced single anticyclone. Figure 2-a) presents a snap-shot of velocity field in a horizontal plane during

the coalescence of two anticyclones measured by PIV. In color scale, we represent also the horizontal divergence of the velocity field and the line along which space-time diagrams are calculated. Figure 2-b) shows such a space-time diagram of the divergence of the velocity field during the coalescence process. Waves whose frequency and horizontal wavenumber are compatible with internal gravity waves are clearly visible. We still have to prove that these waves are not emitted during the creation process of the vortices but are indeed caused by the unbalanced dynamics of their merging.

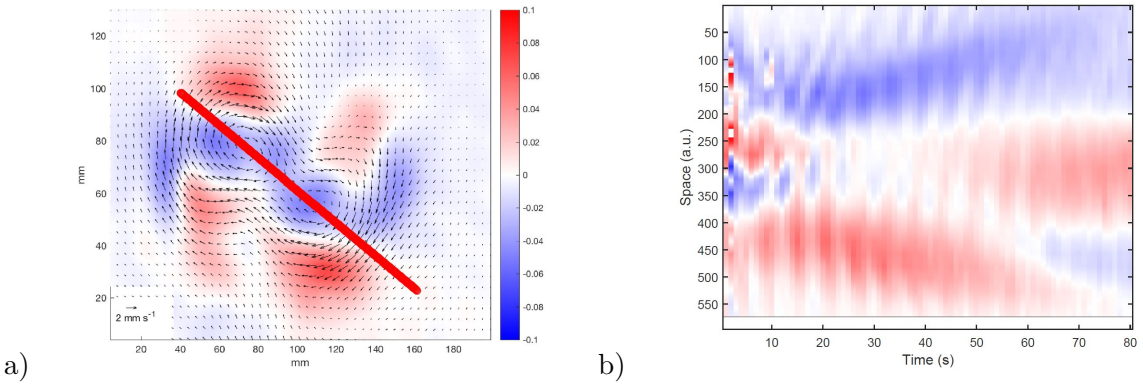

Figure 2: a) PIV velocity field in a horizontal plane during the coalescence of two anticyclones. In color scale, the horizontal divergence of the velocity field and the line along which space-time diagrams are calculated. b) An example of space-time diagrams of the horizontal divergence of the velocity field for a Coriolis frequency $f = 1$ rad/s, a buoyancy frequency $N = 1.18$ rad/s and an initial separation $d_0 = 5$ cm. Waves whose frequency and horizontal wavenumber are compatible with internal gravity waves are clearly visible.

References

[1] P. Hassanzadeh, P. S. Marcus, P. Le Gal, *The universal aspect ratio of vortices in rotating stratified flows: theory and simulation*, J. Fluid Mech. **706**, 4657, 2012.

[2] O. Aubert, M. Le Bars, P. Le Gal, P. S. Marcus, *The universal aspect ratio of vortices in rotating stratified flows: experiments and observations*, J. Fluid Mech. **706**, 3445, 2012.

[3] J.C. McWilliams, *Fluid dynamics at the margin of rotational control*, Environmental Fluid Mechanics, **8(5)**, 441-449, 2008.

[4] K.L.S. Tokos, H.H. Hinrichsen, W. Zenk, *Merging and migration of 2 meddies*, J. Phys. Oceanography **24 (10)**, 2129-2141, 1994.

[5] R.W. Griffiths, E.J. Hopfinger, *Coalescing of geostrophic vortices*, J. Fluid Mech. **178**, 73-97, 1987.

[6] D.G. Dritschel, *Vortex merger in rotating stratified flows*, J. Fluid Mech. **455**, 83-101, 2002.

Instability of the Taylor-Couette-Poiseuille flow with radial flux of a shear-thinning fluid

Cécile Lemaitre[1], Cherif Nouar[2], Yao Agbessil[1], Philippe Marchal[3], Lionel Choplin[4]

[1] LRGP, Université de Lorraine-CNRS, UMR 7274, 1 rue Grandville, 54000 Nancy

[2] LEMTA, Université de Lorraine-CNRS, UMR 7563, 2 av. de la Fort de Haye, 54500 Vandoeuvre-ls-Nancy

---

Cylindrical rotative filters are intensified separation processes used for example to separate blood plasma [1]. They are composed of two concentric cylinders of radii R_1 and R_2. The inner cylinder is porous and rotates at an angular velocity Ω. The suspension flows in the annular space between the two cylinders, under an axial pressure gradient G. During the flow, some liquid leaves the suspension to cross the porous inner wall (with a nondimensional flowrate per unit height q_f). At the outlet, the suspension thus has a higher particle concentration than at the inlet. If the inner cylinder rotates fast enough, Taylor vortices appear, similar to those occurring in Taylor-Couette flow, due to a hydrodynamic instability, but modified by the supplementary axial and radial flows existing in the filter. The stability of the Taylor-Couette-Poiseuille-radial flow occurring in the filter has already been investigated for Newtonian fluids [2], [3]. We generalize here these studies to purely viscous non Newtonian flows.

A radius ratio of $\eta = R_1/R_2 = 0.8$ is considered here, corresponding to a narrow gap between the cylinders. The conservation equations of mass and momentum, perturbated by infinitesimal perturbations are solved for different Reynolds number values $Re = \rho R_1 \Omega (R_2 - R_1)/\mu_0$, with ρ the fluid density and μ_0 its viscosity at low shear rates. We consider the rheological law of Carreau describing a shear-thinning behavior which reads in nondimensional form $\mu = (1 + \lambda^2 \dot{\gamma}^2)^{(n-1)/2}$ where $\dot{\gamma}$ is the second invariant of the nondimensional shear rate tensor. The critical conditions for instability (critical Reynolds number Re_c, axial and azimuthal wavenumbers, k_c and m_c) are calculated for different pressure gradients G, different radial flowrates q_f and different shear-thinning indices n.

The critical Reynolds number Re_c diminishes then grows for increasing flowrate q_f, going through a minimum Re_{cmin}, Fig. 1(a). The minimum locus q_{fmin} is negative (centripetal radial flow rate). Furthermore it is possible to compute critical conditions in a limited radial flowrate range $[q_{f1}, q_{f2}]$. Outside this interval, the flow is unconditionally stable. When the fluid becomes more shear-thinning (diminishing n), Re_{cmin} diminishes. The flowrate q_{fmin} is practically unchanged while the instability interval $[q_{f1}, q_{f2}]$ becomes narrower.

The critical axial wavenumber $k_c also$ presents a minimum k_{min} but its locus q'_{fmin} is different from q_{fmin}, 1(b). The minimum k_{min} decreases with decreasing n, while q'_{fmin} hardly changes. In the presence of an axial pressure gradient, $G = 1$, the curves $k_c(q_f)$ show slope discontinuities corresponding to azimuthal wavenumber m_c changes.

In the absence of axial pressure gradient $G = 0$, the critical azimuthal wavenumber m_c is always zero, indicating closed torus-shaped vortices. For $G = 1$ however, m_c is no longer zero que high enough values of $|q_f|$, Fig. 1(c). In this case, the vortices are helices wrapped around the inner cylinder. The extent of the flowrate interval for which $m_c = 0$ depends on the value of n.

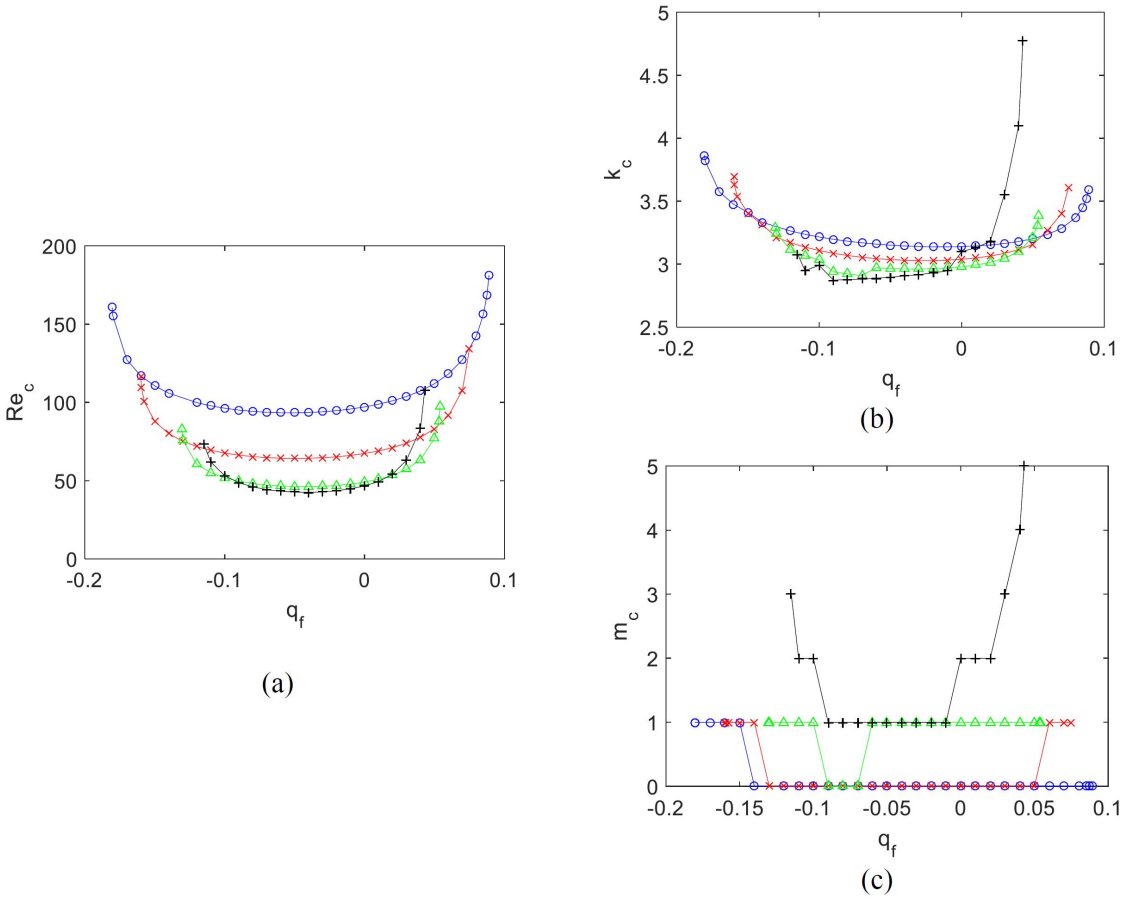

Figure 1: Critical conditions vs radial flowrate q_f for a pressure gradient $G = 1$. (a) Critical Reynolds number Re_c. (b) Critical axial wavenumber k_c. (c) Critical azimuthal wavenumber m_c. (o) Newtonian fluid ($n = 1$). Carreau fluid with $\lambda = 5$ et ($\times$) $n = 0.8$, ($\triangle$) $n = 0.6$, ($+$) $n = 0.5$.

References

[1] G. Beaudoin, M. Y. Jaffrin, *Plasma filtration in Couette flow membrane devices*, Artificial organs **13-1**, 43-51, 1989.

[2] E. C. Johnson, R. M. Lueptow, *Hydrodynamic stability of flow between rotating porous cylinders with radial and axial flow*, Phys. Fluids **9-12**, 3687, 1997.

[3] D. Martinand, E. Serre, R. M. Lueptow, *Absolute and convective instability of cylindrical Couette flow with axial and radial flows*, Phys. Fluids **21**, 104102, 2009.

Subcritical instability of Taylor–Couette flow with stationary inner cylinder

Juan M. Lopez[1],

[1] School of Mathematical and Statistical Sciences, Arizona State University, Tempe, AZ 85287, USA

The presence of endwalls in Taylor–Couette flows has far reaching effects, leading to dynamics that are qualitatively different to the idealized flow involving infinitely long cylinders. This is well known when the inner cylinder is rotating and the outer cylinder is stationary. The effects of endwalls in the centrifugally stable situation with stationary inner cylinder have not been previously considered in detail. The meridional flows induced by the endwalls lead to the formation of a thin sidewall boundary layer on the inner cylinder wall if the endwalls are rotating, or on the outer cylinder wall if they are stationary. At sufficiently high Reynolds numbers, the sidewall boundary layer has concentrated shear, the pressure gradient in the azimuthal direction (which is the streamwise direction for the boundary layer flow) is zero (the flow is axisymmetric) and the boundary layer thickness is constant. At a critical Reynolds number, the sidewall boundary layer loses stability at a subcritical Hopf bifurcation, breaking the axisymmetry of the flow, and for Reynolds numbers slightly above critical, a packet of Hopf modes with azimuthal wavenumbers clustered about the critical wavenumber grow. The early time evolution of the critical Hopf mode is a rotating wave analogous to a Tollmien–Schlichting wave. As the Hopf modes grow, nonlinear interactions lead to modulations, localization of the disturbances and the evolution of concentrated streamwise vortical streaks which become very long and intense via vortex stretching.

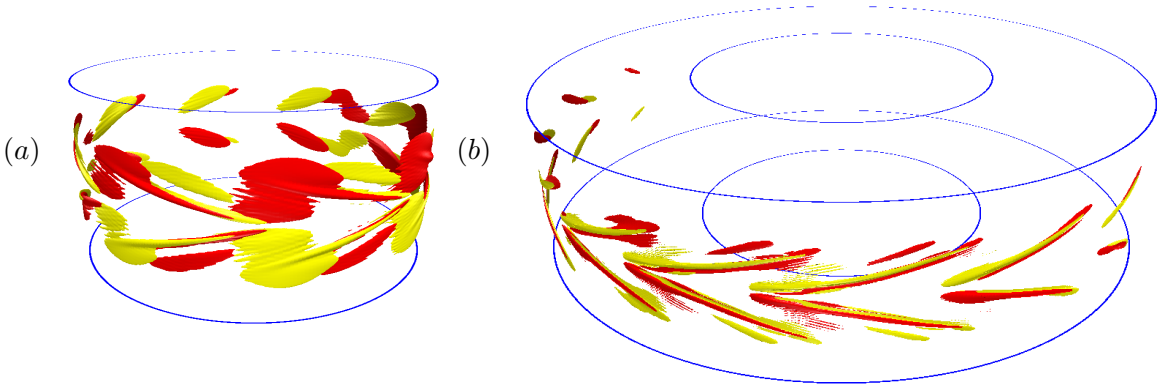

Figure 1: Isosurfaces of helicity He at $Re = 4\times10^5$ for (a) the case with the endwalls rotating with the outer cylinder, with levels $He = \pm7 \times 10^{10}$, and (b) the stationary endwalls case, with levels $He = \pm10^{12}$.

Figure 1 shows isosurfaces of the helicity He at late times for the two case discussed above. The helical structures are very flat and reside inside their respective cylinder boundary layer, whose radial thickness is only approximately 2% of the annular gap. The dark (red) isosurfaces correspond to positive He, where the velocity vector and the vorticity vector point

in the same direction, and the light (yellow) isosurfaces correspond to negative He, where the two vectors point in the opposite direction. The large value of He indicates that the velocity and vorticity are well aligned. The less developed structures have negative helicity in the top half and positive helicity in the bottom half of the boundary layer. These come about because they correspond to the Tollmien–Schlichting wavelike structures being bent by the streamwise azimuthal mean flow in the boundary layer about the mid-height. The wave structures at early times correspond to azimuthally alternating positive and negative axial (spanwise) vorticity cells spanning across the entire boundary layer from top to bottom. At later times, when they are bent into the streamwise (azimuthal) direction near the mid-height, the wave structures with positive axial vorticity are bent producing negative and positive azimuthal vorticity above and below the mid-height, and vice versa for the wave structures with negative axial vorticity. The wave structures with positive axial vorticity are stronger as they are reinforced by the positive axial vorticity from the mean boundary layer flow, which in turn weakens the wave structures with negative axial vorticity. Once the wavelike structures have been bent into the azimuthal direction, they are rapidly stretched and intensified by the mean flow. The azimuthally-turned structures from the alternating wavelike structures with positive and negative axial vorticity also become intertwined. The helicity indicates that the streamwise structures consist of pairs of very closely linked counter-rotating vortices; the velocity is in the streamwise (azimuthal) direction, but one of the vortices is left-handed and the other right-handed, resulting in opposite-signed helicity. This situation rapidly leads to small-scale instability as the vortices are intensified via stretching.

Taylor–Couette flow with endwalls and a stationary inner cylinder is subcritically unstable. The early time form of the perturbation modes consists of rollers of alternating sign of axial vorticity that are aligned in the axial direction in the boundary layer, and behave very much like Tollmien–Schlichting waves in shear boundary layers with zero streamwise pressure gradient, where a band of waves with different wavenumbers grow leading to modulation and secondary instability. The sidewall boundary layer is very thin, implying that curvature effects are not important. The shear flow nature of the instability is initiated by vortex bending and brought to fruition by vortex stretching.

References

[1] J. M. Lopez, *Subcritical instability of finite circular Couette flow with stationary inner cylinder*, J. Fluid Mech., **793**, 589-611, 2016.

Acknowledgements

This work was supported by NSF grant CBET-1336410 and NASA grant NNX13AQ22G.

Taylor Couette Flow with Imposed Radial and Axial Flows– A Weakly Nonlinear Analysis

Richard M. Lueptow[1], Denis Martinand[2], Eric Serre[2]

[1] Northwestern Univ., Evanston, IL, USA

[2] Aix-Marseille Univ., CNRS, Centrale Marseille, M2P2, Marseille, France

---

The linear stability analysis of Taylor-Couette flows where axial and radial through-flows are superimposed is extended to consider the weakly nonlinear behavior of convective-type instabilities using a fifth-order amplitude equation and numerical simulations. Special attention is paid to the influence of the radius ratio η, particularly as the gap increases to become very wide (η increases from top to bottom in Figure 1), which magnifies the impact of the radial Reynolds number α. The instabilities take the form of pairs of counter-rotating

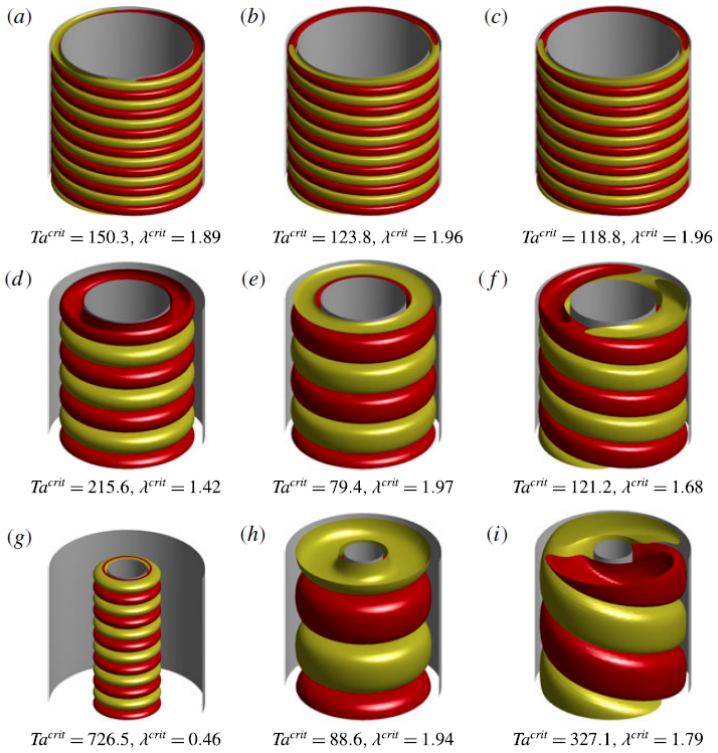

Figure 1: Modes of instabilities for $\beta = 20$ and (a) $\eta = 0.85$ and α = -10, (b) $\eta = 0.85$ and $\alpha = 0$, (c) $\eta = 0.85$ and $\alpha = 10$, (d) $\eta = 0.55$ and α = -10, (e) $\eta = 0.55$ and $\alpha = 0$, (f) $\eta = 0.55$ and $\alpha = 10$, (g) $\eta = 0.25$ and α = -10, (h) $\eta = 0.25$ and $\alpha = 0$, (i) $\eta = 0.25$ and $\alpha = 10$. Isosurfaces of the radial velcoity of the instability are shown at 0.2 (red) and -0.2 (yellow) of the maximum value. The critical Taylor number and wavelength are indicated. Reprinted with permission [1].

toroidal vortices superseded by helical ones as the axial Reynolds number β is increased. Increasing the radial inflow (negative α) draws the vortices toward the inner cylinder, where they shrink relative to the annular gap when the gap is wide (Figure 1(d, g, h)). Strong axial and radial flows lead to steeply sloped helical vortices. Strong radial outflow (positive α) in a wide annular gap results in very large helical vortices (Figure 1(i)). In addition, radial inflows or outflows can change the supercritical bifurcation from laminar to vortical flow to become a subcritical bifurcation. The radial flow above which this change occurs decreases as the radius ratio decreases.

References

[1] D. Martinand, E. Serre, R. M. Lueptow, *Linear and weakly nonlinear analyses of cylindrical Couette flow with axial and radial flows*, J. Fluid Mech. **824**, 438-476, 2017.

Acknowledgements

This work was granted access to the HPC resources of IDRIS under the allocation 2016242 made by GENCI (Grand Equipement National de Calcul Intensif).

Taylor-Couette Flow of Fluid-Particle Suspension

Madhu V. Majji[1], Sanjoy Banerjee[2], Jeffrey F. Morris[3]

[1] Department of Chemical Engineering, Stanford University, Stanford, California 94305, USA

[2] Energy Institute,CUNY City College of New York,New York,NY10031,USA

[3] Benjamin Levich Institute,CUNY City College of New York,New York,NY10031,USA

Diverse flow structures are generated when a fluid is sheared in the annulus between two concentric cylinders. This flow system can be used to probe the dynamical behavior of fluid-particle suspension flows by comparing flow structures and transitions in regime with the extensively studied and well established Taylor-Couette flows of a Newtonian fluid. Fundamental understanding of suspension fluid dynamics is essential due to the applications in wide ranging fields including oil, pharmaceutical and power industries and biological flows including blood flow.

We report the results of experiments in which a neutrally buoyant suspension was sheared between a rotating inner cylinder and a concentric stationary outer cylinder. The radial gap between the two cylinders is $\delta = 7$ mm. The radius ratio and the aspect ratio of the apparatus are $\eta = r_i/r_o = 0.877$ and $\Gamma = L/\delta = 20.5$ respectively where L is the axial height of the cylinders and r_i and r_o are radii of the inner and outer cylinders. The inner cylinder rotation rate, Ω, is non-dimensionalized to give a Reynolds number, $Re = \delta r_i \Omega \rho/\mu$, where ρ and μ are the density and effective viscosity of the working fluid. The suspension was prepared by mixing non-Brownian poly-(methyl methacrylate) particles in a mixture of water and glycerol of 1 : 2 weight ratio to match the fluid density to that of the particles at 20°C. Two particle sizes with average diameters $d_p = 230$ μm and 70 μm to yield $\alpha = \delta/d_p = 30$ and 100, respectively, were used to study the effect of particle size on the flow behavior. Effects of particle concentration were studied by varying the particle volume fraction (ϕ) between $\phi = 0$ and $\phi = 0.3$. Illuminating flakes in very dilute concentration were added to the suspension to visualize and record the flow structures using a high speed camera. The protocol followed in the experiments was to first establish wavy vortex flow (WVF) at higher Re reduce the value of Re slowly until the flow transitioned into circular Couette flow (CCF).

Figure 1 shows the effect of particles on the flow transitions for $\alpha = 30$ suspension. When Re was reduced, pure fluid ($\phi = 0$) transitioned from WVF to Taylor vortex flow (TVF) to CCF. Significant deviations from the pure fluid behavior occur when particles are present. For example, a $\phi = 0.1$ suspension, as shown in the space-time diagrams in figure 1(a), transitioned from WVF to TVF to spiral vortex flow (SVF) to ribbons (RIB) to CCF. In addition to the appearance of non-axisymmetric flow structures (SVF and RIB) between TVF and CCF, the Re corresponding to all the flow transitions for the $\phi = 0.1$ suspension reduced significantly compared to the pure fluid. When the particle size was reduced to yield $\alpha = 100$, the non-axisymmetric region between TVF and CCF disappeared indicating, as expected, that the size of the particles plays a role in the observed deviations. Compiled in figure 1(b) are the effect of particle concentration on various flow transition Re and flow structures for $0 \leq \phi \leq 0.3$. For dilute suspensions ($\phi < 0.05$), the suspension exhibited the same flow structures as the pure fluid but the transition Re reduced with increasing

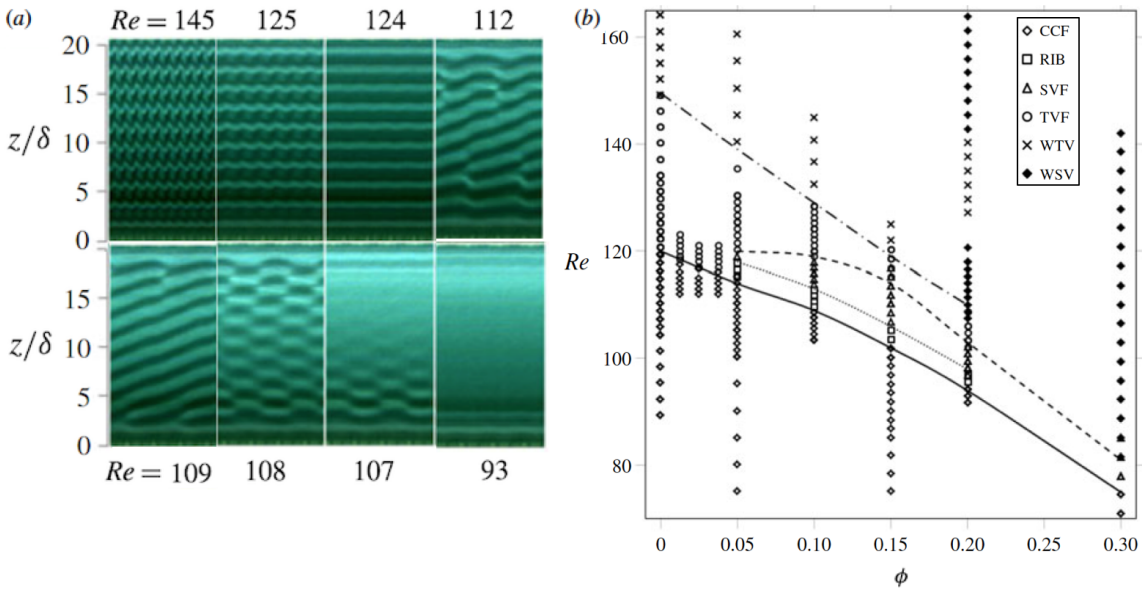

Figure 1: (a) Space-time diagrams showing flow transitions: WVF-TVF-SVF-RIB-CCF (see text for definitions), for $\phi = 0.1$ and $\alpha = 30$ suspension when the inner cylinder Re was reduced from $Re = 145$ to $Re = 93$; (b) Effect of particle concentration on flow transition Re for suspension with $\alpha = 30$. Symbols indicate various flow states and Dashed and solid lines indicate various flow transition boundaries.

concentration. For $0.05 \leq \phi \leq 0.15$, non-axisymmetric flow structures appeared between TVF and CCF. With increasing ϕ, the range of Re yielding stable non-axisymmetric flow structures increased and the transition Re for al the flow transitions was reduced significantly. At higher concentrations, as shown for $\phi = 0.3$, the transition series consisted only of non-axisymmetric structures: wavy spiral vortices (WSV) to SVF to RIB to CCF. In addition, the Re at which flow transitioned into CCF was $Re \approx 75$ compared to $Re = 120$ of the pure fluid. The spiral structures observed here are of mode $m = 1$ and the ribbon structures are a combination of two mode $m = 1$ spirals, one left winding and one right winding. Our experiments with very dilute suspensions ($\phi \ll 0.01$) showed inertial migration of particles in CCF and TVF. Initially uniformly distributed particles in CCF at $Re = 82$ migrated to an equilibrium position that is 0.4δ from the inner cylinder. In TVF, particles focused in a circular equilibrium limit cycle (with radius dependent on Re within the TVF range) in each vortex when observed in $r - z$ cross section. The results are recently published in [1] [2].

References

[1] M.V. Majji, S. Banerjee, J.F. Morris, *Inertial flow transitions of a suspension in Taylor-Couette geometry*, Journal of Fluid Mechanics, 835, 936-969, 2018.

[2] M.V.. Majji, J.F. Morris, *Inertial migration of particles in Taylor-Couette flows*, Physics of Fluids 30(3), 033303, 2018.

Global modes in Taylor–Couette–Poiseuille flow with a permeable inner cylinder

Denis Martinand[1], Nils Tilton[2],

[1] Aix-Marseille Univ., CNRS, Centrale Marseille, M2P2, France

[2] Mechanical Engineering, Colorado School of Mines, Golden, CO 80401 USA

Variations in the local stability of the flow in a Taylor–Couette cell can be imposed by adding an axial Poiseuille flow and a radial flow associated with the a weakly permeable inner cylinder through which the radial flow is governed by Darcy's law. At a given rotation rate of the inner cylinder, this results in adjacent regions of the flow that can be simultaneously stable, convectively unstable, and absolutely unstable, making this system fit for obtaining global, synchronized, modes of centrifugal instability.

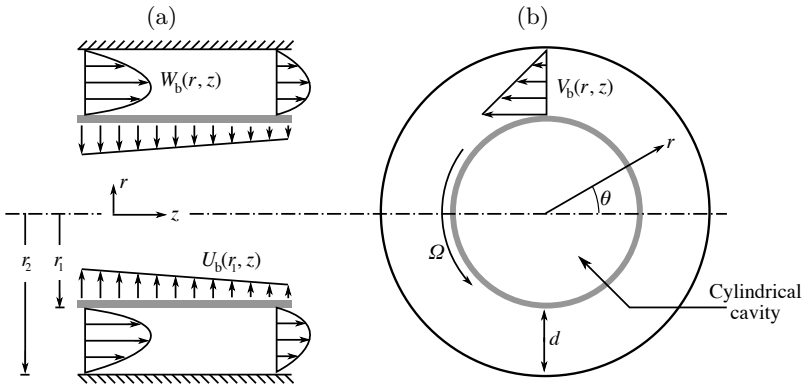

Figure 1: (a) Radial and axial velocities of the laminar Taylor–Couette–Poisuille (TCP) flow. The outer cylinder is impermeable while fluid flows across the inner permeable cylinder, according to Darcy's law, leading to a base flow varying along the axial direction. (b) shows the azimuthal velocity of the base flow in an equatorial plane.

A two-pronged approach is adopted. First, building on the existing convective/absolute stability analysis in the axially invariant TCP flow with impermeable cylinders [1], the analytical frameworks of linear and non-linear global modes are used to obtain the critical conditions and characteristics of the instabilities in the axially varying flow with a permeable inner cylinder. These analyses are based on the selection of a specific axial location that acts as a wavemaker and imposes its unstable dynamics and frequency to the rest of the perturbation. Then, Direct Numerical Simulations using a dedicated pseudospectral method implementing the Darcy's condition on the permeable cylinder [2] are performed to shed new light on the validity of the analyses in global modes. Guided by application to filtration devices, we consider a set-up where fluid extraction occurs along the full length of the inner cylinder. As one moves downstream, the mean axial flow decreases and so does the local stability of the

base flow. Close to critical conditions, the global mode is governed by a linear wavemaker located at the outlet, in agreement with the wavepacket of toroidal vortices obtained in the DNS shown in Figure 2(a). As the rotation rate is increased, the linear global mode evolves to a non-linear global mode governed by wavemaker located at the boundary between the convectively and absolutely unstable regions, in agreement with the DNS shown in Figure 2(b). The global mode analyses do not fully explain, however, that the instabilities observed in the numerical simulations take the form of axial stacks of wave-packets, as observed in Figure 2(b), characterized by step-downs of the temporal frequency.

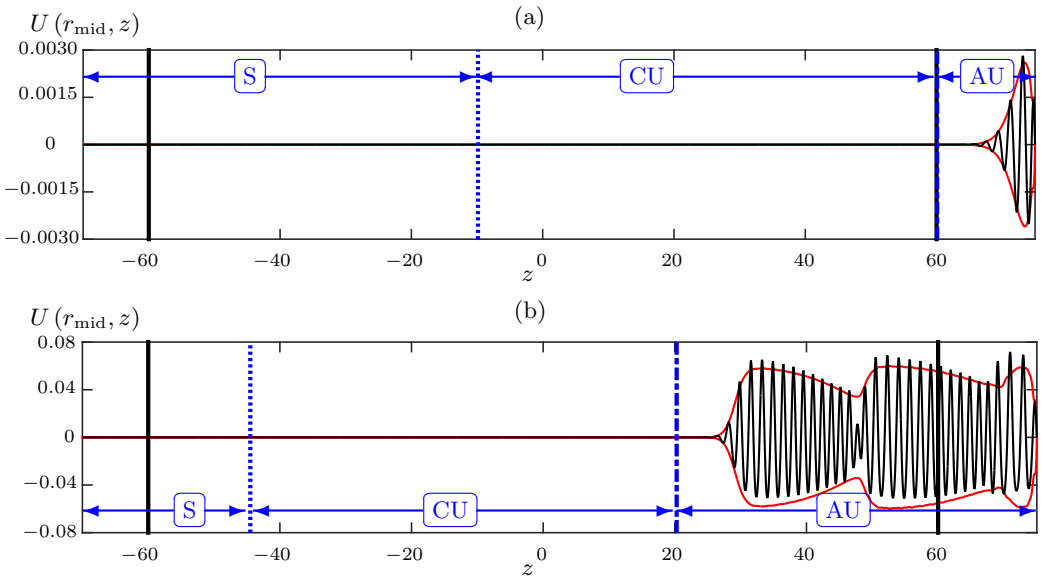

Figure 2: Direct Numerical Simulation of TCP flow with a permeable inner cylinder: radial velocity at mid-gap, as a function of the axial coordinate z. The rotation rate of the inner cylinder is 0.6% (a) and 16% (b) above its analytical critical value. The stable, convectively unstable and absolutely unstable regions are denoted by blue S, CU and AU, respectively.

References

[1] D. Martinand, E. Serre and R. M. Lueptow, *Absolute and convective instabily of cylindrical Couette flow with axial and radial flows*, Phys. Fluids, **21**, 104102, 2009.

[2] N. Tilton, E. Serre, D. Martinand and R. M. Lueptow, *A 3D pseudospectral algorithm for fluid flows with permeable walls. Application to filtration*, Comput. Fluids, **93**, 129–145, 2014.

Vortex Dynamics in Couette-Taylor Flow with Axial Distribution of Temperature

Hayato Masuda[1], Saho Yoshida[2], Takafumi Horie[1], **Naoto Ohmura**[2], Makoto Shimoyamada[1]

[1] School of Food and Nutritional Science, University of Shizuoka, 52-1 Yada, Suruga, Shizuoka 422-8526, Japan

[2] Department of Chemical Science and Engineering, Kobe University, 1-1 Rokkodai, Nada-ku, Kobe 657-8501, Japan

---

This presentation introduces our work [1] which experimentally investigated the vortex dynamics of a Couette-Taylor flow with an axial distribution of temperature. The apparatus comprises concentric cylinders (length: $L = 112.3$ mm), a rotating inner cylinder (outer radius: $R_o = 25$ mm), a fixed outer cylinder (inner radius: $R_i = 38$ mm), and a water jacket divided into two parts, as shown in Figure 1. The temperature of the lower half of the water jacket, T_1, was set as 60 °C and that of the upper half, T_2, was varied from 20 to 50 °C. An aqueous solution of 40 wt% glycerin was used as the working fluid. The flow pattern was visualized using an aqueous solution seeded with Kalliroscope AQ-1000 flakes (0.1 wt%).

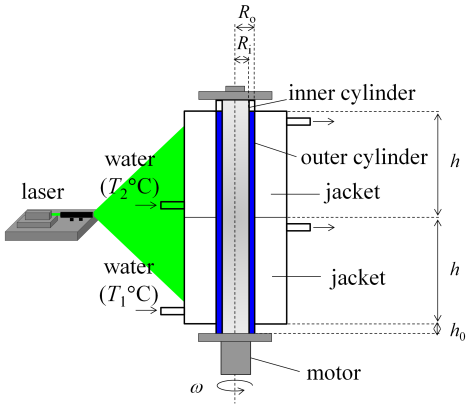

Figure 1: Experimental apparatus.

The flow patterns can be mapped in a Grashof number (Gr) and Reynolds number (Re) plane and they classified into three patterns based on the balance between the centrifugal force and the buoyancy, as shown in Figure 2. If the buoyancy is dominant, global heat convection is observed instead of Taylor vortices (Case I). When the buoyancy is comparable to the centrifugal force, the Taylor vortices and global heat convection appear alternately (Case II). If the centrifugal force is sufficiently high to suppress the buoyancy, stable Taylor vortices are observed (Case III). The characteristics of the mixing/diffusion are investigated by conducting a decolorization experiment on a passive tracer, as shown in Figure 3. In Case II, the tracer is rapidly decolorized in the presence of the global heat convection instead of the Taylor vortices. This result implies that the interaction between the centrifugal force and the buoyancy would induce an anomalous transport.

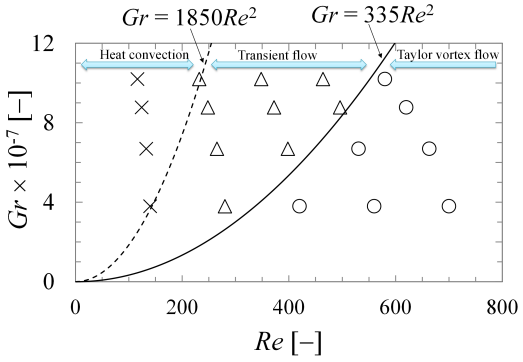

Figure 2: Flow map based on flow visualization. The dash and solid line empirically show the flow boundaries.

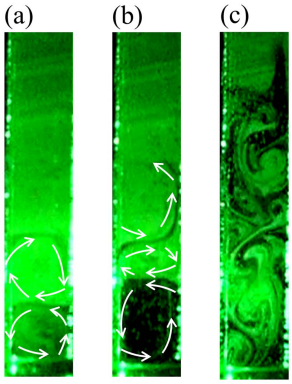

Figure 3: Observed vortices at each stage in Case II ($Re = 496$, $Gr = 8.8 \times 107$): (a) stable Taylor vortices, (b) deformed Taylor vortices, and (c) collapsed Taylor vortices. Arrows in figures denote the vortex motion.

References

[1] H, Masuda, S. Yoshida, T. Horie, N. Ohmura, M. Shimoyamada, *Flow Dynamics in Taylor-Couette Flow Reactor with Axial Distribution of Temperature*, AIChE J., **64**, 1075–1082, 2018.

Acknowledgements

This research project is supported by JSPS KAKENHI Grant Number JP18H03853.

A path following algorithm to compute bifurcation diagrams in confined natural convection problems involving Bingham fluids

Marc Medale[1], Bruno Cochelin[2]

[1] Aix-Marseille Université, CNRS, IUSTI UMR 7343, 13453 Marseille, France.

[2] LMA, Centrale Marseille, UPR 7051 CNRS, 13451 Marseille, France.

The classical way to determine bifurcation diagrams in problems where the base-state solution has no analytical expression usually consists in performing a sequence of two tasks for a series of control parameter values [1]: i) compute the base state associated to a given value of the control parameters; ii) compute the linear stability of the given base state.

The present work presents a computationally efficient solution to the first of these two steps for large size algebraic systems resulting from the discretization of coupled energy and incompressible Navier-Stokes equations. Among continuation algorithms, first order predictor-corrector algorithms with pseudo-arc-length parameterization have been widely used for decades [2, 3, 4]. Nevertheless, it turns out that step-length adaptivity may be in trouble in the vicinity of bifurcation points leading to a weak computational efficiency and sometimes lack of convergence. An alternate way to first order predictor algorithms stands in high-order predictors that have been introduced in continuation algorithms based on the Asymptotic Numerical Method [5]. This method combines high-order Taylor series expansion, discretization technique and parameterization strategy, which results in a general and efficient non-linear solution method. In this framework, power series analysis enables to accurately detect and compute simple bifurcation points in the course of the ANM continuation [6, 7].

This paper presents bifurcation diagrams performed with our numerical model based on ANM continuation for a confined Rayleigh-Bénard configuration where the working fluid obeys the Bingham model under the Boussinesq's approximations. The confining box has aspect ratios of L/h=10 and l/h=4 and the fluid properties are defined by Pr=9, Bn=1. Figures 1 and 2 present bifurcation patterns at threshold and second steady-state bifurcation and corresponding bifurcation diagram, respectively. Unlike Newtonian fluids, the pattern at threshold is a combination of square cells and rolls, and the bifurcation nature at threshold is no longer a pitchfork one, but a transcritical one (subcritical).

References

[1] H. Dijkstra *et al.* Numerical bifurcation methods and their application to fluid dynamics: Analysis beyond simulation. *Commun. Comput. Phys.*, Vol. **15**, 1–45, 2014.

[2] H. B. Keller. *Numerical solution of bifurcation and nonlinear eigenvalue problems.* Academic Press, New York, 1977.

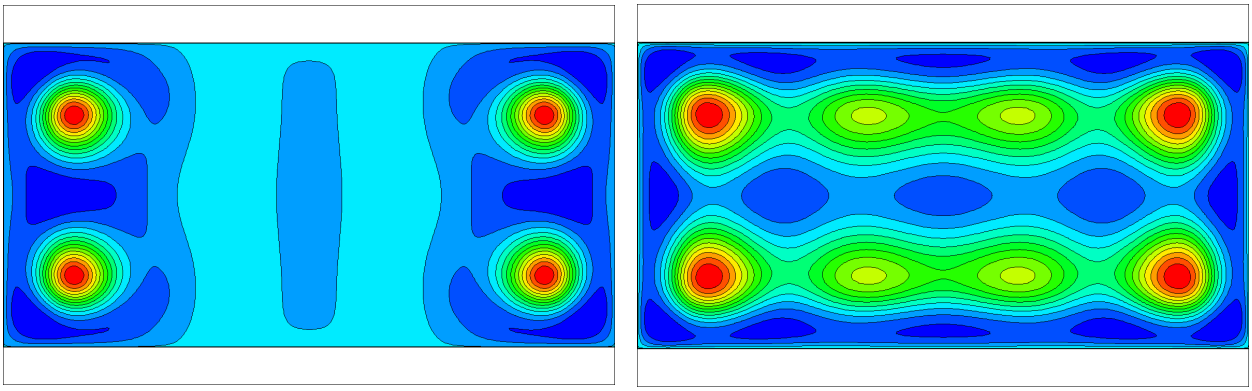

1st bifurcation mode: Ra_{c1}=2671.6 2nd bifurcation mode: Ra_{c2}=3139.1

Figure 1: Bifurcation patterns at threshold (left) and second steady state bifurcation (right).

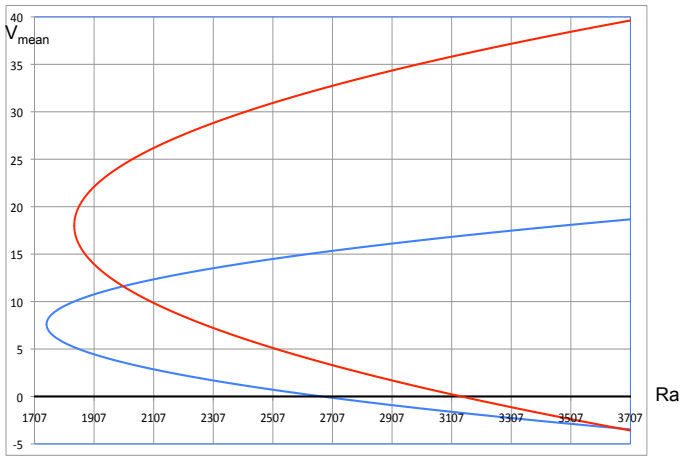

Figure 2: Bifurcation diagram: fondamental branch (black line), bifurcated ones from threshold (bleu line) and second steady state bifurcation (red line).

[3] E. Doedel, H. B. Keller and J. P. Kernevez. Numerical analysis and control of bifurcation problems (i) bifurcation in finite dimensions. *Int. J. Bifurcation and Chaos*, Vol. **3**, 493–520, 1991.

[4] R. Seydel. *Practical bifurcation and stability analysis*. Springer-Verlag, 1994.

[5] B. Cochelin, N. Damil and M. Potier-Ferry. *Méthode Asymptotique Numérique (in french)*. Hermès - Lavoisier, 2007.

[6] B. Cochelin and M. Medale. Power series analysis as a major breakthrough to improve the efficiency of Asymptotic Numerical Method in the vicinity of bifurcations. *J. Comput. Phys.* Vol. **236**, 594–607, 2013.

[7] M. Medale and B. Cochelin. High performance computations of steady-state bifurcations in 3D incompressible fluid flows by Asymptotic Numerical Method. *Journal of Computational Physics*, Vol. **299**, pp. 581–596, 2015.

Experimental Confirmation of Linear Stability Results on Stratified Taylor-Couette Flows

Gabriel Meletti[1], Uwe Harlander[1], Torsten Seelig[1], Stéphane Viazzo[2], Stéphane Abide[3], Andreas Krebs[1], Anthony Randriamampianina[2], Isabelle Raspo[2]

[1] Brandenburg University of Technology CottbusSenftenberg, LAS, Germany

[2] Aix-Marseille Univ., CNRS, Centrale Marseille, M2P2, France

[3] Univeristé de Perpignan Via Domitia, LAMPS EA 4217, Perpignan, France

---

Understanding the mechanisms that can result in an outward transport of angular momentum is a central problem regarding astrophysical objects formation, particularly in the theory of accretion, on which turbulence might explain this phenomenon in accretion discs [1]. Among other candidates, the Strato Rotational Instability (SRI) has attracted attention in recent years as a possible instability leading to turbulent motion in these systems. The SRI is a purely hydrodynamic instability consisting of a classical Taylor-Couette (TC) system with stable density stratification due to, for example, salinity or a vertical temperature gradient.

Many information about the SRI can be obtained from numerical simulations and particularly designed laboratory experiments of axially-stratified TC setups, as the one in the laboratory of Aerodynamics and Fluid Mechanics (LAS) of the Brandenburg University of Technology (BTU) Cottbus-Senftenberg. For obtaining a stable density stratification along the cylinder axis, the bottom lid of the setup is cooled, and its top part is heated, establishing an axial linear temperature gradient between 3K and 5K per 0.7m.

Numerical simulations using the same configuration as the BTU experiment have been performed at the M2P2 laboratory at the Aix-Marseille University (AMU), and at the LAMPS laboratory at the University of Perpignan, with the temperature difference set as 4K between the bottom and top parts of the cylinder.

The inner and outer cylinders on the experimental setup rotate independently, each one driven by a DC motor unit controlled by servo amplifiers. The experimental results presented were obtained at a fixed rotation ratio of $\mu = \Omega_{out}/\Omega_{in} = 0.35$, where Ω is the angular velocity of the cylinder. The velocity profiles shown are obtained from *Particle Image Velocimetry* (PIV), with the camera co-rotating with the outer cylinder. The PIV measurements absolute error is of less than 2%, and all experiments were repeated at least 2 times at different days, so that the result's reproducibility could be guaranteed.

The experimental results obtained with PIV are in agreement with the linear stability curves presented in [2] for constant values of Rn, a stratification related Reynolds number. The linear stability curve for Rn=250 (adapted from [2]) is shown as a black solid line in figure 1, where some of the experimental results obtained during this work are also represented along the vertical red line of constant $\mu = 0.35$.

The red triangles represent unstable flows obtained for $Re = 400$, $Re = 600$, and $Re = 800$, while the blue circle represents the stable case when $\mu = 0.35$, $Rn = 250$, and $Re = 1000$. As it can be seen in fig.1, the stable case is just outside the marginal linear stability line. All the other experiments are inside the unstable regions. The instability can be observed

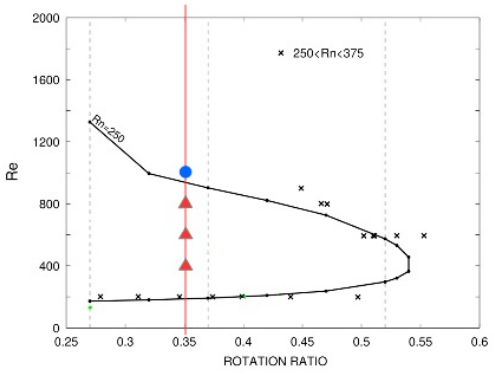

Figure 1: Linear stability map for Rn=250. The solid red vertical line refers to the constant rotation ratio ($\mu = 0.35$) of the performed experiments. The red triangles are unstable cases, and the blue circle represents stable cases.

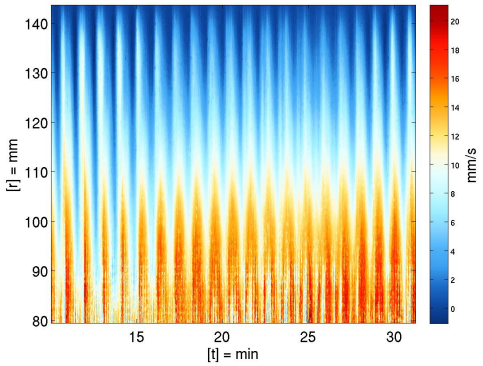

Figure 2: Hovmöller plot showing the azimuthal velocity as function of radius at constant angle and time. Parameters: Re=600, $\mu = 0.35$, $\Delta T \approx 5K$, N=0.320, $Fr \approx 1.2$

in the Hovmöller plots (figure 2), as well as in the analysis of the Reynolds stress tensor components (e.g., $-\rho u'v'$), since it is zero for the stable case, and non-zero when the flow is SRI unstable.

Comparisons of the experimental results with numerical simulations using the codes described in [3] and [4] did show a good agreement regarding the SRI frequencies and the mean velocity profiles obtained. New high-performance numerical simulations considering all the same input parameters as the experiments shown in this abstract are now being performed for further comparison with linear stability analysis.

References

[1] P. J. Armitage. *Astrophysics of Planet Formation.* Cambridge University Press, 2009.

[2] G. Rüdiger, T. Seelig, M. Schultz, M. Gellert, U. Harlander, and C. Egbers. The stratorotational instability of Taylor-Couette flows with moderate Reynolds numbers. *Geophysical & Astrophysical Fluid Dynamics*, 111(6):429–447, 2017.

[3] U. Harlander, T. Seelig, M. Gellert, S. Viazzo, A. Randriamampianina, C. Egbers, and R. Günther. Stratorotational instability in a thermally stratified Taylor-Couette flow. In *EGU General Assembly Conference Abstracts*, volume 17, 2015.

[4] S. Abide, M. S. Binous, and B. Zeghmati. An efficient parallel high-order compact scheme for the 3D incompressible Navier–Stokes equations. *International Journal of Computational Fluid Dynamics*, 31(4-5):214–229, 2017.

Acknowledgements

The authors thank the Deutsche Forschungsgemeinschaft (DFG) for financial support.

DFG Core Facility Center: Physics of rotating Fluids

Sebastian Merbold[1], Uwe Harlander[1], **Christoph Egbers**[1]

[1] Dept. of Aerodynamics and Fluid Dynamics, BTU Cottbus-Senftenberg, Cottbus, Germany

---

The present project aims to establish a new international research center (core facility center) for "Physics of Rotating Fluids (PRF)" with geo-/astrophysical, meteorological and technical applications located at Brandenburg University of Technology Cottbus-Senftenberg. The main goal is to integrate cutting-edge rotating and stratified fluid flow experiments across national boundaries in order to foster internationally competitive experimental research in the field of rotating and stratified fluids by providing an easy access to experimental facilities equipped with state-of-the-art instrumentation.

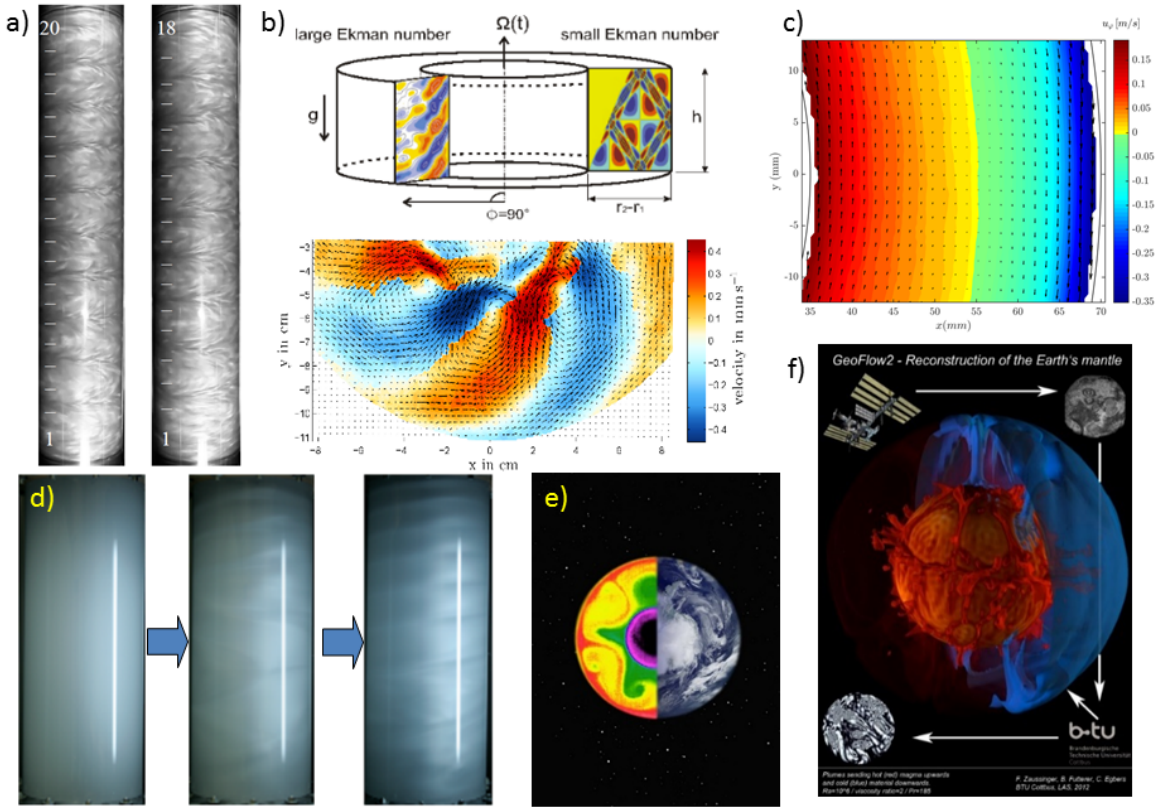

Figure 1: Overview on the DFG Core Facility Centre 'Physics of Rotating Fluids'. a) Turbulent Taylor-Couette flow b) Quasi-Biannual Oscillation c) PIV measurements in rapidly rotating geometries d) Strato-rotational instability e) Waves in tmospheres f) GeoFlow project.

The research areas covered by the experimental facilities inside the new center are: Planetary and astrophysical flows (with focus on disk formation, instabilities and mixing), geophysical

fluid dynamics (with focus on strato-rotational turbulence, mean flow generation and wave interaction) as well as rotating flows with technical applications (centrifuges, turbines, journal bearings and rotor/stator cavities). The new center of "Physics of Rotating Fluids (PRF)" will cover and focus all previous single research and guest scientist exchange activities like EUHIT, CNRS French/German-co-operation and ESA Topical Team with BTU/CFTM2 in the field of rotating and stratified fluid flows. As an overview of the performance of the Core Facility Centre we briefly present various topics involved (Fig. 1).

The experiments on rotating fluids are setup and ready for guest use within the DFG core facility centre. For example turbulent Taylor-Couette flow including torque measurements [1] and velocity measurements [5] are performed within the center, stratorotational instabilities are studied [2], Inertial waves are excited in the quasi-biannual oscillaton tank [3] or wave instabilities in spherical shells are investigated [4]. Apart from this the variety of the Core Facility Center on Physics of Rotating Fluids does not become depleted.

References

[1] S. Merbold, H.J. Brauckmann, C. Egbers *Torque measurements and numerical determination in differentially rotatingnwide gap Taylor-Couette flow.*, Phys. Rev. E , **87**, 023014, 2013.

[2] G. Ruediger, T. Seelig, M. Schultz, M. Gellert, C. Egbers, U. Harlander *The stratorotational instability of Taylor-Couette flows with moderate Reynolds numbers.*, Geophys. and Astro.-Phys. Fluid Dyn. , **111**, 6, 2017.

[3] M. Klein, T. Seelig, M.V. Kurgansky, A. Ghasemi, I.-D. Borcia, A. Will, E. Schaller, C. Egbers, U. Harlander *Inertial wave excitation and focusing in a liquid bounded by a frustrum and a cylinder*, JFM , **751**, 255-297, 2014.

[4] M. Hoff, U. Harlander, C. Egbers *Experimental survey of linear and nonlinear waves and wave instabilities in a spherical shell.*, JFM , **789**, 589-616, 2016.

[5] A. Froitzheim. S. Merbold, C. Egbers *Velocity profiles, flow structures and scalings in a wide-gap turbulent Taylor-Couette flow.*, JFM , **831**, 330-357, 2017.

Acknowledgements

The authors gratefully acknowledge the funding of DFG under grant EG100/23-1 and HA2932/10-1 and European High Performance Infrastructures in Turbulence (EuHIT).

Shear flow instabilities in stretching channels and twisted pipes

Alvaro Meseguer[1], Francisco Marques[1], Fernando Mellibovsky[1], Patrick Weidman[2]

[1] Department of Physics, Universitat Politècnica de Catalunya, Barcelona, Spain

[2] Department of Mechanical Engineering, University of Colorado, Boulder, USA

Extensional self-similar flows appear in channels or pipes with accelerating, pulsating or porous walls with uniform suction and/or injection. In all the aforementioned cases, the boundary conditions at the walls are modelled by assuming the streamwise velocity of the fluid as being linearly proportional to the streamwise coordinate, leading to an exact Navier-Stokes self-similar flow governed by the Proudman-Johnson nonlinear differential equation. Steady flows arising between symmetrically stretching parallel plates and axially stretching pipes were addressed in the early 80s [1]. The emergence of time periodic flows between symmetrically stretching plates and their eventual destabilization to chaotic regimes were identified by many authors in the early 90s [4]. Later studies also explored steady flows arising for the particular asymmetrical case based on one plate at rest and the other stretching [5]. More recent works have addressed the validity of the self-similar anstatz in extensional channels when compared with actual two-dimensional Navier-Stokes direct numerical simulations [2].

In this talk we will outline the most relevant findings recently reported in [3], where we explore steady and time-periodic self-similar flows in channels with general stretching-shrinking boundary conditions, therefore unfolding the particular explorations carried out in the past by many authors to arbitrary stretching rates at the top and lower boundary plates. We numerically integrate the nonlinear boundary value problem using a Legendre spectral method and determine the steady flow solution in the channel. These steady flows are continuated in the two-dimensional parameter space characterized by the Reynolds number and the stretching-shrinking rate of the top and bottom plates. These flows exhibit codimension-2 bifurcations that are carefully studied. These bifurcations lead to instabilities and sometimes to time periodic solutions which are also continuated in the parameter space and whose stability is also monitored through Floquet exponents computation.

In this talk we will also briefly describe current ongoing explorations on flows arising in axially stretching-shrinking and azimuthally twisting pipes, where not only the classical steady flows found in [1] are unfolded throughout the stretch-shrink-twist parameter space, but also new time-periodic regimes (some of them linearly stable) have been identified.

References

[1] Brady, F. and Acrivos, A., *J. Fluid Mech.* **112** (127), 1981.

[2] Espín, L. , Papageorgiou, D. T. , *Phys. Fluids* **21** (113601), 2009.

[3] Marques, F.,Meseguer, A., Mellibovsky, F., Weidman, P. D., Proc. Roy. Soc. A **473** (20170151), 2017.

[4] Watson, E. , Banks, W., Zaturska, M. and Drazin, P., *J. Fluid Mech.* **212** (451), 1990.

[5] Wang, C. A. and Wu, T. C., *Computers Math. Applic.* **30**(1), 1995.

Acknowledgements

supported by the Spanish Government grant no. FIS2017-85794-P. The Catalan Government support of the authors in UPC, members of the research group 2017-SGR-785, is greatly acknowledged.

Experiments on thermoelectric convection induced in a cylindrical annulus under microgravity conditions

Antoine Meyer[1], Marcel Jongmanns[1], Martin Meier[1], Torsten Seelig[1], Changwoo Kang[2], Innocent Mutabazi[2], Christoph Egbers[1]

[1] Lehrstuhl Aerodynamik und Strömungslehre (LAS) - Brandenburgische Technische Universität Cottbus-Senftenberg, Siemens-Halske-Ring 14, 03046 Cottbus, Germany

[2] Laboratoire Ondes et Milieux Complexes (LOMC) - CNRS : UMR6294, Université du Havre - 53, rue de prony, 76058 Le Havre Cedex, France

---

When an a.c. high voltage is applied to a dielectric fluid which exhibits an electric permittivity gradient, the dielectrophoretic (DEP) force appears and can be regarded as a thermal buoyancy associated to an effective electric gravity [1, 2]. We developed an experimental set-up to study thermoelectric convections induced by the DEP force. The dielectric liquid is confined between two concentric cylinders, which are maintained at different temperatures and different electric potentials, creating a radially oriented electric gravity field [3] (Fig. 1 left). In order to avoid the combined effect of Earth's gravity and the electric gravity, the experiment ran under microgravity (μg) conditions obtained during parabolic flight campaigns (Fig. 1 right). A Particle Image Velocimetry method is used to visualize the flow in the axial direction, and a Shadowgraph/Schlieren technique is used to measure the density variation in the azimuthal direction.

Figure 1: Schematic representation of the flow configuration (left) and photo of the A310 ZeroG airplane (right, by courtesy of Novespace).

Various fluids and aspect ratios are investigated in different gravity phases provided by the parabolic flights. The growth rates of instabilities are compared for different initial conditions: the high voltage is applied before the beginning of the μg phase, just when the μg phase started, or some seconds after the μg started. The objective of such investigation is to provide optimal conditions for thermoelectric convection for future experiments such as the TEXUS sounding rocket flight.

References

[1] B. Futterer, A. Krebs, A.-C Plesa, F. Zaussinger, R. Hollerbach, D. Breuer, C. Egbers *Sheet-like and plume-like thermal flow in a spherical convection experiment performed under microgravity*, J. Fluid Mech., **735**, 647-683, 2013.

[2] A. Meyer, M. Jongmanns, M. Meier, C. Egbers, I. Mutabazi, *Thermal convection in a cylindrical annulus under a combined effect of the radial and vertical gravity*, C. R. Mecanique **345**, 11-20, 2017.

[3] H.N. Yoshikawa, O. Crumeyrolle, I. Mutabazi, *Dielectrophoretic force-drivan thermal convection in annular geometry*, Phys. Fluids **25**, 024106, 2013.

Acknowledgements

The project « *Untersuchungen zur thermischen Konvektion im konzentrischen Spalt mit elektrischem Zentralkraftfeld unter verminderter Schwerkraft* » (KIKS) is funded by the BMWi via German Aerospace Center DLR under grant no. 50WM1644.

Effect of the dielectrophoretic force in a rigidly rotating cylindrical annulus

Antoine Meyer[i1], Harunori Yoshikawa[2], Innocent Mutabazi[1], Christoph Egbers[3]

[1] Laboratoire Ondes et Milieux Complexes (LOMC) - CNRS : UMR6294, Université du Havre - 53, rue de prony, 76058 Le Havre Cedex, France

[2] Laboratoire J-A Dieudonné (LJAD) - CNRS : UMR7151, Université de Nice Sofia Antipolis - Parc Valrose, 06108 Nice Cedex, France

[3] Lehrstuhl Aerodynamik und Strömungslehre (LAS) - Brandenburgische Technische Universität Cottbus-Senftenberg, Siemens-Halske-Ring 14, 03046 Cottbus, Germany

---

The application of an electric field, together with a temperature gradient on a dielectric liquid can generate thermal convection, in particular under weightlessness where the Archimedean buoyancy is negligible [1, 2]. We consider an incompressible dielectric fluid confined in a cylindrical annulus rotating about its axis in a microgravity environment. The two cylindrical surfaces are maintained at different temperatures and an alternating difference of electric potential is applied between them (Figure 1). The centrifugal acceleration $\boldsymbol{g}_c$ acts on the density stratification to produce the centrifugal buoyancy. With an analogous mechanism, the radial electric field acts on the electric permittivity stratification and gives rise to the dielectrophoretic (DEP) force which can be seen as a thermal buoyancy force induced by an effective electric gravity $\boldsymbol{g}_e$.

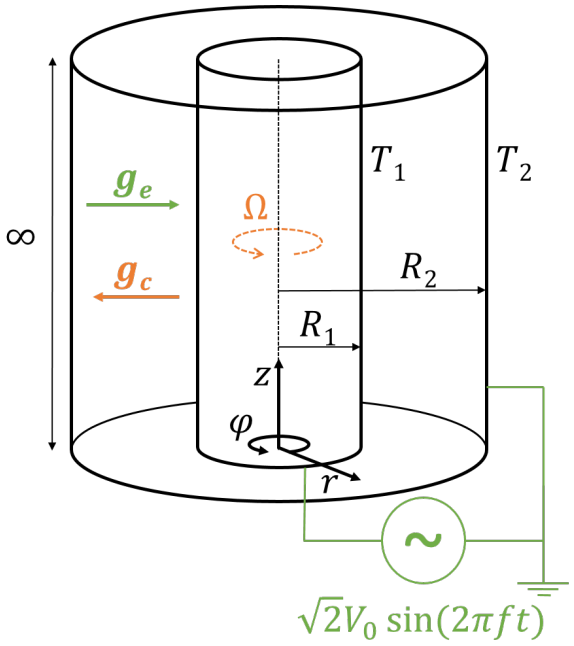

Figure 1: Sketch of the flow configuration.

---

[i]Present address: [3] LAS, BTU Cottbus Senftenberg

The instability driven by the two competing thermal buoyancies is studied through a linear stability analysis. For low rotation rates, convection cells take the form contra-rotating helical vortices [3]. However, the rotation of the cylindrical annulus favours vortices which are aligned with the axis when the rotation rate is sufficiently large [4]. We will see that the heating direction has an important role in this problem, and a careful analysis of the frequency of wave propagation is performed.

References

[1] B. Futterer, A. Krebs, A.-C Plesa, F. Zaussinger, R. Hollerbach, D. Breuer, C. Egbers *Sheet-like and plume-like thermal flow in a spherical convection experiment performed under microgravity*, J. Fluid Mech., **735**, 647-683, 2013.

[2] A. Meyer, M. Jongmanns, M. Meier, C. Egbers, I. Mutabazi, *Thermal convection in a cylindrical annulus under a combined effect of the radial and vertical gravity*, C. R. Mecanique **345**, 11-20, 2017.

[3] H.N. Yoshikawa, O. Crumeyrolle, I. Mutabazi, *Dielectrophoretic force-drivan thermal convection in annular geometry*, Phys. Fluids **25**, 024106, 2013.

[4] M. Auer, F.H. Busse, R.M. Clever, *Three-dimensional convection driven by centrifugal buoyancy*, J. Fluid Mech. **301**, 371-382, 1995.

Acknowledgements

The present work has benefited from a partial support from the French Spatial Agency (CNES) and from the French National Research Agency (ANR) through the program "Investissements d'Avenir (No. ANR-10LABX-09-01)", LABEX EMC^3. A. M. was supported by a doctoral fellowship from the Région Normandie. H. N. Y. acknowledges financial support from the French National Center for Scientific Research (CNRS) through the program PEPS-PTI OndInterGE.

Numerical investigation of the flow structures in a vertical Taylor-Couette system with a large radial temperature gradient

Innocent Mutabazi[1], Changwoo Kang[1], Arnaud Prigent[1]

[1] Normandie Université, UNILEHAVRE, CNRS-UMR 6294, LOMC, Le Havre, France

---

We consider the Taylor-Couette system with rotating inner cylinder and a radial temperature gradient. The gap between the cylinders has the width d=0.5cm and the length L=57cm. The inner cylinder of radius a=2cm rotates with the angular frequency Ω. The geometrical control parameters are the radius ratio η=0.8 and the aspect ratio Γ=114. The annular gap is filled with a Newtonian fluid with the density ρ, the thermal expansion α and the thermal diffusivity κ. The physical control parameters are the Taylor number Ta=$Re(d/a)^{1/2}$ (with Re=$\Omega ad/\nu$)) which is a measure of the rotation rate of the inner cylinder and the Grashof number Gr=$\alpha\Delta Tgd^3/\nu\kappa$ which is a measure of the temperature difference acting on the fluid.

The stability of the flow in this configuration has been reported in a recent study in which an experimental diagram of flow sates has been provided together with few states checked with DNS [1]. For Ta=0, the flow consists of a large convective cell with an ascending flow is ascending near the hot cylinder and a descending near the cold surface. For a weak rotation rate with $Ta < Ta_c$=12, the base flow consists of a superposition of the circular Couette flow induced by the rotation and the large convective flow. Such a base flow is characterized by two vorticity components: the azimuthal vorticity induced by the temperature gradient(baroclinic vorticity) and the axial vorticity due to the rotation of the inner cylinder. The baroclinic flow has an inflexion point in which the vorticity reaches its maximum and, according to Rayleigh-Fjortoft criterion[2] , the flow is unstable. According to the Rayleigh circulation criterion, the circular Couette flow is unstable. In this flow, it is possible to excite two types of instabilities depending on the relative importance of each driving force [3].

We perform direct numerical simulations of different flows obtained for a fixed value of Gr=4,000 in order to determine the flow structures, the momentum and heat transfer coefficients when the Taylor number Ta is increased from 0 to 500. We use a finite-volume in a cylindrical coordinate system [1,4]. The endplates are assumed adiabatic and stationary. The value Gr=4,000 is the largest value for which the Boussinesq approximation is still valid for our flow system.

At Ta=Ta_c=12, the base flow bifurcates to a state of localized modulated spiral pattern (MSPI)(Fig. 1(a)). The pattern is formed in the central part of the flow system and vanishes before reaching the endplates. This state is observed in a small range of Ta above Ta_c. Such types of localized structures have been obtained in numerical simulations of the quintic Swift-Hohenberg equation [5]. A small increase of Ta just above Ta_c results in the occurrence of the disordered spiral pattern (DSPI) which exhibit light zones in which azimuthal vorticity components have very low values leading to irregular spiral vortices (Fig. 1(b), (c)). These light zones have the signature of solitary states. For large values of Ta, the disordered flow bifurcates to a wavy spiral pattern (WSPI) (Fig. 1(d), (e)), and then to the wavy vortex flow (WVF) (Fig. 1(f)). The disappearance of the disordered character of the spiral flows

corresponds to the dominance of the centrifugal force over the temperature gradient. The competition between the centrifugal force and the temperature gradient is determined by the Richardson number $Ri{=}Gr/Re^2$. Guillerm et al.[1] found that, for the flow with η=0.8, the disappearance of the temperature gradient effects occur at Ri^*=0.03. Fig. 1(f) corresponds to Ri=0.011< Ri^*.

The variation of the friction coefficients with Ta shows the transition from the regime dominated by the baroclinic vorticity and the wave dominated by the centrifugal force. This transition corresponds also to the change of the slope of the variation of the Nusselt number with Ta.

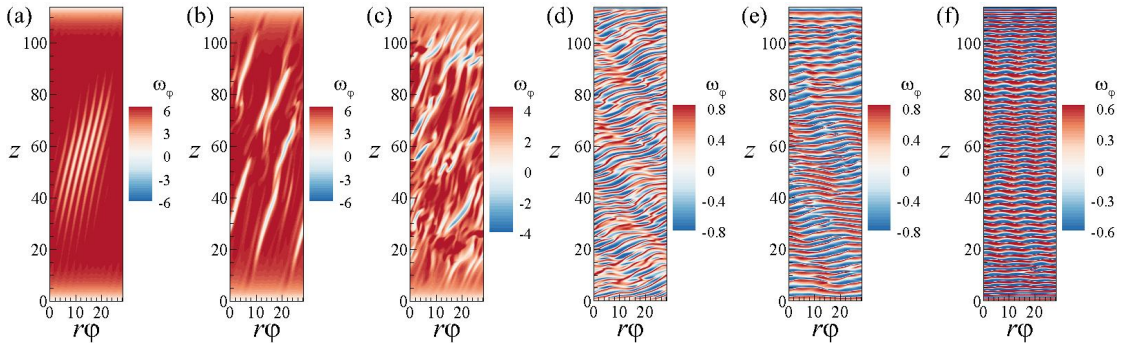

Figure 1: Instantaneous contours of azimuthal vorticity component (ω_φ) in the centre surface of the annulus for Gr=4,000; (a) Ta=12, (b) Ta=13, (c) Ta=20, (d) Ta=80, (e) Ta=170, (f) Ta=300.

References

[1] R. Guillerm, C. Kang, C. Savaro, V. Lepiller, A. Prigent,K.-S. Yang, I. Mutabazi, *Flow regimes in a vertical Taylor-Couette system with a radial thermal gradient*, Phys. Fluids **27**, 094101(2015).

[2] P.G. Drazin, *Introduction to Hydrodynamic Stability*, Cambridge University Press (2002).

[3] M. Ali and P.D. Weidman, *On the stability of circular Couette flow sith a radial heating*, J. Fluid Mech. **220**, 53-84 (1990).

[4] C. Kang, K.-S. Yang, I. Mutabazi *Thermal effect on large-aspect-ratio Couette-Taylor system: numerical simulations*, J. Fluid Mech., **771**, 57-78(2015).

[5] J. Burke and E. Knobloch, *Localized states in the generalized Swift-Hohenberg equation*, Phys. Rev. E **73**, 056211 (2006).

Acknowledgements

The present work has been realized within the LIA ISTROF (CNRS LIA n1092), and it was partially supported the French National research Agency (ANR) through the programme Investissements d'Avenir (ANR-10 LABX-09-01), LABEX EMC^3/TUVECO. C.K. has a financial support from the project BIOENGINE/CPER-FEDER/Normandie.

Bifurcation in rotating plane Couette flow revisited

Masato Nagata[1,3], Darren P. Wall[2], Takashi Noguchi[3]

[1] School of Mechanical Engineering, Tianjin University, Tianjin, 300072 PRC

[2] Graduate School of Engineering, Kyushu University, Fukuoka, 819-0395 Japan

[3] Graduate School of Engineering, Kyoto University, Kyoto, 615-8510 Japan

---

Regarding the problem of transition from laminar to turbulent motions, plane Couette flow subject to a span-wise system rotation has been serving as a testing ground for comparison between experiments ([1, 2]) and theories ([3, 4, 5]).

The fluid motion for this system is governed by two non-dimensional parameters, R (shear-induced Reynolds number) and Ω (system rotation). It is known that, at a fixed R, the basic state loses stability to stream-wise-independent perturbations as Ω is increased, resulting in the onset of secondary flow with a stream-wise-independent roll-cell structure possessing the span-wise wavenumber, $\beta = 1.5585$.

Although it is believed that instability property of the secondary flow has been understood quite well, we re-examine the property in the present paper, especially for small R, with a surprising result. Namely, the secondary flow becomes unstable to perturbations with small stream-wise wavenumbers, α, as soon as it bifurcates from the basic state at $\Omega = 1.079$ (for $R = 100$), so that there exists no *stable* stream-wise-independent roll-cell structures.

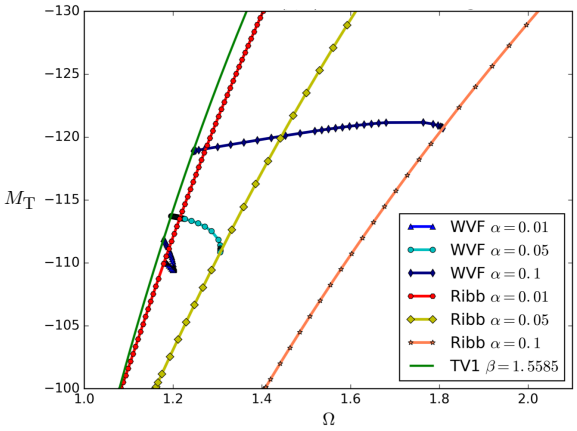

Figure 1: Bifurcation structure for small α against the momentum transport M_T at the channel wall when $R = 100$. TV1: two-dimensional stream-wise-independent roll-cells; WVF: tertiary flows; Ribb: Ribbons. The span-wise wavenumber, β, is 1.5585 for all flows.

As shown in Figure 1, three-dimensional tertiary flows (WVF's) for small α resulting from the afore-mentioned secondary instability connect with the so-called Ribbons[4] (Ribb's), which possess double-layered stream-wise vortex structures. The stream-wise component

of the vorticity for each vortex changes signs alternately in the stream–wise direction (see Figures 2(a,c)).

The velocity directions in the top/bottom layers at particular span-wise positions (Figures 2(b,d)) are consistent with the direction of flow around the central vortex - i.e. the vortex, as described by the velocity vectors, extends across the full height of the channel.

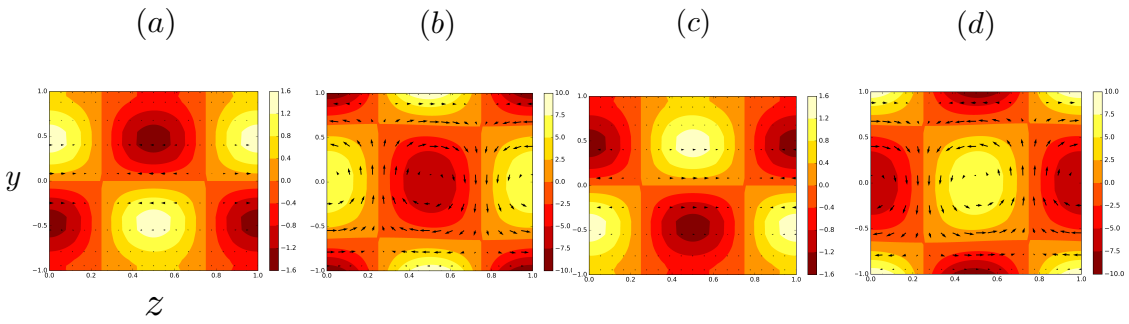

Figure 2: The flow pattern of Ribbon with $\alpha = 0.01$ and $\beta = 1.5585$ at $\Omega = 1.18$ for $R = 100$. The stream-wise component of the vorticity is indicated by colour code and the velocity vectors are projected on the span-wise(z) - wall normal(y) cross-section at the stream-wise(x) stations at (a):$x = 0$, (b):$(2\pi/\alpha)(3/10)$, (c):$(2\pi/\alpha)(5/10)$, (d):$(2\pi/\alpha)(8/10)$.

In conclusion, there exist no stable two-dimensional stream-wise-independent roll-cells theoretically. What are observed in experiments might be actually Ribbons with a long stream-wise wave length $\lambda = 2\pi/\alpha$.

References

[1] T. Tsukahara, N. Tillmark, P. H. Alfredsson, *Flow regimes in plane Couette flow with system rotation*, J. Fluid Mech., **648**, 5-33, 2010.

[2] A. Kawata, P. H. Alfredsson, *Experiments in rotating plane Couette flow - momentum transport by coherent roll-cell structure and zero-absolute vorticity state*, J. Fluid Mech., **791**, 191-213, 2016.

[3] M. Nagata, *Tertiary solutions and their stability in rotating plane Couette flow*, J. Fluid Mech., **358**, 357-378, 2015.

[4] M. Nagata, *A note on the mirror-symmetric coherent structure in plane Couette flow*, J. Fluid Mech., **727**, R1, 2013.

[5] C. A. Daly, T. M. Schneider, P. Schlatter, N. Peake, *Secondary instability and tertiary states in rotating plane Couette flow*, J. Fluid Mech., **761**, 27-61, 2014.

Aggregation of silica micro particles in chaotic mixing field

Yusuke Ochi[1], Takafumi Horie[1], Naoto Ohmura[1]

[1] Department of Chemical Science and Engineering, Kobe University, 1-1 Rokkodai, Nada-ku, Kobe 657-8501, Japan

---

Our experimental work which investigated the aggregation of micro-scale silica particles in a chaotic mixing field will be introduced. The experimental apparatus comprises two rotating cylinders (diameter : 15 mm) and a vessel (inner diameter : 130 mm) as shown in Figure 1. The cylinders rotated at a constant rate ω and paused for a fixed time T with a phase difference to give rise to the chaotic mixing [1]. Silica particle (diameter : 2.5 μm, density: 1.9 g cm^{-3})-silicone oil (kinetic viscosity : 50 mm^2 s^{-1}, density : 0.96 g cm^{-3}) suspension was used as the working fluid and pure glycerol was introduced to make the friction of the bottom surface be negligible. The solid content was 0.1% w/w. Particle size analyses were done with a microscope on samples taken from the sampling point shown in Figure 1.

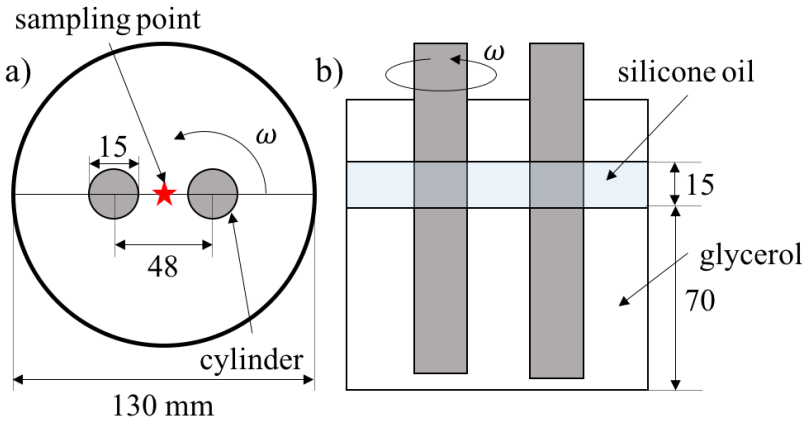

Figure 1: Experimental apparatus; a) top and b) side views.

The median diameter d_{50} after 20 min of the process had a minimum value when plotted against ωT as shown in Figure 2. Representative particle distributions are shown in Figure 3. If ωT is small, the particle size distribution curve was monomodal as well as the initial distribution, which implies that aggregates form from the same scale of particles. On the other hand, when ωT is large, it drastically changed to the bimodal distribution compare to the initial monomodal distribution. This result implies that aggregates form from different scale of particles. The mechanism of aggregation in a chaotic mixing field would be able to control by changing ωT.

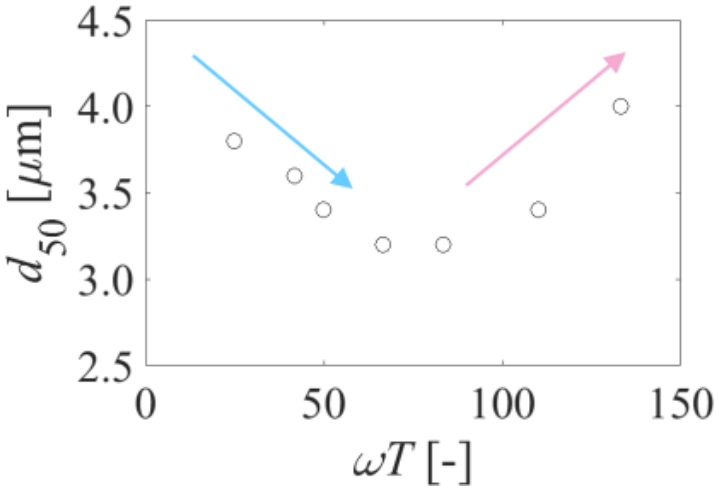

Figure 2: Relationship between ωT and d_{50} at $t = 20$ min.

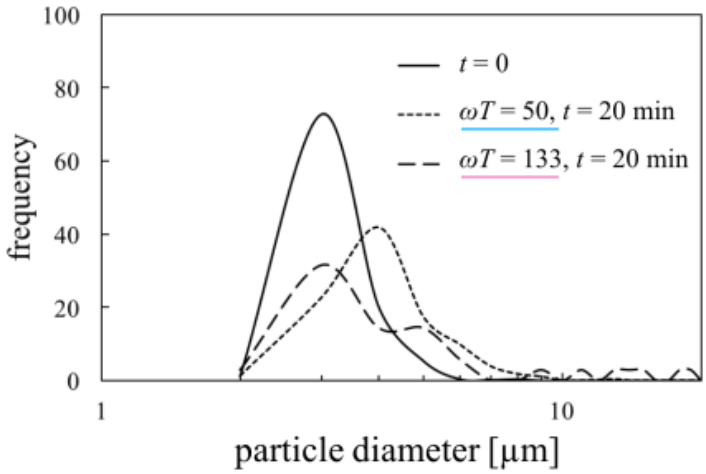

Figure 3: Particle size distributions at different ωT.

References

[1] H. Aref, *J. Fluid Mech.*, **143**, 1–21, 1984.

Acknowledgements

This research project is supported by JSPS KAKENHI Grant Number JP18H03853.

NUMERICAL SIMULATION OF PASSIVE SCALAR TRANSPORT IN TURBULENT TAYLOR-COUETTE FLOWS IN SHORT ANNULUS WITH ROTATING OUTER WALL

Nabila OUAZIB[1], **Yacine SALHI**[1] El-Khider SI-AHMED[1,2] Jack LEGRAND[2] Abdellah ARHALIASS[2] Gérard DEGREZ [3]

[1] USTHB, Faculty of Physics, LMFTA, Algiers, Algeria

[2] GEPEA, CNRS - UMR 6144, CRTT, Université de Nantes, France

[3] Aero-Thermo-Mechanics Department, Université Libre de Bruxelles, Belgium

Abstract

In this paper, we investigate numerically the Taylor-Couette flow between independently rotating cylinders with a relatively small aspect ratio $\Gamma = 2.4$. For this purpose, direct numerical simulations (DNS) have been achieved to study the effects of the gravitational and the centrifugal potentials on the stability of incompressible Taylor-Couette flow as well as on passive scalar transport. The flow is confined between two concentric cylinders both the inner cylinder and the outer one are allowed to rotate. The Navier-Stokes equations and the uncoupled convection diffusion reaction (CDR) equation are solved using a spectral development in one direction combined together with a finite element discretization in the two remaining directions. When the cylinders are abruptly rotating, it is shown that the counter rotation promotes the appearance of the abnormal mode.

Introduction

Flow between independently rotating concentric cylinders, which is commonly called Taylor-Couette flow has attracted great interest since the publication of the classical Taylor [1] paper, because of its complex dynamic behavior and it numerous engineering applications. In the most of the previous works the effect of the end walls is neglected, theoretically by assuming innitely long cylinders, experimentally by using long cylinders compared to the gap between the cylinders, and computationally by using periodic boundary conditions at the axial extrema of the computational domain. However these end walls have a significant influence on the flow dynamics [2]. In the classical setup where only the inner cylinder is allowed to rotate and with stationary end walls, Benjamins studies [3] [4] reveal a new dynamical aspect in short annulus and classified the observed flow into primary mode which is usually develops smoothly with increasing the Reynolds number and uniquely possible at small values of Re, and secondary modes witch are possible only above a respective critical value of Re, these modes can be normal if the flow is inward close to the end wall, or anomalous if the flow is outward near the end wall.

Results

The codes ability to solve three-dimensional flow in axisymmetric geometries including passive scalar transport with uniform boundary and initial conditions with both LES and DNS

methods was previously established [5] . In these simulations we examine the effect of both weak and strong counter rotation on the flow structure in a Taylor-Couette apparatus with small aspect ratio, This is reached by starting the two cylinders from rest and keeping the end walls at rest, the inner Re_i numbers explored here are ranging between 300 to 700, and outer Re_o numbers between -10 to -300, the modes uncountred here are summarized in Fig.1, the first Remarque that we can make is that all the modes produced with the counter rotation in our range of Reynolds numbers are anomalous, and two new anomalous modes appeared when a counter rotation is imposed, these modes are anomalous two-cell and anomalous four-cell flows, the anomalous four-cell flow (fig. 1 b. c. f. i) is formed by a pair of normal cells at the center and two anomalous cells at both end walls, the anomalous two-cell flow is also constituted by two anomalous cells and the flow is outward at both end walls, which also the case in the anomalous four-cell flow.

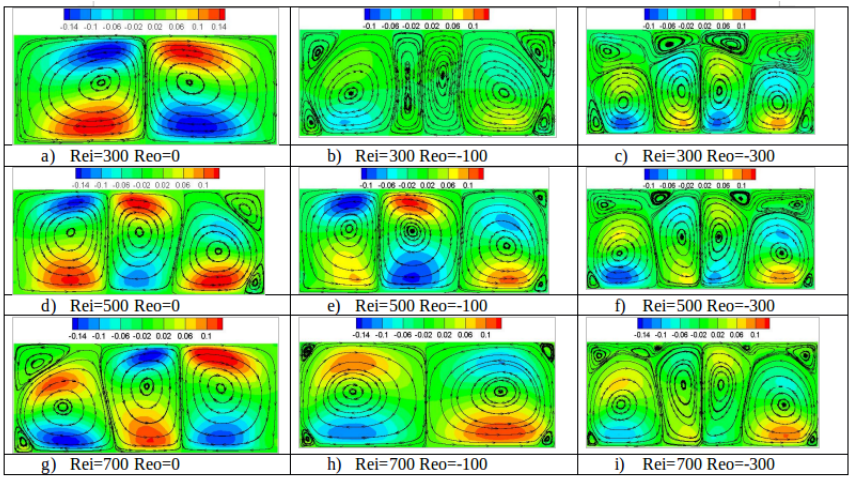

Figure 1: Instantaneous axial velocity u_z contours and streamstraces for the cylinder geometry $\eta = 0.615$ and $\Gamma = 2.4$

References

[1] GI Taylor. Stability of a viscous liquid contained between two rotating cylinders phil. trans. r. soc. lond. a january. 1923.

[2] T Mullin. Mutations of steady cellular flows in the taylor experiment. *Journal of Fluid Mechanics*, 121:207–218, 1982.

[3] TB Benjamin. Bifurcation phenomena in steady flows of a viscous fluid i. theory. 1978.

[4] T. B Benjamin and Mullin T. *Proc. Roy. London Ser*, 311, 1981.

[5] Yacine Salhi, El-Khider Si-Ahmed, Gérard Degrez, and Jack Legrand. Numerical investigations of passive scalar transport in turbulent taylor-couette flows: Large eddy simulation versus direct numerical simulations. *Journal of Fluids Engineering*, 134(4):041105, 2012.

Acknowledgements

Simulations were performed with computing resources granted by Centre de Calcul Intensif des Pays de la Loire (CCIPL).

Experimental study of the flow produced in a vertical Taylor-Couette system submitted to a large radial temperature gradient

Arnaud Prigent[1], Clément Savaro[1], Innocent Mutabazi[1]

[1] Normandie Université, UNILEHAVRE, CNRS-UMR 6294, LOMC, Le Havre, France

---

The Taylor-Couette system has long been studied as a model for the study of centrifugal effects and the transition to turbulence in closed flows. In realistic situations, it is often necessary to take into account the presence of thermal effects. Thus, the first observation of the complications caused by these thermal effects is generally attributed to Taylor himself [1]. He reported in some cases the appearance of a spiral instead of the Taylor vortex flow. This phenomenon, not predicted by theory in the context of an isothermal fluid, was a posteriori associated with the presence of an axial flow created by a radial temperature gradient [2]. Here we are interested in the study of the flow produced in a Taylor-Couette system submitted to a large radial temperature gradient.

Our system is composed of two vertical coaxial cylinders of same length $L = 57$ cm (figure 1a). The inner cylinder made of black anodized aluminium has a radius $a = 2$ cm, the outer cylinder made of glass has a radius $b = 2.5$ cm. The gap between the cylinders $d = b - a = 0.5$ cm is filled by water. Two stationary Teflon rings are used to seal the annulus, giving the gap length $H = 55.4$ and the radii and aspect ratios $\eta = a/b = 0.8$ and $\Gamma = H/d = 111$. The inner cylinder is rotated with angular frequency Ω whereas the outer cylinder is at rest. The inner and outer cylinders are maintained at fixed temperatures T_1 and T_2 by constant temperature water circulating inside the inner cylinder and between the outer and a third glass cylinder which surrounds the system. Therefore, the flow can be described by three physical control parameters: the Taylor number $Ta = (\Omega a d/\nu).(d/a)^{1/2}$, the Grashof number $Gr = g\alpha\delta T d^3/\nu^2$ and the Prandtl number $Pr = \nu/\kappa$.

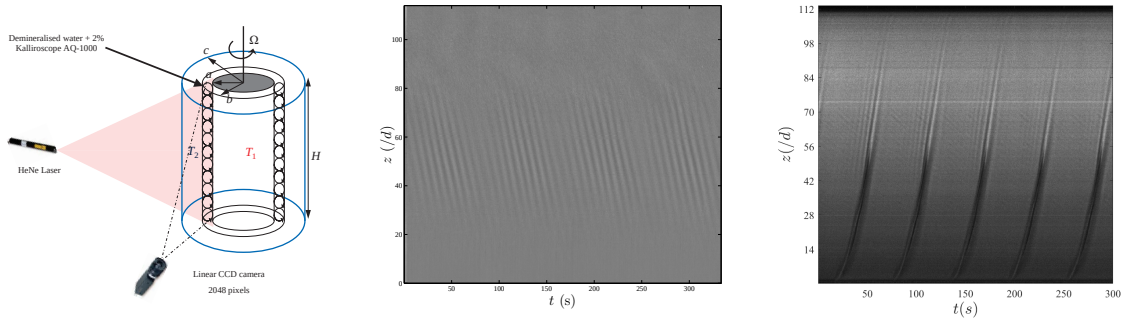

Figure 1: Schematic drawing of the experimental setup (a). Space-time diagrams of the spiral pattern for $Gr = 4270$ and $Ta = 12.4$ (b) and $Gr = -8800$ and $Ta = 15.8$ (c).

The flow is characterized using two complementary techniques. Using Kalliroscope AQ1000 concentrate, the flow pattern are visualized along the whole length of the system in the $r - z$ plane. We also use encapsulated Thermochromic Liquid Crystals (TLC) to perform temperature and velocity measurements in a 11 cm wide portion of the same plane taken at mid-height.

As soon as a radial temperature gradient is imposed between the cylinders, the flow takes the form of a convective cell with particles moving upwards along the heated wall and downwards along the cooled one. When the inner cylinder starts to rotate, the classical circular Couette flow is added to this convective cell. Then, when the rotation of the inner cylinder is further increased and the Taylor number reaches a critical value Ta_c which depends on the Grashof number, this base flow is destabilized [4]. For $Gr = 0$, $Ta_c = 47$ and the base flow is replaced by the Taylor vortex flow [1, 3]. For $Gr \neq 0$ a spiral flow, sets in when Ta_c is reached. The onset of the instability first decreases as $|Gr|$ increases until $|Gr| \simeq 800$. For $|Gr| \geq 800$, Ta_c remains roughly constant.

For $Gr \neq 0$, two distincts behaviours can be observed according to the Grashof number. For $|Gr| \leq 800$ the pattern appearing at the onset of the first instability has already been described in [5]. The spiral only appears at the bottom of the cavity and has a regular time behaviour inducing the temporal frequency spectrum to be caracterized by one single mode. For $|Gr| \geq 800$, the time behaviour of the pattern is no longer regular. A low frequency time modulation can be seen on the space-time diagrams. The pattern evolves from the bottom to the mddle of the heigth of the system. Its axial extension icreases with the Grashof numbe and reaches half the length of the system at $Gr = 4270$ (figure 1b). For $|Gr| \geq 2500$, as soon as the Taylor number is slightly increased above its critical value (an increase of $\delta Ta = 0.4$ is sufficient), a pattern called solitary wave appears on the background of the modulated spiral. This solitary wave is a robust structure and persists even when Ta is further increased. It takes the form of one to three helical stripes depending on the Grashof number (figure 1c). Its helicity follows the same rules as the other patterns observed in the system [6] but it is much more intense than the modulated spiral which is barely visible in the same conditions. It extends vertically over 3/4 of the system from the top (bottom) when the inner (outer) cylinder is hotter and propagates around the cylinders following the inner cylinder rotation.

References

[1] G.I. Taylor, *Stability of a Viscous Liquid Contained between Two Rotating Cylinders*, Phil. Trans. R. Soc. Lond. A **223**, 289-343 (1923).

[2] R. Tagg, *The Couette-Taylor problem*, Nonlinear Science Today **4**, 1-25 (1994).

[3] C. Andereck, S. Liu and H. Swinney, *Flow regimes in a circular Couette system with independently rotating cylinders*, J. Fluid Mech. **164**, 155-183 (1986).

[4] R. Guillerm, C. Kang, C. Savaro, V. Lepiller, A. Prigent,K.-S. Yang, I. Mutabazi, *Flow regimes in a vertical Taylor-Couette system with a radial thermal gradient*, Phys. Fluids **27**, 094101(2015).

[5] V. Lepiller, A. Goharzadeh, A. Prigent and I. Mutabazi, *Weak temperature gradient effect on the stability of the circular Couette flow*, Eur. Phys. J. B **61**, 445-455 (2008).

[6] M. Ali and P.D. Weidman, *On the stability of circular Couette flow sith a radial heating*, J. Fluid Mech. **220**, 53-84 (1990).

Acknowledgements

The present work has been realized within the LIA ISTROF (CNRS LIA n1092), and it was partially supported the French National research Agency (ANR) through the programme Investissements d'Avenir (ANR-10 LABX-09-01), LABEX EMC^3/TUVECO. C.S. had a financial support from the project BIOENGINE/CPER-FEDER/Normandie.

Low Mach Number Modeling of Stratorotational Instability in a water-filled Taylor-Couette cavity

Isabelle Raspo[1], Stéphane Viazzo[1], Anthony Randriamampianina[1], Gabriel Meletti[2], Uwe Harlander[2], Torsten Seelig[2], Andreas Krebs[2]

[1] Aix-Marseille Univ, CNRS, Centrale Marseille, M2P2, Marseille, France

[2] Department of Aerodynamics and Fluid Mechanics, Brandenburg University of Technology, Cottbus-Senftenberg, Germany

---

The Stratorotational Instability (SRI) is a purely hydrodynamic instability with distinctive local features occuring in centrifugally stable flows. It is suspected to contribute to the outward angular momentum transport in accretion discs, which is a central problem of planet formation. Only turbulence can achieve such a large angular momentum transport. SRI can be studied from specifically designed laboratory experiments and numerical simulations in an axially-stratified Taylor-Couette setup [1, 2]. Recent studies [3, 4] mentioned that, at fixed values of the Froude number, $Fr = \Omega_i/N$ (with N the buoyancy frequency and Ω_i the angular velocity of the inner cylinder), and of the angular velocity ratio $\mu = \Omega_o/\Omega_i$ (with Ω_o the angular velocity of the outer cylinder), there exists an upper limit of the Reynolds number $Re = \Omega_i R_i(R_o - R_i)/\nu$ for the occurrence of SRI. These authors also showed that the value of Re where the flow becomes stable again increases as Fr decreases. Therefore, at high Reynolds number values relevant to transition to turbulence regimes, SRI can only be obtained at small Froude number values and, consequently, for large temperature difference ΔT between the top and bottom endplates. When liquid water is used in simulations, the validity of the Boussinesq approximation may be questioned under such conditions. Indeed, Shalybkov and Rüdiger [5] suspected non-Boussinesq effects to be responsible for large discrepancies between numerical and experimental results for strong stratifications, e.g small values of Fr. Medale and Haddad [6] reported non-Boussinesq effects in a mixed convection problem using liquid water. The Boussinesq approximation can theoretically be applied with liquid water at 298.15K for temperature differences ΔT less than 5.2K [7]. We investigated the influence of non-Boussinesq effects on the characteristics of SRI by performing 3D simulations with both Low Mach number and Boussinesq approximations based on spectral methods in the configuration of experiments at the BTU Cottbus-Senftenberg, Germany [4]. For the Low Mach number modeling, the specific equation of state proposed for water by Pátek *et al.* [8] is implemented, which allows for an accurate representation of the density and other thermodynamic properties of water, with a mean deviation of 0.01% for the density compared with data provided by NIST. The simulations show that non-Boussinesq effects modify the value of the Froude number for the threshold of occurrence of SRI. Significant changes are also observed for the azimuthal wavenumber, as illustrated in figure 1, and for the fundamental frequency of the instability. The present studies will serve to guide future simulations based on High Performance Computing in order to reach higher values of governing parameters relevant to turbulence regimes [9].

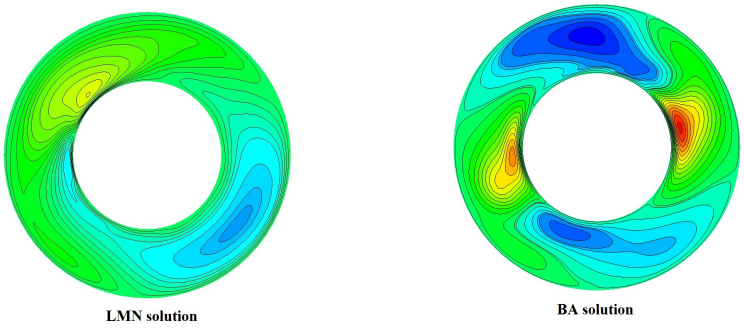

Figure 1: Iso-contours of radial velocity at mid-height of the cavity for $Re = 1000$, $Fr = 0.58$ ($\Delta T = 24$K) and $\mu = 0.35$. Left: Low Mach number approximation (azimuthal wavenumber $m = 1$, frequency ω/Ω_i=0.54). Right: Boussinesq approximation (m=2, ω/Ω_i=1.12).

References

[1] M. Gellert, G. Rüdiger, *Stratorotational instability in Taylor-Couette flow heated from above*, Journal of Fluid Mechanics **623**, 375–385, 2009.

[2] M. Le Bars, P. Le Gal, *Experimental analysis of the stratorotational instability in a cylindrical Couette flow*, Physical review letters **99 (6)**, 064502, 2007.

[3] R. Ibanez, H. L. Swinney, B. Rodenborn, *Observations of the stratorotational instability in rotating concentric cylinders*, Phys. Rev. Fluids **1**, 053601, 2016 **doi:10.1103/PhysRevFluids.1.053601**.

[4] G. Rüdiger, T. Seelig, M. Schultz, M. Gellert, C. Egbers, U. Harlander, *The stratorotational instability of Taylor-Couette flows with moderate Reynolds numbers*, Geophysical & Astrophysical Fluid Dynamics **111 (6)**, 429–447, 2017.

[5] D. Shalybkov, G. Rüdiger, *Stability of density-stratified viscous Taylor-Couette flows*, Astronomy & Astrophysics **438**, 411–417, 2005.

[6] M. Medale, A. Haddad, *A 3D Low Mach Number model for high performance computations in natural or mixed convection Newtonian liquid flows*, Journal of Physics: Conference Series **395**, 012095, 2012. **doi:10.1088/1742-6596/395/1/012095**

[7] D.D. Gray, A. Giorgini, *The validity of the Boussinesq approximation for liquids and gases*, International Journal of Heat and Mass Transfer **19**, 545–551, 1976.

[8] J. Pátek, J. Hrubý, J. Klomfar, M. Soucková, *Reference correlations for thermophysical properties of liquid water at 0.1MPa*, Journal of Physical and Chemical Reference Data **38**, 21–29, 2009.

[9] S. Abide, S. Viazzo, I. Raspo, A. Randriamampianina, *High-Order Compact scheme for High-Performance Computing of stratified rotating flows*, Computers & Fluids 2018 (submitted).

Acknowledgements

This work was granted access to the HPC resources of Aix-Marseille Université financed by the project Equip@Meso (ANR-10-EQPX-29-01) of the program "Investissements d'Avenir" supervised by the "Agence Nationale de la Recherche". The authors acknowledge financial support from "Ministère des Affaires étrangères", France, in the framework of a PROCOPE project (PHC 35299PM).

Paper offer for the

International Taylor-Couette Workshop, Marseille, 2018

Taylor-Couette Flow with Cavitation

Prof. Peter Reinke, Tom Beckmann, Dr. Marcus Schmidt

HAWK Göttingen, Faculty of Natural Sciences and Technology.

The work on hand presents a new flow phenomenon which has yet not seen any research: the combination of the transistion from Couette to Taylor vortex flow and the formation of vapor. In other words, the one-phase and two-dimensional Couette flows becomes a two-phase (liquid/vapor) and three-dimensional Taylor vortex flow. This flow is studied inside the gap between a rotating inner cylinder and fixed outer cylinder. Initially the gap is filled with a liquid, only. If the rotational speed is increased and exceeds a critical value, torodial vortices begin to fill the gap in pairs according to gap and diameter ratio. The onset of vortex formation is known as first linear instabilty of the Couette flow and is widely investigated numerically and experimentally, both. The parameter which drives the vortex formation is the radial pressure gradient across the gap. When reaching a critical value the pressure gradient causes a radial flow which in turn becomes a component of the three-dimensional vortices. The motivation to investigate a fluid that has a boiling point near the stability limit of the Couette flow led to the work on hand targeting the interaction of cavitation and vortex formation. The results yield a better understanding of the physics and the parametrization of a newly developed numerical model. As a matter-of-fact, numerical studies indicate the initiation of cavitation near the wall of the inner cylinder due to the radial pressure gradient and the pressure minimum adjacent to the inner wall. The work on hand presents numerical results as well as experimantal data, which are in good agreement. A special fluid is used for the experiments, which fulfills three conditions: a viscosity to reach the instabilty of the Couette flow, a vapor pressure to provide boiling at the operating point and an optical refractive index compatible with the housing material. A specifically designed experimental set-up allows optical accessibilty to the flow that makes the application of non-intrusive measurement techniques possible. Numerical and experimental results are presented and discussed.

Contact:

Prof. Dr.-Ing. Peter Reinke
HAWK Göttingen
Von-Ossietzky-Str. 99
D-37085 Göttingen
Germany
peter.reinke@hawk.de

Subharmonic instabilities on modulated Taylor-couette flow

Mehdi Riahi, Said Aniss, Mohamed Ouazzani Touhami

[1] Laboratory of Mechanics, Faculty of Sciences Ain Chock, University Hassan II Casablanca, Morocco.

Abstract

This paper deals with the centrifugal instability of time-periodic flow in Taylor-Couette geometry where both the inner and outer cylinders are oscillating with equal amplitude and frequency, $\Omega_1(t) = \Omega_o \cos(\omega\ t)$ and $\Omega_2(t) = \varepsilon\ \Omega_o \cos(\omega\ t)$ respectively. Attention is focused on the case of co-oscillating and counter-oscillating cylinders corresponding to $\varepsilon = 1$ and $\varepsilon = -1$ respectively. The Floquet analysis is employed to solve the partial differential equations governing the stability of the system. Results obtained in this framework show that the subharmonic responses are present, in contrast to previous works where only harmonic responses are observed. In addition, it turns out that the most dangerous mode in the intermediate frequency is the subharmonic one. Also, transitions between harmonic and subharmonic responses are occurred by decreasing the frequency number. In the low frequency limit, these responses are likewise since the system approaches the steady configuration.

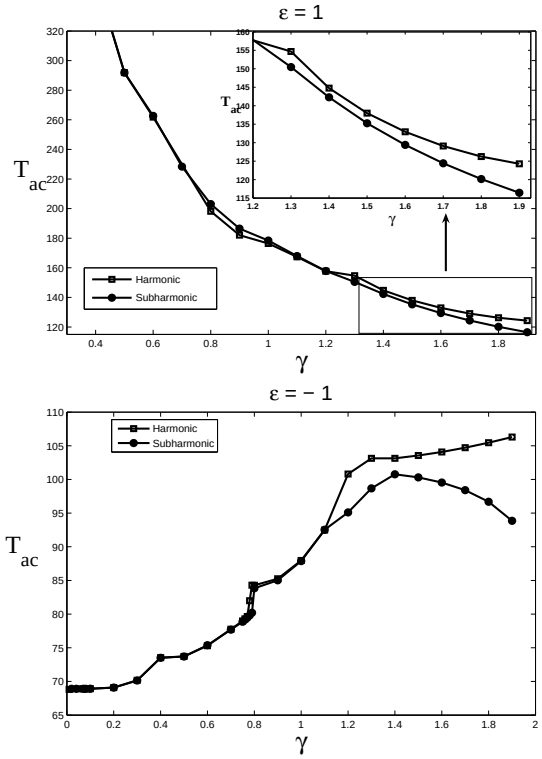

Figure 1: Stability diagrams related to the in-phase $\varepsilon = 1$ and out-of phase $\varepsilon = -1$ modulations.

Numerical and theoritical study of extremely rare collapse and build-up of turbulence in stochastic models of wall flows

Joran Rolland[1]

[1] Institut PPrime, ENSMA, UPR CNRS 3348, Chasseneuil du Poitou, France.

Using skin friction measurements [1], it has been know for decades, that in pipe flow, turbulence can be maintained down to Reynolds number $R = UD/\nu \simeq 2000$ and that it coexists with laminar flow up to Reynolds number $\simeq 2600$. In this transitional range, turbulence in localised in *turbulent puffs* which are actually metastable. They undergo three typical events: turbulence collapse [2], puff splitting, and build up of turbulence from the linearly stable laminar flow, possibly passing nearby the minimal seed of turbulence [3]. The quantitative knowledge on these events is actually far more recent. One important feature of these metastability events is that they can become extremely rare as R is varied. This can make them hard to study by traditional means.

Recently, numerical methods have been proposed that can exponentially accelerate the calculation of rare events, of the trajectories that lead to these events and of the mean first passage time before they occur [4]. One strong advantage of these methods is that they come along proofs of convergence and well documented convergence rates. I specifically use one of these methods, called Adaptive Multilevel Splitting (AMS), which performs a mutation selection procedure on N clones of the system to calculate the trajectories. In this presentation I show the result of the use of AMS on two stochastic models of transitional wall flows [5, 6]. The core results, the trajectories, indicate us what are the paths followed by the flow during collapses of pipes or isolated puffs (figure 1 (a)), isolated puffs splitting, or during the build up of turbulence from the laminar flow under a noise of vanishing variance. Among other things, the calculations yield the Reynolds number R and pipe length L dependence of the mean first passage time T before collapse of turbulence in initially laminar-turbulent pipes. This dependence can written in a *Large Deviation* form in the large size limit $\lim_{L\to\infty} \ln(T)/L = Ar - B$ (figure 1 (b)) [7]. This result confirms and extend a former numerical find in classical simulations of pipe flow [2].

Numerical methods like AMS come hand in hand with a theoretical formalism to study rare events. Many of these methods are asymptotic in the variance of the noise felt by the system going to zero (in that case the pipe length L increasing). These theories write mean first passage times in a large deviations form $\ln(T)/L = f(R, L)$. In the case of the model by Dauchot & Manneville, I *derived analytically* the mean first passage time before collapse of turbulence. This again confirms the $\ln(T)/L = AR - B$ dependence, in quantitative agreement with numerical calculations (figure 1 (c)). One fundamental physical point of this derivation is the separation of the system between slow, leader, modes (which typically represent streamwise vorticity) and fast, slave modes (which typically represent the streamwise flow) [8]. This analysis shows that in the Dauchot & Manneville model, the affine dependence of $\ln(T)/L$ in Reynolds comes from the amplitude of the flow leader mode that has to be collapsed and which grows like an affine function of the Reynolds number.

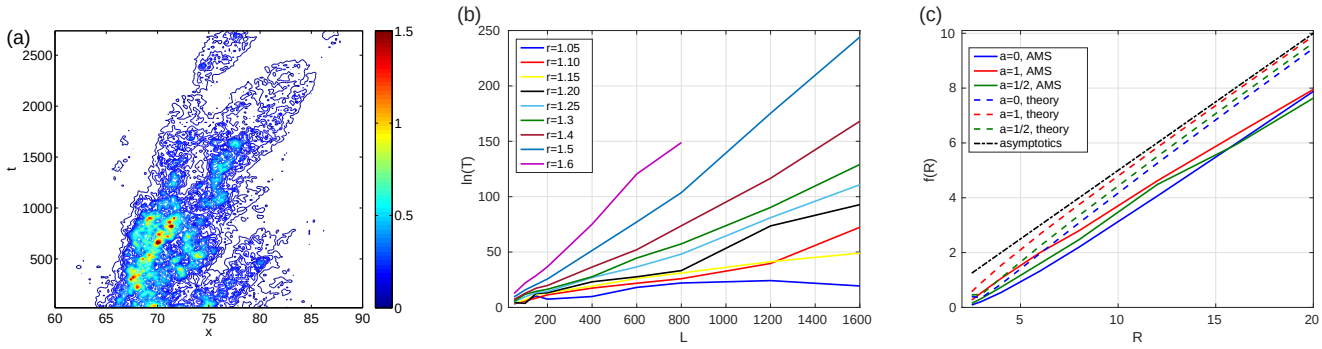

Figure 1: (a): Spatiotemporal diagram of the intensity of turbulence in the model of D. Barkley [5] during the collapse of an isolated turbulent puff. (b): logarithm of the mean first passage time before collapse T of initially laminar-turbulent pipes as a function of size for increasing Reynolds numbers (model of D. Barkley). (c): rate function $f(R) = \ln(T)/L$ as a function of Reynolds number R of mean first passage time before collapse of turbulence in the model by O. Dauchot & P. Manneville [6].

These results could provide a new approach for calculating the mean first passage time before collapse of turbulence very efficiently in direct numerical simulations of transitional wall flows. This could be applied to flow configurations uninvestigated so far, or this could be applied to more academical configurations to check scalings in details. The approach is also currently being used to calculate build-up trajectories in direct numerical simulations of Couette flow. This could confirm the relevance of minimal seed, edge states *etc.* calculations.

References

[1] H. Schlichting, McGraw-Hill (1968).

[2] T. Schneider, B. Eckhardt, Phys. Rev. E **78**, 046310 (2008).

[3] S. M. E Rabin, C. P. Caulfield, R. R. Kerswell, J. Fluid Mech. **712**, 244 (2012).

[4] F. Cérou, A. Guyader, Stochastic Anal. Appl. **25**, 417 (2007).

[5] D. Barkley, J. Fluid Mech. **803**, 1 (2016).

[6] O. Dauchot, P. Manneville, J. Phys. **2**, 371 (1997).

[7] J. Rolland, Phys. Rev. E **97**, 023109 (2018).

[8] T. Grafke, F. Bouchet, T. Tangarife, E. Vanden Eijnden, J. Stat. Phys. **162**, 793 (2016).

Acknowledgements

The author wishes to thank CICADA, centre de calcul interactif de l'université de Nice Sopha-Antipolis for supporting this work. The author also thanks the hospitality of institute for atmospheric and environmental science of Goethe Frankfurt University where the author worked when some the research presented here was performed.

Exact Coherent Structures in Weakly Turbulent Couette-Taylor Flow: Experiments and Numerics

Michael F. Schatz, Christopher J. Crowley, Michael Krygier & Roman O. Grigoriev
School of Physics, Georgia Institute of Technology, Atlanta, GA 30332-0430

Recent work suggests turbulent shear flow behaviors may be captured by Exact Coherent Structures (ECS), which are particular unstable solutions of the Navier-Stokes equations with nontrivial spatial structure and simple temporal dynamics. We report preliminary results on the direct comparision of predicted ECS with output from direct numerical simulations and observations from lab experiments in Couette-Taylor flow. The studies are carried out in a small-aspect-ratio ($\Gamma = 1$) system at radius ratios $\eta = 0.5, 0.71$ in a counter-rotating regime (inner Reynolds number $R_i > 0$, outer Reynolds number $R_o < 0$). Predictions are quantitatively compared with experimental measurements from tomographic particle image velocimetry of all velocity components, fully resolved in space and time, throughout the entire flow domain.

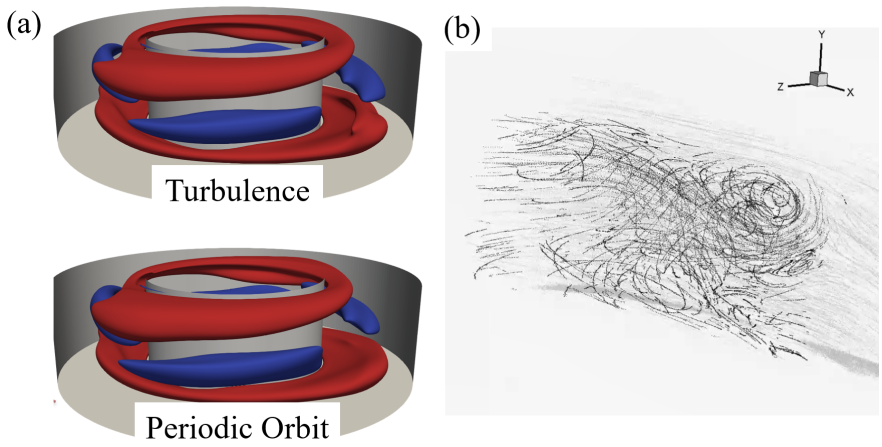

Figure 1: Snapshots of radial velocity level sets are nearly identical for (a) direct numerical simulation of turbulence (top) and an ECS (relative periodic orbit, bottom) at $\Gamma = 1$, $\eta = 0.5$, with $R_i = 1200$, $R_o = -1200$. (b) 3D tomographic velocimetry yields particle track measurements in turbulent flow experiments at $\Gamma = 1$, $\eta = 0.71$, with $R_i = 600$, $R_o = -600$.

Acknowledgements
This work is supported by the US Army Research Office.

Onset of dielectrophoretic force-driven convection in annular geometry under Earth's gravity

Torsten Seelig, Marcel Jongmanns, Antoine Meyer, Martin Meier, Christoph Egbers

Dept. of Aerodynamics and Fluid Mechanics, BTU Cottbus – Senftenberg, Germany

---

Radial outward heating and the influence of a gravitational central-force field is subjected to planetary flows like the motion in Earth's atmosphere or its liquid mantle. Another interesting set-up is the **ca**sk for **s**torage and **t**ransport **o**f **r**adioactive material 'castor' or encapsulated heat exchanger systems [1]. An improvement of heat transfer due to the application of a central-force field is of general interest. To simulate the central nature of the gravitational field Smylie (1966) suggested the use of a strong non-homogeneous electric field in dielectric liquids. When we apply a radial alternating electric field to a dielectric fluid with temperature dependent permittivity confined in a concentric vertical annulus and additionally apply a radial temperature gradient, mainly the dielectrophoretic force contributes to the flow field [3, 4]. Warmer fluid adjusts to regions with less intense electric field and cooler fluid to regions with more intense electric field. This force can be seen as a buoyancy force referring to an 'electrical gravity' that superposes Earth's gravity. Nowadays known as thermal electro-hydrodynamic (TEHD) driven flow.
The experimental work investigates the onset of convective instability and its coherent structures in two experiment cells with two different aspect ratios. The cells have an inner cylinder radius $R_1 = 5$ mm, an outer cylinder radius $R_2 = 10$ mm and heights of $h = 100/300$ mm leading to aspect ratios $\Gamma = h/(R_2 - R_1) = 20/60$. With two different flow visualization techniques, namely the shadowgraph method [5] and particle image velocimetry (PIV) [6] we are able to characterize perturbations of the base flow. We show that the unicellular base flow induced by Archimedian buoyancy first undergoes transition to a stationary axially aligned columnar structure and compare the result with 3D numerical simulation. From all measurements available we draw a regime diagram and compare the lines of marginal stability with linear stability analysis [4].

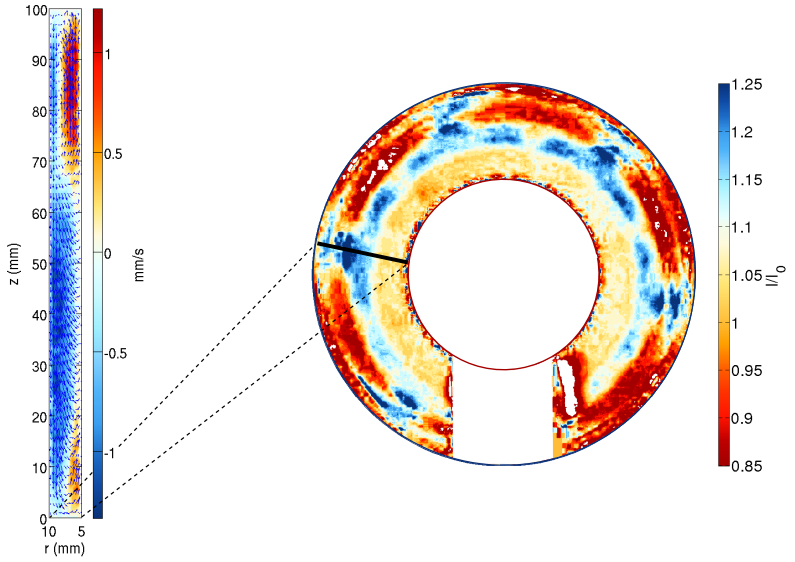

Figure 1: The flow in the annular gap of aspect ratio $\Gamma = 20$ induced by a temperature gradient of $\Delta T = 7$ K and an electric potential of $V_{rms} = 7$ kV. Left: PIV measurement in the meridional plane. Blue/red color refers to down/upward flow. Right: Top view shadowgraph image showing the normalized light intensity I/I_0 as function of density of the axially integrated flow. Blue/red color refers to denser/lighter fluid.

References

[1] Dahley, D., *Dielectrophoretic flow control of thermal convection in cylindrical geometries*, Cuvillier Verlag Göttingen, PhD-thesis, 2014.

[2] Smylie, D. E., *Thermal convection in dielectric liquids and modelling in geophysical fluid dynamics*, Earth and Planetary Science Letters **1**, 339-340, 1966.

[3] Futterer, B., Dahley, N., Egbers, C., *Thermal electro-hydrodynamic heat transfer augmentation in vertical annuli by the use of dielectrophoretic forces through a.c. electric field*, Int. J. Heat Mass Transfer **93**,144-154, 2016.

[4] Meyer, A., Jongmanns, M., Meier, M., Egbers, C., Mutabazi, I., *Thermal convection in a cylindrical annulus under a combined effect of the radial and vertical gravity*, C. R. Mecanique **345(1)**,11-20, 2016.

[5] Schöpf, W., Patterson, J. C., Brooker, A. M. H., *Evaluation of the shadowgraph method for the convective flow in a side-heated cavity*, Experiments in Fluids **21(5)**, 331-340, 1996.

[6] Adrian, R. J., Westerweel, J. *Particle Image Velocimetry*, Cambridge University Press, 2010.

Acknowledgements

This work was supported by the DFG grant ""Thermo-elektro-hydrodynamisch TEHD getriebene Wärmetransporterhöhung im vertikalen Zylinderspalt - Experimente und numerische Simulation im Kontext von Messunsicherheiten und optimaler Versuchsplanung (EG 100/20-1)". M. Jongmanns, A. Meyer and M. Meier acknowledge the support of the BMWi via German Aerospace Center DLR under grant no. 50WM1644.

Recent Developments of the Liquid Metal Taylor Couette Experiment PROMISE

Martin Seilmayer, Frank Stefani, Thomas Gundrum

Helmholtz-Zentrum Dresden-Rossendorf, Bautznerlandstrasse 400, 01328 Dresden, Germany

---

In the beginning of the 20th century Taylor-Couette (TC) experiments were carried out with transparent liquids like water or air, which are electrical no-conducting. With the first experiments of Donnelly [1] in the sixties, a more general approach with liquid metal experiments started to investigate the interaction between magnetic fields and the TC flows of electrically conducting fluids. Two challenges of opaque liquid metal experiments are the measurement technique to investigate the flow structure inside the liquid and the precision and strength of the magnetic field.

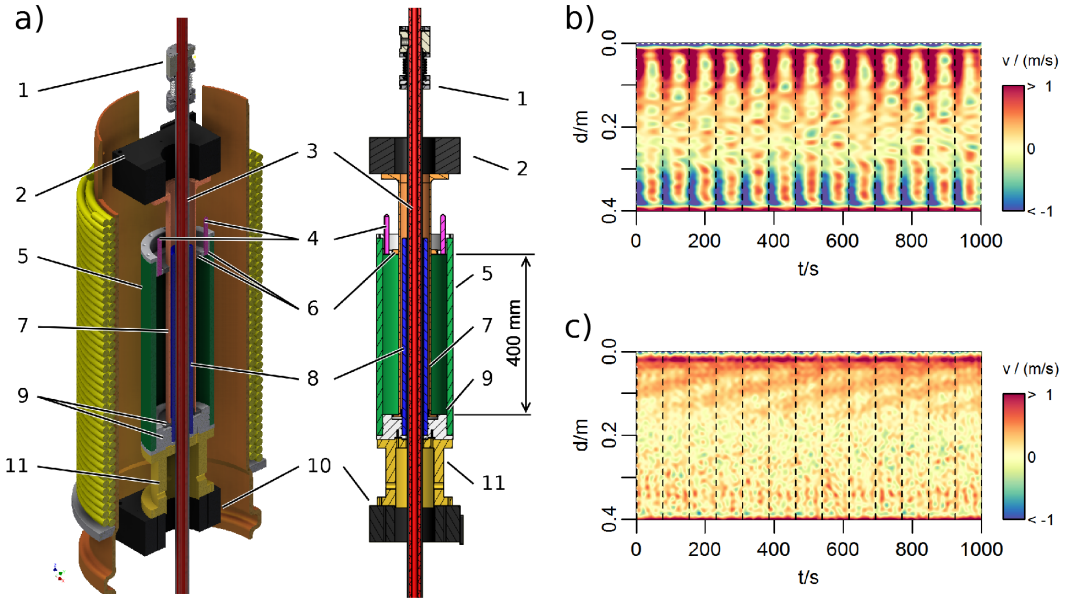

Figure 1: a) Sketch of the PROMISE facility. (1) Vacuum insulation; (2) Upper motor; (3) Current carrying copper rod; (4) UDV – Sensors, fixed with the outer cylinder; (5) Outer cylinder; (6) Top acrylic glass split rings; (7) Inner cylinder; (8) Center cylinder; (9) Bottom split rings; (10) Bottom motor; (11) Interface – Dimensions: $h = 0.4$ m, $r_i = 40$ mm, $r_o = 80$ mm. b) shows the filtered time series of one sensor, with characteristic disturbance originating from magnetic field imperfections. c) same as b) but with optimized magnetic field distribution. The dashed lines indicate the rotation period of the outer cylinder.

In the present setup magnetic field support is realized by a cylindrical coil (yellow wires in Figure 1) generating B_z and a central rod carrying up to 20 kA DC current creating B_φ. The former current supply for B_φ consisted of an upper feed line and a lower one,

which together formed a frame coil with approximated two meters in height and width. The effect of this design was that the magnetic field component B_φ in the cylindrical gap on the inside was about 6% larger than on the outer side. In addition to that, also a small B_r component was created which acted on the flow. All this imperfections lead to an $m = 1$ distributed stationary (in the frame of laboratory) residual background flow as seen in Figure 1b. Nevertheless the results on the AMRI experiment in 2014 [2] confirmed the predicted features of the investigated instability such as amplitude, frequency and wave number.

We like to report recent results carried out with a quasi coaxial return path, which was introduced to the PROMIS experiment in the last years. Instead of the former frame coil an axial-symmetric return path closes the electrical circuit, which improves the field symmetry inside the experiment and minimizes the stray field outside the setup. Since this arrangement consists of an electrical parallel connection of the return conductors and the parallel connection of the hydraulic cooling circuit, it must be checked whether stability problems can occur in the current distribution in the return conductors. It turned out that the current return design can be controlled by simple and cheap proportional heater valves [3].

The improved magnetic field configuration minimized side effects of geometric imperfections which leads to an unperturbed evolution of AMRI-wave. As an example, Figure 1c depicts results at $Ha = 124$ ($I_{\mathrm{rod}} = 16\,\mathrm{kA}$), $\mathrm{Re} = 1480$ and $\Omega_{\mathrm{out}}/\Omega_{\mathrm{in}} = 0.26$, which indicate a clean AMRI-wave in the upper half plane of the experiment. In a future experimental campaign the transition from HMRI [4] to AMRI is to be investigated.

A new liquid metal Taylor Couette Experiment is currently under development in the frame of DRESDYN-Project. In contrast to the PROMISE facility the new machine will be in 1 m - scale, which enables $\mathrm{Re} = \mathcal{O}(10^6)$, $\mathrm{Rm} \approx 21$ and $\mathrm{Ha} = \mathcal{O}(10^3)$ to achieve conditions necessary for standard MRI – the "holy grail" in liquid metal shear-flow experiments.

References

[1] R. J. Donnelly and M. Ozima, *Hydromagnetic Stability of Flow Between Rotating Cylinders*, Phys. Rev. Lett., 4(10), 497–498, 1960.

[2] M. Seilmayer et al., *Experimental Evidence for Nonaxisymmetric magnetorotational instability in a rotating liquid metal exposed to an azimuthal magnetic field*, Phys. Rev. Lett. 113, 024505, 2014.

[3] M. Seilmayer and N. Krauter, *Balanced 20 kA DC Distributor for Magnetized Taylor Couette Systems, Utilizing Thermostatic Controlled Water Valves with CO2 Adsorption Charge Sensors as Current Controller*, IEEE Sensors Journal, 18(3), 1256–1264, 2018.

[4] F. Stefani et al., *Helical magnetorotational instability in a Taylor-Couette flow with strongly reduced Ekman pumping*, Physical Review E, 80(6), 2009.

[5] F. Stefani et al., *The DRESDYN project: planned experiments and present status*, arXiv preprint arXiv:1704.03157, 2017.

Acknowledgements

This work was supported by the Helmholtz-Gemeinschaft Deutscher Forschungszentren (HGF) in the framework of Helmholtz Alliance LIMTECH, as well as by the Deutsche Forschungsgemeinschaft under SPP 1488 (PlanetMag).

Quasi-periodic mixing events in two-layer stably-stratified turbulent Taylor-Couette flow

Kanwar Nain Singh[1], Jamie Partridge[1], Stuart Dalziel[1] C. P. Caulfield[2,1]

[1] DAMTP, Centre for Mathematical Sciences, University of Cambridge

[2] BP Institute, University of Cambridge

We consider mixing in stratified Taylor-Couette flow between two concentric cylinders driven at different angular rotation rates when the fluid in the annular region between the two cylinders is stably stratified, with (statically stable) density variation in the axial (vertical) direction. If the fluid is initially linearly stratified, for certain flow parameters such stratified Taylor-Couette flow is known to be prone to the so-called 'strato-rotational instability' (SRI), even when the unstratified flow is (centrifugally) stable. At finite amplitude, the SRI develops into helical structures[1], growing due to resonance between boundary trapped inertia-gravity waves.

Conversely, when the flow is centrifugally unstable (with the inner cylinder rotating at some angular rotation rate Ω, and the outer cylinder fixed) at sufficiently high rotation rates, layers spontaneously form in an initially linearly stratified flow, with turbulent motions ensuring the relatively deep 'layers' are well-mixed, and separated by apparently robust 'interfaces' of substantially higher density gradient[2]. Interestingly, the buoyancy flux through these layers matches the equivalent flux through a two-layer stratification, independently of the height or number of layers [2].

Even in two layer flows with a single interface, such interfaces appear always to support $m = 1$, inherently nonlinear perturbations with characteristic period $\sim 6 * 2\pi/\Omega$ for an inner cylinder of 100 mm and outer cylinder of 240 mm, where $T = 2\pi/\Omega$ is the characteristic period of rotation of the inner cylinder. These perturbations are observed to disrupt the interface completely yet transiently, inducing the dominant irreversible mixing within such flows. Crucially, these perturbations are not observed in experiments using immiscible fluids, indicating that inherently nonlinear processes are central to the maintenance of these perturbations, which still survive even in highly turbulent flows. Through the use of PIV and LIF measurements, we characterise the growth, maintenance, and mixing of momentum or mass by these largely coherent perturbations.

For example, we find that the azimuthal velocity also increases and decreases periodically with the same period as the observed mixing event. The interface periodically becomes very sharp (O[1 mm]) in the high shear regions close to the inner and outer cylinders, with the dominant mixing processes occurring at intermediate radii in the annulus. Due to the mixing, the density difference across the interface steadily decreases, which ultimately causes the region of the flow with substantially higher frequency content (as shown in figure 1(a)) to penetrate across the entire annulus, as shown in figure 1(b).

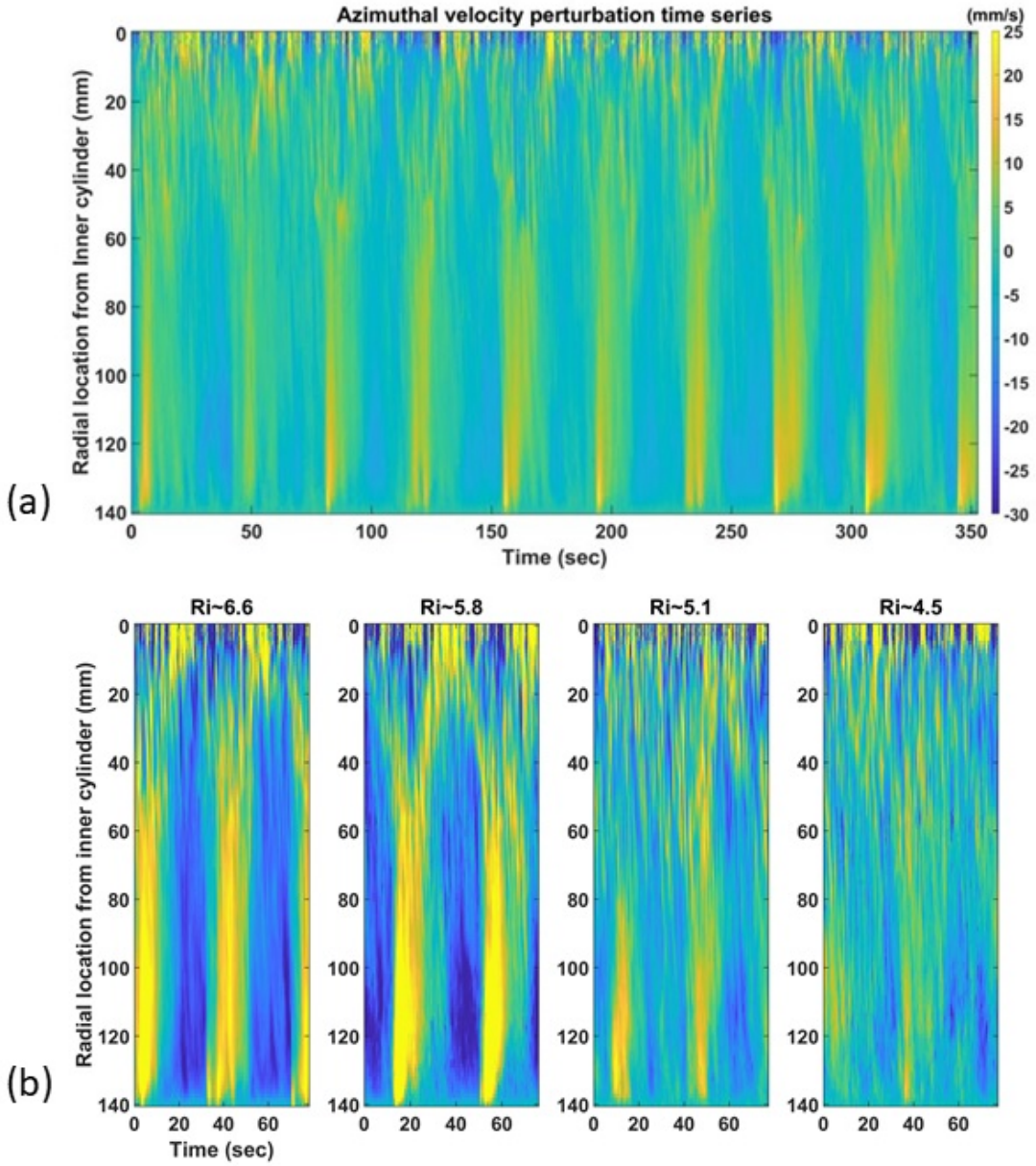

Figure 1: (a)Time-series of azimuthal velocity perturbation along one radial line. (b)Phase averaged azimuthal velocity perturbation time-series at the same line with reducing Richardson number (density difference).

References

[1] M. Le Bars & P. Le Gal, *Phys. Rev. Lett.*, **99**, 064502, 2007.

[2] R.L. Oglethorpe ,C.P. Caulfield ,A.W. Woods, *J. Fluid Mech.* **721**, 2013.

Acknowledgements

The authors would like to acknowledge EPSRC for the Programme grant (EP/K034529/1) entitled *Mathematical Underpinning of Stratified Turbulence* (MUST) which funded this project.

Symmetry in Taylor Couette Flow

Yasushi Takeda[1], Lea Pokorny[1], Erich J. Windhab[1]

[1] Laboratory of Food Process Engineering, Institute of Food, Nutrition and Health, Swiss Federal Institute of Technology Zurich, yasushi.takeda@hest.ethz.ch

---

A symmetry assumption is revisited and tested. A highly resolved measurement of axial distribution of radial velocity of Taylor Couette system (TCF) was performed for Taylor Vortex Flow (TVF) and Wavy Vortex flow (WVF). A shift-reflect symmetry was found visually to be well reproduced as known from early time. Quantitatively, an auto-correlation function of radial velocity at the mid gap position with respect to vertical position grows from 0.6 at just after onset of TVF to larger than 0.9 just before WVF appears, which verifies a high degree of shift symmetry. The value is flat to be at 0.8 for WVF regime, which shows a validity of shift symmetry of TCF for all the covered range of Reynolds number including the wavy vortex mode. Evaluation using a folding coefficient (defined here) indicates, however, that the reflect symmetry is also valid for TVF but it abates after WVF sets in.

1 Introduction

A symmetry assumption is revisited and tested. A highly resolved measurement of axial distribution of radial velocity of Taylor Couette system (TCF) was performed for Taylor Vortex Flow (TVF) and Wavy Vortex flow (WVF). A shift-reflect symmetry was found visually to be well reproduced as known from early time. Quantitatively, an auto-correlation function of radial velocity at the mid gap position with respect to vertical position grows from 0.6 at just after onset of TVF to larger than 0.9 just before WVF appears, which verifies a high degree of shift symmetry. The value is flat to be at 0.8 for WVF regime, which shows a validity of shift symmetry of TCF for all the covered range of Reynolds number including the wavy vortex mode. Evaluation using a folding coefficient (defined here) indicates, however, that the reflect symmetry is also valid for TVF but it abates after WVF sets in.

2 Results and Discussion

2.1 Shift symmetry

As expected, it appears that shift symmetry dominates for the range of Reynolds number studied here. All axial distributions indicate no violation of this symmetry. In order to investigate this quantitatively, it is readily studied by computing the auto-correlation function of these distributions, showing the shift symmetry is valid for long distances in the axial direction. Variation of the correlation function with respect to Reynolds number shows that, in the regime of TVF ($R^*<1.4$), the correlation coefficient grows from 0.57 to 0.97 with increasing R^*, which implies the development of Taylor vortices, while the wave length stays

constant. For R*>1.44 where WVF sets in, both the correlation coefficient and the wave length becomes smaller but quite constant. This is an interesting nature that shift symmetry may be valid also for WVF.

2.2 Reflect symmetry

We define a folding coefficient as follows; $K(z) = \frac{1}{2L}(\sum_{i=1}^{L} \sqrt{(v(z+i) - v(z-i))})$ where z is axial position, $2L$ corresponds to the axial wave length of Taylor rolls. The value would be zero if reflect symmetry is perfect around the symmetry axis at z. Figure 1a is the distribution of the computed folding coefficient for R*=1.07. The value of the minima is, in

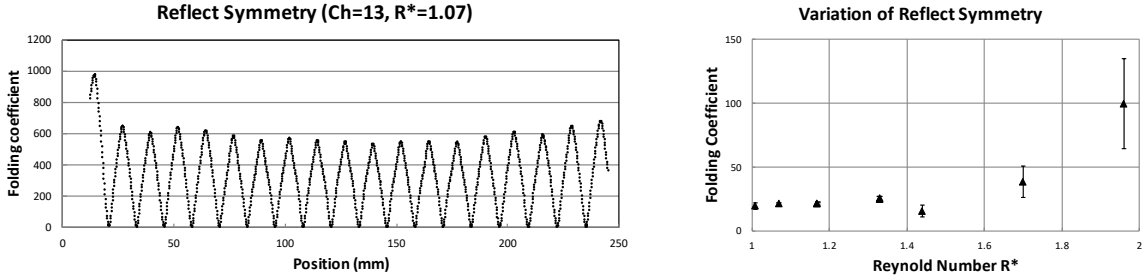

(a) (b)

Figure 1: (a) Computed reflection coefficient for R*=1.07. (b) Variation of the averaged minimal values of reflection coefficient.

this example, roughly 20 which is far smaller compared to the value of maxima, roughly 550. Therefore, it could be judged that reflect symmetry is almost perfect in this example. The average over all minimum values is plotted against Reynolds number as shown in Figure 1b. It is found that reflect symmetry is good and remains good for TVF and beginning of WVF, but it grows for larger R*.

3 Conclusion

Shift- and Reflect-symmetry was quantitatively investigated. An auto-correlation coefficient close to unity was obtained, which indicates a very high symmetry of TVF, and it remains symmetric even for WVF. On the other hand, reflect symmetry was investigated by defining a folding coefficient, which shows a good symmetry only for TVF, and it departs from symmetry just after WVF sets in. Our observation and quantitative evaluation of shift-reflect-symmetry confirms the validity of the assumption of symmetry used in theoretical and numerical work, as long as for TVF, but reflect symmetry must be treated carefully for the higher mode of WVF.

2D oscillatory convections in a bounded liquid metal layer under an imposed horizontal magnetic field

Yuji Tasaka[1], Takatoshi Yanagisawa[2], Tobias Vogt[3], Sven Eckert[3]

[1] Laboratory for Flow Control, Hokkaido University, Sapporo, Japan

[2] Japan Agency for Marin-Earth Science and Technology (JAMSTEC), Yokosuka, Japan

[3] Helmholtz Zentrum Dresden-Rossendorf, Dresden, Germany

Applying horizontal magnetic field to Rayleigh-Beénard convection in a layer of electrically conductive fluids restricts convective motions into two-dimensional (2D). We examined the onset and development of oscillatory convections formed in a liquid metal layer confined by aspect-ratio-five box imposed by a horizontal magnetic field. The onset and development were controlled by decreasing Chandrasekhar number Q at fixed Rayleigh numbers Ra in relatively larger Q ranges. Experimental investigations using ultrasonic velocity profiling (UVP) and following numerical simulations elucidated that the oscillatory convection is 2D at the onset, and is possibly caused by instability on recirculation vortex pair between the main rolls aligned parallel to the magnetic field (see Fig. 1). Variations of the Reynolds number, Re_{2D}, estimated from velocity profiles perpendicular to the rolls measured by UVP (Fig. 2) indicate the oscillations appear at $Re_{2D} \sim 900$ even for different Ra values. The increases of Re_{2D} with relaxation of the magnetic field obey power law, $Re_{2D} \sim Q^{\alpha}$, $-0.25 < \alpha < -0.2$. According to Prandtl's free-fall theory and using effective Ra values reduced by critical Ra values, Ra_c, depending on Q, the relation between Re_{2D} and Ra can be described as $Re_{2D} \sim [Ra/Ra_c(Q)]^{1/2}$. In the fluid layer confined by electrically insulated side walls, viscous dissipation by Hartmann breaking on the walls perpendicular to the magnetic field restricts the onset of convection. Linear stability analysis with considering Hartmann breaking performed in Burr & Müller [2] derived $Ra_c \sim Q^m$, where the exponent m increases with respect to Q and approaches to 1/2 for sufficiently large Q. This derives the relation, $Re_{2D} \sim Ra^{1/2}Q^{-m/2}$, and the exponent for Q becomes -1/4 for sufficiently large Q values

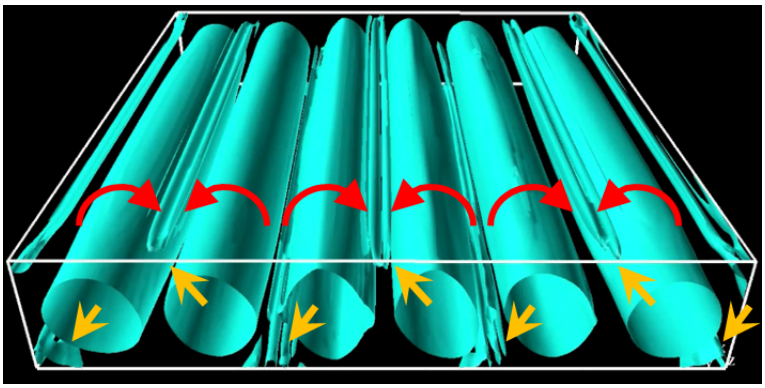

Figure 1: 2D oscillatory convections visualized by isosurface of Q_{3D} value [1]

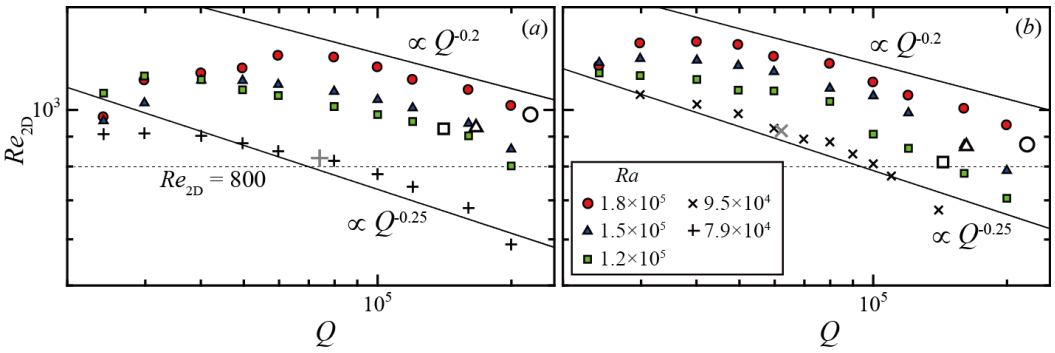

Figure 2: Variations of Reynolds number for quasi-2D flows, Re_{2D}, with decreasing Q at different Ra values and different number of rolls; (a) $n = 5$ and (b) 6, respectively; Bigger open symbols (grey lines for crosses) indicate estimated value of Re_{2D} corresponding to Q_{os}.

and increases with decreasing of Q. This relation has reasonable agreement with the power law found in the present experiment shown in the figure.

References

[1] T. Yanagisawa, Y. Hamano, A. Sakuraba, *Flow reversals in low-Prandtl-number Rayleigh-Bénard convection controlled by horizontal circulations*, Phys. Rev. E, **92**, 023018, 2015.

[2] U. Burr, U. Müller, *RayleighBénard convection in liquid metal layers under the influence of a horizontal magnetic field*, J. Fluid Mech., **453**, 345-369, 2002.

Acknowledgements

The present study was supported by JSPS KAKENHI 15KK0219.

From Bubbles to Cells: A decade of investigation into the phenomenon of object motion in the Taylor-Couette flow

Jia Heng Teoh, Rensheng Deng, Chi-Hwa Wang*

Department of Chemical and Biomolecular Engineering, National University of Singapore, 4 Engineering Drive 4, Singapore 117585

*Corresponding Author. Tel: +65 65165079; Fax: +65 67791936;
Email: chewch@nus.edu.sg (C. H. Wang)

The discovery of the phenomenon known as the Taylor-Couette flow, some aspects of which were first noted by Sir Isaac Newton in the 17th century has sprouted numerous studies and development in this area of fluid dynamics. Among the unknowns surrounding the Taylor-Couette flow, our research group has delved into the behaviour of objects trapped in this flow. This review looks into computational and experimental studies that we have carried out over the past decade on object motion in the Taylor-Couette flow. This review first begins with our investigation into the motion of bubbles trapped in Taylor vortices. Our study found interesting observations, including uniform spacing between bubbles travelling in the same axial plane and orbit crossing of small and large bubbles. From bubbles, we move on to droplet and particle motion in Taylor vortices respectively. Differences in behaviour exist between these three objects, such as the deformation of droplets trapped in Taylor vortices and variation in droplet and particle trajectories with increasing Reynolds number. Finally, this review looks into our studies pertaining to the cultivation of rBMS and QM7 cells respectively in a Taylor-Couette bioreactor for biomedical applications. One key benefit of this application is the improvement of mass and oxygen transport, which improves cell proliferation and cell secretion. Overall, these studies demonstrate the unique phenomenon of object motion in the Taylor-Couette flow and its potential application in particle-laden processes such as mixing, extraction and cell cultivation.

Dr. Chi-Hwa Wang is currently a Professor of Chemical and Biomolecular Engineering at the National University of Singapore (NUS). He had the following joint appointments in his service to the same university (i) Assistant Dean for Research at the Faculty of Engineering, NUS (2006-2008), and (ii) Faculty Fellow, Singapore-MIT Alliance (2001-2006). He received his B.S. degree (Chemical Engineering) from the National Taiwan University, M.S. degree (Biomedical Engineering) from Johns Hopkins University, M.A. and PhD degrees (both in Chemical Engineering) from Princeton University, respectively. He was holding several visiting appointments throughout different stages of his career: National Taiwan University (1999-2000, 2002, Visiting Assistant Professor), Kyoto University (2003, JSPS Visiting Fellow), Cambridge University (2004, Sabbatical Academic Visitor), Massachusetts Institute of Technology (2004, Visiting Associate Professor). His current research interests include transport & reaction in particulate systems and drug delivery systems. He is on the editorial boards of *Journal of Controlled Release (2009 - present)*, *Powder Technology (2008 - present)*, and *Advanced Powder Technology* (2009 – present, also Executive Editor, 2009-2012. He is currently an Executive Editor for *Chemical Engineering Science* (Elsevier, 2013 - present).

Experimental and Numerical Modelling of fluid flow between rotating spheres

Zahia Tigrine[1,2], Ahcene Bouabdallah[1],

[1] USTHB Univ., Thermodynamics and Energetic Systems Laboratory, B.P 32 El Alia, 1611 Bab Ezzouar Algiers, Algeria

[2] Unite de Developpement des Equipements Solaires UDES/EPST-CDER., Tipaza, Algeria

---

This paper presents an experimental and numerical study of hydrodynamic instabilities of an incompressible viscous fluid contained between two concentric spheres whose the inner one rotating ($\Omega_1 \ddagger 0$)while the outer is at rest ($\Omega_2 = 0$). The flow system, totally or partially filled through the aspect ratio $\Gamma_{HF} = H/d$ of the fluid is defined by clearance ratio in small gap configuration ($\delta = 0.11$). The main aim is to investigate the effect of the aspectratio on the instabilities in completely illed flow system and with free surface using two immiscible fluids. Experiments are performed for different aspect ratio values,and Laser photometric technique is sed for visualization. Our observations are compared to the flow system totally filled using a single fluid studied by M. Wimmer [1], K.Nakabayashi et al [2]. Three-dimensional numerical simulations are performed using the finite volume method in order to set up and solve the free-surface problem in spherical Taylor-Couette flow. The simulation confirms our experimental measurements that a surface cell exists and wavy mode flow is accelerate for aspect ratio ($\Gamma_{HF} = 13$). The numerical results of the flow pattern and critical Taylor numbers were analyzed and compared to the experimental results [3] which are in good agreements.

References

[1] A. M.Wimmer, *Experiments on a viscous fluid flow between rotating spheres*, J.Fluid Mech., **78**, part 2, 317-335, 1976.

[2] K.Nakabayashi, Y. Tsuchida, *Modulated and unmodulated traveling azimuthal waves on the toroidal vortices in a spherical Couette system*, J. Fluid Mech. **195**,495-522, 1988.

[3] Z.Tigrine, F. Mokhtari, A.Bouabdallah, M. Mahloul, *Experiments on two immiscible fluids in spherical Couette flow*, Acta Mechanica Journal. **225**,233242, 2014.

The influence of wall roughness on bubble drag reduction in Taylor-Couette turbulence

Ruben A. Verschoof[1], Dennis Bakhuis[1] Pim A. Bullee[1] **Sander G. Huisman**[1], Chao Sun[2,1] Detlef Lohse[1,3]

[1] Physics of Fluids, Max Planck Institute for Complex Fluid Dynamics, MESA+ Institute and J. M. Burgers Center for Fluid Dynamics, University of Twente, P.O. Box 217, 7500 AE Enschede, The Netherlands

[2] Center for Combustion Energy and Department of Thermal Engineering, Tsinghua University, 100084 Beijing, China

[3] Max Planck Institute for Dynamics and Self-Organization, Am Fassberg 17, 37077 Göttingen, Germany

---

We experimentally study the influence of wall roughness on bubble drag reduction in turbulent Taylor-Couette flow, see figure 1. We measure the drag in the system for the cases with and without air, and add roughness by installing transverse ribs on either one or both of the cylinders. We operate our system at Re = $\mathcal{O}(10^6)$. For the smooth wall case (no ribs) and the case of ribs on the inner cylinder only, we observe strong drag reduction up to DR = 33% and DR = 23%, respectively, for a void fraction of $\alpha = 6\%$. However, with ribs mounted on both cylinders or on the outer cylinder only, the drag reduction is weak, less than DR = 11%, and thus quite close to the trivial effect of reduced effective density. Flow visualizations show that stable turbulent Taylor vortices are induced in these two cases, i.e. the cases with ribs on the outer cylinder. These strong secondary flows move the bubbles away from the boundary layer, making the bubbles less effective than what had previously been observed for the smooth-wall case. Measurements with counter-rotating smooth cylinders, a regime in which pronounced Taylor rolls are also induced, confirm that it is really the Taylor vortices that weaken the bubble drag reduction mechanism. Our findings show that, although bubble drag reduction can indeed be effective for smooth walls, its effect can be spoiled by e.g. biofouling and omnipresent wall roughness, as the roughness can induce strong secondary flows.

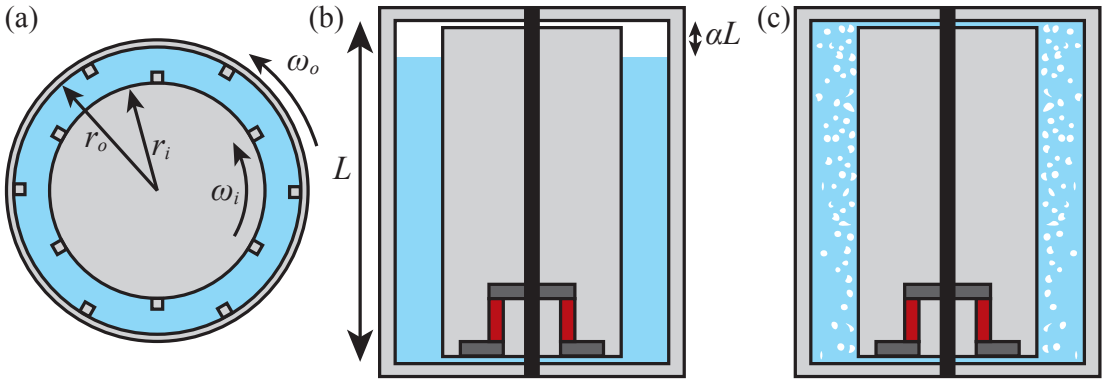

Figure 1: (a) Top view schematic of the T3C facility. We attached 6 vertical transverse ribs (not to scale) equally distributed around the perimeter of the inner cylinder, the outer cylinder, or both cylinders. We also measure a smooth-wall case without any ribs. (b) Vertical cross-section of the setup at rest, showing the position of the torque sensor. To control the void fraction, we fill the cylinder only partially with water, so that the void fraction α is controlled by measuring the relative height of the water level. (c) Vertical cross-section of the setup during a measurement. The free surface disappears, and all air is entrained by the turbulent flow (bubbles not to scale).

Acknowledgements

We thank Tom van Terwisga (MARIN, TU Delft) for the continuous and stimulating collaboration over the years on drag reduction in the marine context. We also thank Dennis van Gils, Gert-Wim Bruggert, and Martin Bos for their technical support. The work was financially supported by NWO-TTW (project 13265). We acknowledge support from EuHIT and MCEC. Sun and Bakhuis acknowledge financial support from VIDI grant No. 13477, and the Natural Science Foundation of China under grant no. 11672156. Bullee acknowledges NWO-TTW (project 14504).

Structures in a rotating flow with free surface: simulations and experiments.

Wen Yang[1,2], Ivan Delbende[3,4], Yann Fraigneau[4], Laurent Martin Witkowski[3,4]

[1] Sorbonne Université, Collège Doctoral, F-75005 Paris, France

[2] FAST, UMR 7608, Parc-Club Orsay Université, F-91405 Orsay Cedex, France

[3] Sorbonne Université, Faculté des Sciences et Ingénierie, UFR d'Ingénierie, F-75005 Paris, France

[4] LIMSI, CNRS, Bât. 507, rue du Belvédère, F-91405 Orsay Cedex, France

---

We are interested in the free surface rotating flow driven by the rotation of the bottom in an open cylinder with radius R. Given an initial filling depth H, increasing the rotation disk frequency f_d breaks the flow axisymmetry. Two kinds of instability patterns can be observed: a modal structure with almost no free surface deformation (Fig. 1a) similar to those observed in [3] at intermediate Reynolds number values; a pattern of rotating polygons at high Reynolds numbers (Fig. 1b) with large free surface deformations [4]. In the present work, we carry out a detailed study of the flow structure for the intermediate Reynolds number regime by characterizing the influence of Froude number, aspect ratio and Reynolds number. The ultimate goal is to understand if the structures prevailing in the two regimes are related.

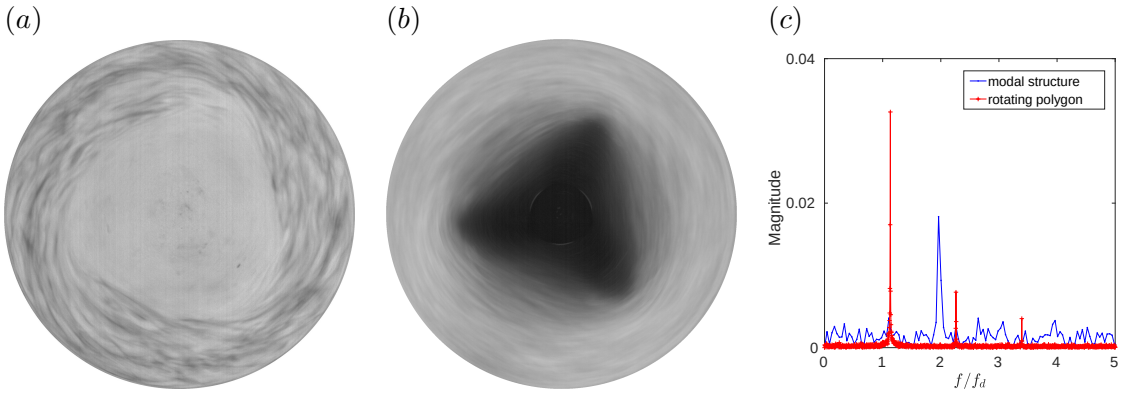

Figure 1: (a)-(b) Top view of the experiment using kalliroscope to visualise the flow structure ($H = 26$ mm, $R = 140$ mm). (a): azimuthal mode $m = 3$ for $f_d = 14.6$ rpm (no surface deformation is observed). (b): rotating triangle with a dry core at $f_d = 139$ rpm. (c): typical spectrum of the azimuthal velocity component [probe location $(r, z) = (112,\ 13)$ mm].

The intermediate Reynolds number regime has been investigated using several numerical techniques – computations of steady solutions, mean unsteady two-dimensional and three-dimensional direct simulations – as well as Laser-Doppler Velocimetry measurements. Simulations reveal the structure of a toroidal flow located at the periphery of a central solid body rotation region. This flow cell is found bordered by four layers in the meridional plane, a bottom layer on the disk, a side layer along the wall, a core layer separating the solid body rotation (discussed also in [1]) and a layer at the free surface. The Froude number that

quantifies surface deformation and the Reynolds number are shown to have little effect on the flow structure when the Reynolds number is sufficiently large. By increasing the aspect ratio, we find that the toroidal flow is composed of an upper sub-region with sinuous core layer and a mostly z-independent lower region. The mean flow and the rms of fluctuations in 3D simulations obtained through space and time averaging are compared with LDV measurements. A fair agreement is obtained for azimuthal and axial velocity distributions, except some local discrepancies.

Preliminary experiments show that the modal structure at intermediate Reynolds number is robust over a large range of f_d as long as the free surface does not touch the bottom disk. The spectrum shown in figure 1(c) indicates that this instability is observed always at a frequency close to $2f_d$ before moving abruptly to $1.13f_d$ when the rotating triangle occurs. Yet, the transition between the two regimes seems complex and depends on the protocol used to increase the disk speed [2].

References

[1] K. Iga, *Axisymmetric flow in a cylindrical tank over a rotating bottom. Part I. Analysis of boundary layers and vertical circulation*, Fluid Dyn. Res., **49(6)**:065502, 2017.

[2] J. Mougel, *Ondes et instabilités dans les écoulements tournants à surface libre*, PhD thesis, 2014.

[3] S. Poncet and M. Chauve, *Shear-layer instability in a rotating system*, J. Flow Visual. Image Process., **14(1)**:85-105, 2007.

[4] G. H. Vatistas, *A note on liquid vortex sloshing and Kelvins equilibria*, J. Fluid Mech., **217**:241-248, 1990.

Transition to turbulence in the rotating disk boundary layer of a rotor-stator cavity

Eunok Yim[1,3], J.-M. Chomaz[2], D. Martinand[1] E. Serre[1]

[1] Aix-Marseille Univ., CNRS, Centrale Marseille, M2P2, France

[2] LadHyX, CNRS-Ecole Polytechnique, F-91128 Palaiseau, France

[3] current address LFMI, EPFL, Lausanne, Swiss

The transition to turbulence in the rotating disk boundary layer is investigated in a closed cylindrical rotor-stator cavity via direct numerical simulation using spectral vanishing vistocity method (DNS-SVV) and linear stability analysis (LSA). As shown in the Figure 1,

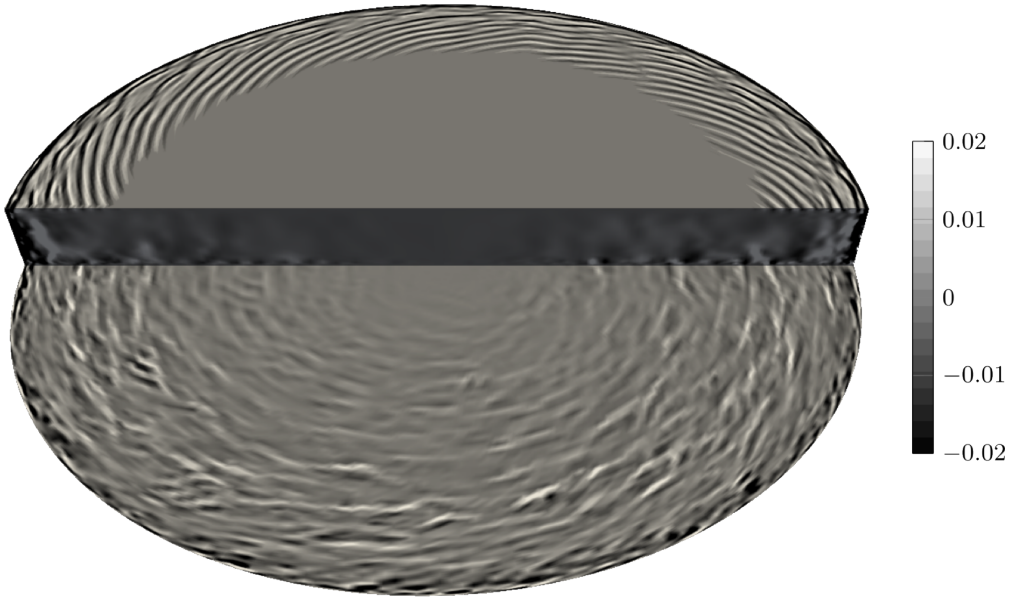

Figure 1: Instantaneous flow pattern in the whole cavity for $Re = 4 \times 10^5$. The stator is below. Iso-surfaces and iso-contours of the instantaneous axial velocity w. Three dimensional view. The rotor and stator boundary layers are shown for $z = \pm 0.97H$, respectively.

the stator boundary layer (lower part) is already turbulent while the rotor boundary layer (upper part) remains stable until very high Reynolds number $Re = U/\nu R$ then shows an organised behaviour followed by incipient turbulence. We focus on the global stability and the transition to turbulence of the rotor boundary layer. The mean flow in the rotor boundary layer is qualitatively similar to the von Kármán self-similarity solution [1]. The mean velocity profiles, however, slightly depart from theory which is developed on the infinite disk assumption [2] as the rotor edge is approached. Such meanflow modification near the edge seems to affect the stability behaviour of the system [3, 4]. Shear and centrifugal effects lead to a locally more unstable mean flow than the self-similarity solution, which acts as a

strong source of perturbations. Fluctuations start rising there, as the Reynolds number is increased, eventually leading to an edge-driven global mode, characterized by spiral arms rotating counter-clockwise with respect to the rotor (see Figure 1). At larger Reynolds numbers, fluctuations form a steep front, no longer driven by the edge, and followed downstream by a saturated spiral wave, eventually leading to incipient turbulence. Numerical results show that this front results from the superposition of several *elephant* front-forming global modes, corresponding to unstable azimuthal wavenumbers m, in the range $m \in [32,\ 78]$. The spatial growth along the radial direction of the energy of these fluctuations is quantitatively similar to that observed experimentally on the infinite single disk [5]. This superposition of *elephant*-modes could thus provide an explanation for the discrepancy observed in the single disk configuration, between the corresponding spatial growth rates values measured by experiments on the one hand, and predicted by LSA and DNS performed in an azimuthal sector [6], on the other hand.

References

[1] Th. von Kármán, *Über laminare und turbulenteReibung.*, Z. Angew. Math. Mech **1**, 233-252, 1921.

[2] R. J. Lingwood, *Absolute instability of the Ekman layer and related rotating flows.*, J. Fluid Mech. **331**, 405-428, 1997.

[3] J. Healey, *Model for unstable global modes in the rotating-disk boundary layer*, J. Fluid Mech. **663**,148–159, 2010.

[4] B. Pier, *Transition near the edge of a rotating disk*, J. Fluid Mech. **737**,R1, 2013.

[5] S. Imayama, P.H. Alfredsson, R.J. Lingwood, *On the laminar-turbulent transition of the rotating-disk flow: the role of absolute instability*, J. Fluid Mech. **745**,132–163, 2014.

[6] E. Appelquist, P. Schlatter, P.H. Alfredsson, R.J. Lingwood, *On the global nonlinear instability of the rotating-disk flow over a finite domain*, J. Fluid Mech. **803**,332–355, 2016.

Acknowledgements

This work was supported by the Labex MEC (ANR-10-LABX-0092) funded by the Investissements d'Avenir program of the French National Research Agency (ANR). This work was granted access to the HPC resources of Aix-Marseille University under the project Equip@Meso (ANR-10-EQPX-29-01) and of IDRIS, under the allocation i20170242 made by GENCI.

Formation of spiral liquid curtains in a Rayleigh-Taylor system

Harunori Yoshikawa[1], Shu Satoh[2], Christian Mathis[1]

[1] Universit Côte dAzur, CNRS, UMR 7351, Laboratoire J.-A. Dieudonn, 06108 Nice Cedex 02, France

[2] Faculty of Engineering, Hokkaido University, N13W8, Sapporo 060-8628, Japan

---

Spiral patterns have attracted much interest due to their striking topological features [1]. The patterns are often found in excitable media, e.g., in the Belousov-Zhabotinsky reaction, but also observed in dissipative pattern forming systems, e.g., in the Rayleigh-Bénard convection [2].

We report an experimental investigation on the liquid curtains falling from a horizontal liquid film beneath a grid plate (Fig. 1). Liquid is fed continuously to the film from a depressurized reservoir at a given volumetric flux density U through the grid holes. The film lower surface is exposed to air so that it is unstable against the gravitational acceleration. The development of the Rayleigh-Taylor instability leads to the discharge of the same amount of liquid as U from the film surface per unit area. Different modes of discharge (drops, columns, curtains, bells) are observed, depending on the flow rate [3, 4, 5]. We are interested in a particular dynamical regime where liquid is discharged in the form of rotating spiral curtains.

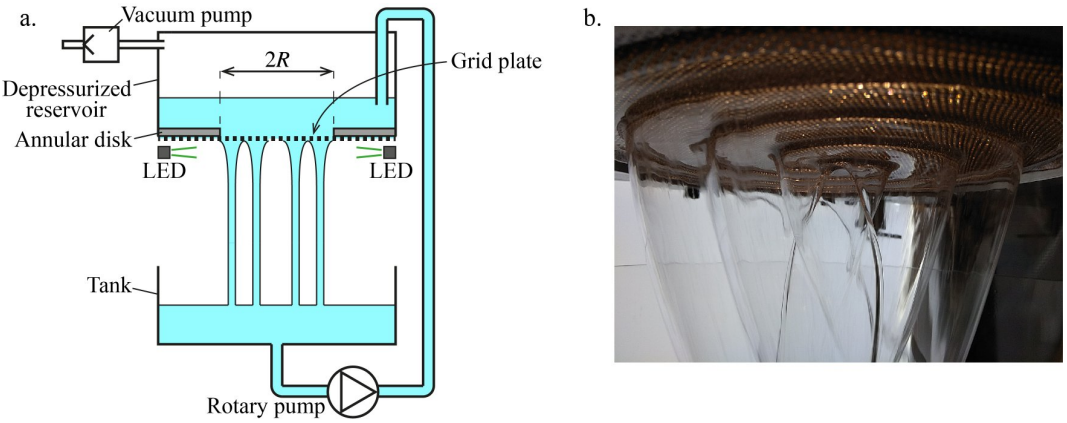

Figure 1: The experimental rig (a) and spiral liquid curtains (b).

Experiments are performed with different liquids of different viscosities ν under different geometrical constraints (i.e., the radius R of the grid plate). The motion of liquid curtain is monitored in the top view along the center axis of the system, where the roots of curtains on the film are visualized by an optical technique (Fig. 2). Patterns with different numbers of rotating arms are observed at a given control parameters (ν, U) in a given geometry as shown in Fig. 2. The time scale of their rotation is given by the viscous time $\tau_\nu = (\nu/\mathrm{g}^2)^{1/3}$ and the rotation speed Ω is inversely proportional to the number m of arms. The averaged wave length $\overline{\lambda}$ of patterns decreases with the flow rate but is insensitive to the viscosity. It does not seem to be sensitive to the geometrical constraint.

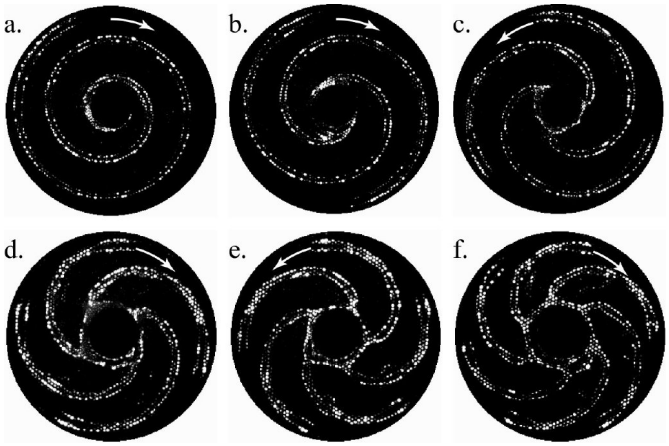

Figure 2: Patterns exhibited by the roots of spiral curtains on the liquid film. The directions of rotation are indicated by arrows.

We develop a simple theoretical model to get insights into the formation mechanism of the spiral patterns. By considering the mass conservation for the liquid supply to the curtain from the film, we obtain the following shape of spiral:

$$r = r_0 \sec\alpha, \quad \varphi - \Omega t = \tan\alpha - \alpha + \varphi_0,$$

in a parametric representation, where α is a parameter varying from 0 to $\pi/2$, (r, φ) are the cylindrical polar coordinates of a spiral arm, and φ_0 is a constant. The single length scale r_0 involved in this theoretical shape depends on the flow rate and related to the wavelength $\overline{\lambda}$ by $2\pi r_0 = \overline{\lambda}$. This predicted shape shows a good agreement with experimental ones.

References

[1] M. Cross, H. Greenside, *Pattern Formation and Dynamics in Nonequilibrium Systems*, Cambridge University Press, Cambridge, UK, 2009.

[2] E. Bodenschatz, J.R. de Bruyn, G. Ahlers, D.S. Cannell, *Transitions between patterns in thermal convection*, Phys. Rev. Lett., **67**(22), 3078, 1991; S.W. Morris, E. Bodenschatz, D.S. Cannell, G. Ahlers, *Spiral defect chaos in large aspect ratio Rayleigh-Bénard convection*, Phys. Rev. Lett., **71**(13), 2026, 1993; B.B. Plapp, D.A. Egolf, E. Bodenschatz, *Dynamics and selection of giant spirals in Rayleigh-Bnard convection*, Phys. Rev. Lett., **81**(24), 5334, 1998.

[3] C. Pirat, C. Mathis, P. Massa, L. Gil, *Structures of a continuously fed two-dimensional viscous film under a destabilizing gravitational force*, Phys. Rev. Lett., **92**(10), 104501, 2004.

[4] C. Pirat, A. Naso, J.-L. Meunier, P. Massa, C. Mathis, *Transition to spatiotemporal chaos in a two-dimensional hydrodynamic system*, Phys. Rev. Lett., **94**, 134502, 2005.

[5] C. Pirat, C. Mathis, M. Mishra, P. Massa, *Destabilization of a viscous film flowing down in the form of a vertical cylindrical curtain*, Phys. Rev. Lett., **97**, 184501, 2006.

Wall roughness induces asymptotic ultimate Taylor-Couette turbulence

Xiaojue Zhu[1], Ruben A. Verschoof[1], Dennis Bakhuis[1], Sander G. Huisman[1], Roberto Verzicco[2,1], Chao Sun[3,1], Detlef Lohse[4,1]

[1] Physics of Fluids Group and Max Planck Center for Complex Fluid Dynamics, MESA+ Institute and J. M. Burgers Centre for Fluid Dynamics, University of Twente, P.O. Box 217, 7500AE Enschede, The Netherlands

[2] Dipartimento di Ingegneria Industriale, University of Rome "Tor Vergata", Via del Politecnico 1, Roma 00133, Italy

[3] Center for Combustion Energy, Department of Energy and Power Engineering, Tsinghua University, 100084 Beijing, China.

[4] Max Planck Institute for Dynamics and Self-Organization, 37077 Göttingen, Germany

---

Turbulence governs the transport of heat, mass, and momentum on multiple scales. In real-world applications, wall-bounded turbulence typically involves surfaces that are rough; however, characterizing and understanding the effects of wall roughness for turbulence remains a challenge. Here, by combining extensive experiments and numerical simulations, we examine the paradigmatic Taylor-Couette system, which describes the closed flow between two independently rotating coaxial cylinders. We show how wall roughness greatly enhances the overall transport properties and the corresponding scaling exponents associated with wall-bounded turbulence. We reveal that if only one of the walls is rough, the bulk velocity is slaved to the rough side, due to the much stronger coupling to that wall by the detaching flow structures. If both walls are rough, the viscosity dependence is thoroughly eliminated, giving rise to asymptotic ultimate turbulence – the upper limit of transport – the existence of which was predicted more than fifty years ago [1]. In this limit, the scaling laws can be extrapolated to arbitrarily large Reynolds numbers.

References

[1] R. H. Kraichnan, *Turbulent thermal convection at arbitrary Prandtl number*, Phys. Fluids, **5**, 1374-1389, 1962.